Abstract

Title of Dissertation:	GLUTAMINE EFFECTS ON ENDOTHELIAL AND RED BLOOD CELL METABOLISM AND FUNCTION IN DIABETES.
	Marzyeh Kheradmand-Hajibashi, Doctor of Philosophy, 2026
Dissertation directed by:	Professor Alisa Morss Clyne, Fischell Department of Bioengineering

Cardiovascular complications are the leading cause of morbidity and mortality in individuals with diabetes, yet strategies that reduce cardiovascular disease (CVD) risk beyond glycemic control remain limited. Endothelial cells and red blood cells (RBCs) become dysfunctional under diabetes-associated hyperglycemia, partly due to increased oxidative stress and impaired vasodilation. These effects may be further influenced by interactions between RBCs and endothelial cells through extracellular vesicles (EVs), which can transfer bioactive cargo that alters endothelial function. Glutamine, the most abundant amino acid in the body, is reduced in individuals with diabetes and has reported antioxidant and anti-inflammatory effects. However, its impact on endothelial cells and diabetic RBCs remains poorly understood. In this thesis, the impact of glutamine on endothelial cells and RBCs was investigated. I showed that glutamine supplementation increased NADPH production and glutathione synthesis in endothelial cells under both normal and hyperglycemic conditions, thereby reducing oxidative stress. Glutamine also systemically altered endothelial metabolism by increasing oxidative respiration, succinate dehydrogenase activity, and UDP-GlcNAc synthesis, while decreasing polyunsaturated fatty acids and one-carbon metabolites. In contrast, RBCs from diabetic subjects showed similar basal ROS levels compared to controls but exhibited reduced antioxidant capacity, evidenced by lower

intracellular glutamate and a greater increase in oxidative stress following oxidant exposure. Glutamine supplementation did not improve RBC oxidative stress or enhance glutathione synthesis. Finally, mechanically generated RBC-EVs from diabetic and non-diabetic subjects did not induce oxidative stress or inflammation in endothelial cells, highlighting the potential impact of EV generation methods on their pathological effects. This work increases our understanding of how glutamine impacts endothelial cells and RBCs and suggests that glutamine supplementation alone may have limited beneficial effects. Instead, metabolic engineering of glutamine-related pathways in both endothelial cells and RBCs may be required to optimize therapeutic strategies for CVD.

GLUTAMINE EFFECTS ON ENDOTHELIAL AND RED BLOOD CELL METABOLISM AND FUNCTION IN DIABETES.

By

Marzyeh Kheradmand-Hajibashi

DISSERTATION SUBMITTED TO THE FACULTY OF THE GRADUATE SCHOOL OF THE UNIVERSITY OF MARYLAND, COLLEGE PARK, IN PARTIAL FULFILLMENT OF THE REQUIREMENTS FOR THE DEGREE OF DOCTOR OF PHILOSOPHY IN BIOENGINEERING
2026

Advisory Committee:
Professor Alisa Morss Clyne, Chair
Professor Kashif Munir
Associate Professor Helim Aranda-Espinoza
Associate Professor Steven Jay
Associate Professor Ganesh Sriram

Dedication

I wholeheartedly dedicate this dissertation to my beloved parents, Mr. Mohsen Kheradmand and Mrs. Fatemeh Attaran, for their unwavering love, encouragement, and support throughout this journey.

Acknowledgements

I would like to express my deepest gratitude to my advisor, Dr. Alisa Morss Clyne, for her guidance, support, and mentorship throughout my doctoral journey. Her insight, patience, and encouragement have been invaluable, shaping not only this work but also my growth as a scientist. I am also sincerely thankful to all current and former members of the Clyne Lab. Your collaboration, support, and the many discussions we shared made this experience both intellectually enriching and enjoyable. I am especially grateful for the friendships formed along the way, which made even the most challenging days more manageable. I would like to extend special thanks to several individuals who made a lasting impact on my journey.

To Dr. Callie Weber, thank you for being an incredible mentor and friend. I will always cherish our tea times and your 'Good morning, sunshine,' which I still miss every day. To Dr. Bilal Moiz, my greatest night-shift mentor, thank you for spending countless late nights troubleshooting mass spectrometry with me and teaching me so much along the way.

To Dr. Gurneet Sangha, thank you for pushing me beyond my comfort zone and giving me the confidence to do things I once thought I could not. I am still waiting to get my $200K/year postdoc offer in your lab. To Dr. Michael Sun, it was truly a pleasure to work with you. Thank you for always listening, helping troubleshoot, and for the many coffee breaks and delicious food you made us. And thanks for understanding that birds are not dinosaurs. To Lauren Smith, thank you for your constant positivity and encouragement, you were truly the energy of the lab and kept me going during the hardest times. I am also grateful for the humor you brought into the lab, including your memorable reminders about my height. To Claire, thank you for being such a wonderful friend and for sharing so many memorable moments and stories with me. I look forward to the day I can visit you at your future farm, surrounded by many animals and a fit Zelda. To Xinyao, thank

you for your hard work, your help with metabolic modeling, and for all the amazing Chinese treats you shared. I am proud of you and excited for your future success. Finally, thank you to Zoya Naseem and Vicky Chen for your support and for bringing joy to the lab.

To my friends, Dr. Shakiba Nikfarjam, Farinaz Asgari, and Dr. Angelica Rose Galvan, thank you for your constant encouragement, understanding, and for being a source of joy and balance throughout this journey. Your presence has meant more than I can fully express.

I would like to express my deepest appreciation to my beloved parents, Mr. Mohsen Kheradmand and Mrs. Fatemeh Attaran, for their unconditional love, unwavering support, and sacrifices. None of this would have been possible without you. To my sister, Mahdyeh, and my brother, Amirhossein, your love and support have always carried me through this journey.

Finally, I am profoundly grateful to my partner, Vahid Bakhshi, for his endless support, patience, and understanding, especially during the most challenging times. Thank you for always being there for me, for supporting my well-being, and for contributing your skills to help me through this work. I will always remember the snack you made me the night before my dissertation. Your presence has been a constant source of comfort and strength.

Table of Contents

List of Tables

List of Figures

Chapter 1: Introduction

1.1 Clinical motivation

Cardiovascular disease (CVD) includes a broad range of disorders affecting the heart and blood vessels, and it remains the leading cause of death worldwide[1]. Major forms of CVD are coronary artery disease (CAD), cerebrovascular disease, peripheral arterial disease (PAD), and heart failure (HF). Coronary artery disease results from atherosclerotic plaque formation in the coronary arteries. When the plaque bursts and occludes the entire coronary artery, a condition referred to as myocardial infarction (MI), downstream blood supply is restricted leading to myocardial cell death due to ischemia. Characteristic electrocardiographic changes and a rise in cardiac troponin biomarkers typically are used to diagnose MI. Cerebrovascular disease, commonly referred to as stroke and defined as an acute neurologic deficit caused by interruption of blood flow to the brain, is similarly caused by atherosclerotic plaques and is diagnosed with neuroimaging[2]. Peripheral arterial disease is a condition in which atherosclerosis narrows arteries in the legs to reduce the blood flow to the limbs, leading to symptoms like leg pain and slow healing wounds[3]. Heart failure, a syndrome of impaired cardiac pump function leading to symptoms such as shortness of breath, fatigue, and edema, is identified by clinical exam and imaging evidence of structural or functional cardiac abnormality[4]. Each of these CVD conditions have well-established diagnostic criteria and represent a significant clinical burden in affected patients. The dysfunction of endothelial cells, which cover the innermost surface of blood vessels, is an initiating event and early sign of atherosclerotic CVD; however endothelial function testing is not part of routine clinical evaluation for CVD risk[5]. This highlights the necessity of research

on prevention or reversal strategies for endothelium dysfunction in pathological conditions that increase the risk of CVD.

Diabetes mellitus (DM) is a chronic metabolic disorder characterized by hyperglycemia due to impairment in insulin secretion, insulin action, or both. Diabetes is highly prevalent and its prevalence is rising. By 2030 the global diabetes burden is projected to increase by approximately 25%. Diabetes incidence increases with age and in populations with obesity and certain genetic predispositions[6]. There are two types of diabetes: type 1 diabetes (T1D) and type 2 diabetes (T2D)[7]. T1D, an autoimmune destruction of pancreatic β-cells leading to insulin deficiency, often arises in childhood. T2D, which accounts for ~90% of cases, is caused by insulin resistance combined with inadequate insulin secretion[6,7].

Diabetes is a well-known risk factor for endothelial dysfunction through the detrimental effects of persistent hyperglycemia. Epidemiological studies have shown that individuals with diabetes have about two-fold higher risk of coronary artery disease, stroke, and other cardiovascular events compared to non-diabetic individuals[6]. Approximately one-third of adults with diabetes have coexisting CVD[8]. Chronic hyperglycemia in diabetes leads to both micro- and macrovascular complications. Examples of common microvascular complications are diabetic retinopathy, nephropathy, and neuropathy, while coronary artery disease, cerebrovascular disease, and peripheral arterial disease are macrovascular complications that impact the larger vessels[9]. Notably, coronary artery disease is present in roughly 21% of diabetes patients, cerebrovascular disease in about 8%, and heart failure in about 15%[10]. Hyperglycemia, combined with dysregulated lipid metabolism, lead to endothelial dysfunction and increased plaque formation in arteries. People with diabetes also commonly have hypertension, high triglycerides, and low HDL (dyslipidemia), which further exacerbate atherogenesis[9]. These systemic impacts make diabetes a

leading cause of CVD[6,7]. This strong epidemiological and biological link between diabetes and CVD highlights the need for cardiovascular risk management in diabetic patients.

Currently, treatment for diabetes aims not only to control blood glucose but also to prevent or mitigate cardiovascular complications by co-treating patients to lower blood pressure, lipid levels, and platelet aggregation (thrombosis). T1D is treated with lifelong insulin replacement, along with blood glucose monitoring and lifestyle modifications. T2D treatment typically begins with lifestyle management to maintain normal weight and cholesterol, alongside first-line diabetic medications such as metformin to improve insulin sensitivity. As diabetes progresses, additional drugs may be added to maintain glycemic control as well as vascular health[6]. For example, statin trials in people with diabetes show ~30% or more relative risk reductions in major cardiovascular events with between 10 to 40 mg statin per day for an average of 4 years[11]. In recent years, sodium–glucose cotransporter-2 inhibitors (SGLT2) and GLP-1 receptor agonists, two glucose-lowering medications, have shown promise in improving cardiovascular outcomes. Specifically, in patients with T2D at high cardiovascular risk, SGLT2 inhibitors and GLP-1 agonists significantly reduce rates of major adverse cardiovascular events, cardiovascular mortality, and hospitalization for heart failure[12].

Despite the advances in integrated glucose lowering and vascular protection therapy, gaps remain in targeting diabetic CVD. Diabetic patients continue to face a higher risk of CVD. Many patients do not reach risk factor targets in practice, and even when they do, the risk of CVD, while reduced, is still higher than in the non-diabetic population due to persistent inflammation, dyslipidemia and other metabolic abnormalities. Moreover, no therapy reverses endothelial and vascular damage from years of hyperglycemia. This gap is a major clinical and research priority,

highlighting the necessity for continued research in treatments and more targeted approaches to diabetes-specific CVD.

1.2 Endothelial cells in health and disease

1.2.1 Healthy endothelial cell function

Endothelial cells (ECs) cover the innermost layer of blood vessels (intima) and form a dynamic endocrine organ that helps maintain vascular homeostasis by releasing a broad range of signaling molecules. In healthy vessels, ECs produce vasodilators and vasoconstrictors in a balanced manner, and they secrete both pro- and anti-inflammatory mediators as well as oxidants and antioxidants to regulate vascular tone, inflammation, and thrombosis[13,14]. ECs produce nitric oxide (NO) via endothelial nitric oxide synthase (eNOS), which is essential for vasodilation and vascular homeostasis [15]. eNOS phosphorylation at regulatory site (Ser1177) is required for its activity. Once activated, eNOS uses L-arginine as a substrate with nicotinamide adenine dinucleotide phosphate (NADPH) and tetrahydrobiopterin (BH_4) as cofactors to produce NO and L-citrulline. Generated NO then diffuses to adjacent smooth muscle cells and activates soluble guanylate cyclase, raising cGMP and causing vasorelaxation[15]. Endothelial NO is anti-thrombotic by inhibiting platelet adhesion and aggregation as well as anti-inflammatory by reducing chemokines and leukocyte adhesion molecules [15]. Thus, NO signaling plays a crucial role in maintaining EC function and protecting against atherogenesis.

ECs continually generate reactive oxygen species (ROS), including superoxide (O_2^-), and hydrogen peroxide (H_2O_2) from sources like mitochondrial respiration and NADPH oxidase [16]. Under healthy conditions, ECs maintain a low basal ROS level by matching generation with powerful antioxidant systems [17]. When ROS production exceeds antioxidant capacity, ECs experience oxidative stress. Common antioxidant defenses in ECs are reduced glutathione

(GSH), superoxide dismutase (SOD), and catalase. GSH is essential in maintaining redox hemostasis. Glutathione peroxidase (GPx) uses GSH to convert H_2O_2 into water and GSSG. Then, glutathione reductase regenerates GSH using NADPH [18]. SOD converts O_2^- to H_2O_2, leaving it for catalase and GSH to convert to water and harmless byproducts. Another important class of EC antioxidant defense is the transcription factor Nrf2-dependent signaling. A major Nrf2 target is heme oxygenase-1 (HO-1). When there is oxidative stress, Nrf2 gets phosphorylated and translocated into the nucleus, where it interacts with antioxidant response elements (AREs). The AREs promote HO-1 transcription. HO-1 then degrades the pro-oxidant molecule heme and produces the antioxidant molecule biliverdin along with carbon monoxide and iron [19]. Together, in healthy vasculature these antioxidant systems ensure cellular redox homeostasis.

1.2.2 Endothelial cell dysfunction in hyperglycemia

Endothelial dysfunction is a critical early step in the development of atherosclerotic plaques[20,21]. Endothelial dysfunction is marked by reduced endothelium-dependent vasodilation (reduced NO) and an excessive production of pro-oxidants (oxidative stress) and pro-inflammatory (inflammation) signals[21,22]. EC dysfunction initiates plaque formation through increased permeability, which allows circulating lipoproteins to pass through the ECs and into the vascular wall. These lipoproteins accumulate and become oxidized, which triggers an inflammatory response. Monocytes adhere to the EC surface due to increased EC adhesion molecule expression, and these adhered monocytes then transmigrate into the arterial wall where they differentiate into macrophages, take up modified lipids, and finally become lipid-laden foam cells. Gradually, accumulation of these foam cells forms atherosclerotic plaques. Over time, persistent

inflammation, oxidative stress, reduced vasodilation and endothelial activation lead to plaque rupture resulting in acute cardiovascular events such as myocardial infarction or stroke [23].

Long-lasting high glucose or even glucose fluctuations in people with diabetes leads to endothelial oxidative stress, inflammation, and reduced NO and vasodilation, making hyperglycemia a major initiator of endothelial dysfunction in diabetes[13,24,25]. Many studies have shown that high glucose increases endothelial oxidative stress *in vitro* and *in vivo*. Kemeny *et al.* measured 50.6% increase in ROS in primary porcine aortic endothelial cells (PAECs) after two days exposure to 30 mM glucose [26]. Incubation of human aortic endothelial cells with 25 mM glucose for 24 hours doubled NADPH oxidase (NOX) expression, which was accompanied by increased oxidative stress. Inhibition of NOX1 using the chemical inhibitor GKT137831 and siRNA reduced oxidative stress by 30% and 77% in normal and high glucose, respectively[27]. *In vivo*, oxidative stress increased by around 80% in the rat aortic endothelium after 48 hours of infusion with continuous 50% glucose in saline to keep the blood glucose at 20 mM[28].

High glucose promotes a pro-inflammatory endothelial state. Hyperglycemia activates the nuclear factor kappa-B (NF-κB) signaling pathway, causing endothelial cells to produce cytokines and chemokines[29]. In HUVECs, 24 hour incubation with 25 mM glucose significantly increased p65 in the nuclear fraction and reduced it in cytosolic fraction, indicating NF-κB activation. In addition, this high glucose condition significantly increased both mRNA and secreted protein concentrations of the inflammatory molecules ICAM-1, VCAM-1, E-selectin, and IL-1β [30]. *In vivo*, rats infused with 50% glucose for 48 hours exhibited elevated plasma concentrations of IL-6, TNF-α, and ICAM-1, along with increased endothelial mRNA expression of these inflammatory mediators[28].

Hyperglycemia decreases vasodilation by increasing NO scavenging and decreasing its production. In clinical studies, flow mediated dilation (FMD) is used to measure endothelium dependent vasodilation, and reduced NO dependent vasodilation is an indicator of increased cardiovascular risk [31]. In a clinical study, fasting brachial artery flow mediated vasodilation was assessed in 33 control subjects and 43 patients with newly diagnosed T2D. Flow mediated vasodilation was significantly reduced in the T2D group, indicating impaired endothelium-dependent vasodilation[32]. Hyperglycemia and glycemic fluctuations elevate oxidative stress which directly interacts with NO to form peroxynitrite (NOO^-), a potent oxidant[25]. This reaction both reduces NO bioavailability and increases oxidative stress by generating NOO^- to cause a double hit on EC function. Aljofan *et.al* measured 50% decreased NO in mouse microvascular endothelial cells incubated with 40 mM glucose for 3 days [33]. *In vivo*, in streptozocin-induced diabetic rats, acetylcholine induced endothelium dependent relaxation was significantly impaired[34]. Additionally, hyperglycemia-induced oxidative stress promotes oxidation of BH_4, forming dihydrobiopterin (BH_2), which destabilizes the eNOS homodimer resulting in eNOS uncoupling. In uncoupled eNOS, electrons flow from NADPH to oxygen, forming superoxide, instead of NO. This further increases oxidative stress[35]. Together, these mechanisms sharply reduce endothelial NO bioavailability and vasodilation.

1.3 Red blood cells in health and disease

1.3.1 Healthy red blood cell function

Red blood cells (RBCs) are the most abundant cells in circulation. RBCs are traditionally recognized for oxygen and carbon dioxide delivery between the lungs and peripheral tissues, a function enabled by their high hemoglobin (Hb) content[36]. Beyond gas transport, RBCs have

specialized structural and vascular roles among which mechanical flexibility and low adhesion are important for vascular function. RBCs deform readily under shear stress so they can squeeze through capillaries even narrower than their resting diameter[37]. RBC deformability is vital for circulatory flow. In healthy conditions, although RBCs interact with endothelial cells, they do not adhere to endothelial cells or to each other. Their surfaces are coated with negatively charged sialic acids on glycoproteins and glycolipids, and removal of these sialic acids increases RBC adhesion[38]. Together, these factors ensure RBCs flow smoothly without sticking to endothelium.

RBCs have also recently been investigated for their ability to regulate vascular function due to their potential interactions with ECs[36,39,40]. Indeed, RBCs are now shown to exert an 'erythrocrine' function by acting as an endocrine organ, releasing signaling molecules like ATP and NO, which can regulate vascular tone and blood flow[41]. RBCs primarily release ATP in response to mechanical deformation or hypoxia. In a study on young individuals (25±3 years, n=12), RBC ATP release increased in hypoxia compared to normoxia[42] . ATP released from RBCs can act on endothelial purinergic P2 receptors to cause endothelium-dependent vasodilation. In a clinical study, vasodilation was measured using forearm blood flow (FBF) and vascular conductance. In young adults (n=10), hypoxia increased plasma ATP, forearm blood flow, and vascular conductance versus normoxia. In older adults (n=8), hypoxia failed to increase venous ATP, and local vasodilation, measured as forearm blood flow and vascular conductance, was essentially absent, indicating an age related impairment in RBC ATP release[43] .

Recent studies in our lab and others have identified endothelial nitric oxide synthase (eNOS) within RBCs. RBC eNOS generates NO, and this RBC-derived NO may have a functional role in blood flow regulation in hypoxia[44–46]. Early work by Ulker *et al.* showed that shear stress activates eNOS within RBCs, and perfusion of sheared RBCs induced vasodilation of

endothelium-denuded resistance arteries specifically under hypoxic conditions[44]. Our group demonstrated that RBC eNOS activation is mechanosensitive and mediated by the ion channel Piezo1. Piezo1 stimulation with agonist yoda1 increased intracellular Ca^{2+} and phosphorylated eNOS at its activating Ser^{1177} site via a protein kinase C (PKC)–dependent pathway. This signaling mechanism is distinct from the canonical Akt-dependent eNOS activation pathway in endothelial cells [47]. Leo et al. provided *in vivo* evidence that RBC eNOS plays a physiologically relevant role in vascular regulation. In mice, deletion of RBC specific eNOS resulted in hypertension and reduced circulating nitrite/nitrate, indicative of reduced NO [45]. Despite these studies, the capacity of RBCs to produce and export NO remains a subject of debate. RBC hemoglobin scavenges available NO to form methemoglobin and nitrite, diminishing NO availability for the vasculature. Notably, if NO is bound to hemoglobin's heme in a more stable form like S-nitrosothiol, it may be able to escape from scavenging and contribute to vasodilation[48–50]. Hence, whether the RBC-derived NO can successfully escape the RBC cytosol to act on the vasculature is uncertain.

1.3.2 Dysfunctional red blood cells in hyperglycemia

Prolonged hyperglycemia in people with diabetes significantly affects RBC function. High glucose interacts with Hb in RBCs to form glycated hemoglobin (HbA1c). This altered form of Hb exhibits an increased affinity for oxygen, subsequently reducing oxygen delivery to tissues. Consequently, diabetic RBCs deliver oxygen less effectively, and higher HbA1c levels correlate with tissue hypoxia and microvascular complications like retinopathy[36]. Hyperglycemia also increases RBC adhesion to the vascular wall[51]. Glycation of band3 protein on RBC membranes promotes their binding to the AGE receptors on ECs. This mechanism increases RBC sticking to the endothelium in diabetes, leading to flow disturbance especially in the microvasculature[52].

Normally, RBCs release ATP in response to external stimuli like shear stress or hypoxia to aid in endothelial cell NO production. Mahdi *et al.* incubated healthy and T2D RBCs with rat aortic rings for 18 hours and then measured endothelial dependent relaxation by wire myography using increasing doses of acetylcholine. They observed a significant reduction in endothelial-dependent relaxation in vessels incubated with T2D RBCs. They showed that T2D RBCs exhibit reduced ATP release, limiting ATP-mediated activation of endothelial purinergic receptors and subsequent NO production, consequently impairing endothelial dependent vasodilation and vascular tone[53].

Oxidative stress is a contributing factor to diabetic RBC dysfunction [40]. RBC-derived ROS can exacerbate endothelial oxidative stress along with scavenging vascular NO. Zhuge *et al.* co-incubated RBCs from global eNOS knockout (KO) and wildtype (WT) mice with healthy aortic rings and measured a significant increase in superoxide in aortic rings incubated with eNOS KO compared to WT RBC. Inhibition of NOX4 using a chemical inhibitor during the co-incubation, but not after RBC removal, reduced the ROS signal in the aortic rings. Additionally ROS scavenging with TEMPOL during indirect contact of RBCs and aortic rings using 0.4 μm pore Transwell inserts reduced ROS in the aortic rings in indirect contact with WT compared to eNOS KO RBC. Because TEMPOL selectively rescued vessels exposed to eNOS KO RBC, and separation of RBCs from the vessel wall completely prevented oxidative stress, the authors concluded that RBC oxidative stress increased endothelial oxidative stress when RBCs were in close proximity [54].

Multiple studies confirm that arginase 1 (Arg1) is present in RBCs. Arg1 hydrolyzes L-arginine to ornithine and urea, which limits arginine availability for eNOS[55] . Arg1 is significantly elevated in RBCs under diabetic conditions. Zhou *et al.* showed that RBCs from people with T2D had significantly elevated Arg1 protein and activity. Jiang *et al.* also reported ~1.55 fold higher

arginase activity in RBC from T2D patients vs age matched healthy subjects [56,57]. The increased RBC Arg1 content and activity hydrolyzes more L-arginine in the RBCs, causing eNOS uncoupling and ROS generation. There is strong evidence that oxidative stress mediates the diabetes-induced increase in RBC Arg1. When T2D RBCs were co-incubated for 24 hours with N-acetylcysteine (NAC), which can directly scavenge ROS, the rise in RBC Arg1 activity and expression was prevented[56].

Thus, RBCs become dysfunctional in diabetes, as indicated by increased HbA1C, increased endothelium adhesion, reduced ATP, increased ROS, and decreased NO. These dysfunctional RBC may contribute to vascular complications in diabetes. Targeting specific pathways in RBCs, like antioxidant defense pathways, may serve as a strategy to overcome diabetic cardiovascular complications.

1.4 Interaction between red blood cells and endothelial cells via extracellular vesicles

RBCs secrete extracellular vehicles (EVs) under both pathological and physiological conditions[46,58]. RBC-EVs are small lipid-membrane-bound particles (40 – 1000 nm) loaded with active signaling biomolecules including proteins, miRNAs, lipids, and metabolites. Once released, RBC-EVs can be taken up by other recipient cells, enabling them to serve as messengers in intercellular communication [59]. RBC-EVs have been associated with and studied in various vascular diseases such as pulmonary hypertension, obstructive sleep apnea, and acute coronary artery syndrome[60,61]. Researchers examining RBC-EVs reported that these vesicles display externalized phosphatidylserine and carry Hb, making them highly pro-coagulant. For instance, Sweeney *et al.* confirmed the presence of phosphatidylserine on RBC-EVs isolated from stored RBCs via flow cytometry. They showed RBC-EVs facilitate thrombin formation in human plasma under thromboelastographic conditions [62,63]. In another study, An *et al.* exposed human pulmonary

microvascular endothelial cells to sickle cell RBC-EVs for 2 hours using a microfluidic flow assay. They then perfused sickle RBCs through the microfluidic channel and observed increase sickle RBC adhesion to endothelium, which can mediate vascular injury[64] . RBC-EVs can also cause EC dysfunction by scavenging NO, which occurs even faster than with RBCs due to the small size and higher membrane permeability of RBC-EVs [65]. RBC-EVs also may promote excess ROS production in vascular cells by carrying pro-oxidants like hemoglobin, phosphatidylserine, iron, and NOX. RBC-EVs can transfer these to other circulating cells. For example, RBC-EV heme and oxidized hemoglobin activated TLR4-dependent signaling in neutrophils and monocytes, leading to NF-κB activation and NOX upregulation. This then led to a respiratory burst, defined as a rapid induction of oxidative stress, which triggered inflammatory signaling and pro-inflammatory gene expression[58,66]. RBC-EVs also deliver Arg 1 to the endothelium and cause eNOS uncoupling, which not only reduces NO production but also increases oxidative stress[67]. Such observations suggest that RBC-EVs can actively transfer bioactive molecules to the recipient cells and impact their function.

Chronic hyperglycemia can impact RBC biology by altering protein glycation, metabolic pathways, and oxidative stress, which in turn impacts RBC-EV contents and characteristics. Freeman *et al*. examined serum EV concentration from 38 individuals (16 healthy and 22 T2D), and they found 50% higher EV concentration (from ~1.0×10^{12} to 1.5×10^{12}), particularly CD235a-positive EVs from RBCs, in the serum of T2D patients[68] . *In vitro*, Sukati *et al.* found that RBCs incubated with hyperglycemic media (45 mM and 100 mM) for 24 hours at 37°C increased RBC-EV release two to three times compared to RBCs incubated with 5 mM glucose. This was connected to increased oxidative stress in RBCs exposed to high glucose, as the addition of N-acetylcysteine (NAC) reduced EV formation [69].

In addition to the quantity of EVs, RBC-EV composition may change with diabetes. Recent studies have shown that diabetic EVs have higher Arg1[67]. Additionally, in diabetes, glycation of RBC-EV surface proteins may enhance EV internalization by ECs. A recent study by Collado *et al.* revealed that RBC-EVs derived from T2D patients were taken up by EC and internalized more avidly than RBC-EVs from healthy patients. They demonstrated that due to the transfer of Arg1, RBC-EVs from T2D patients impaired endothelium-dependent vasodilation by depleting L-arginine and increasing oxidative stress[67]. Inhibition of Arg1 or ROS scavenging protected the ECs from T2D RBC-EV induced dysfunction. So in diabetes, EVs may have changes in their content and protein post-translational modifications that enhance their pathogenic potential.

In summary, RBCs become dysfunctional in diabetes. These dysfunctional RBCs shed more EVs with different content that impacts recipient vascular cells such as EC. However, our understanding of how hyperglycemia alters RBC-EV production, EV internalization, and EC impact remains limited. Understanding the mechanisms behind hyperglycemia-induced changes in RBC-EVs could potentially enable RBC manipulation to generate EVs that are beneficial to the vasculature in diabetes.

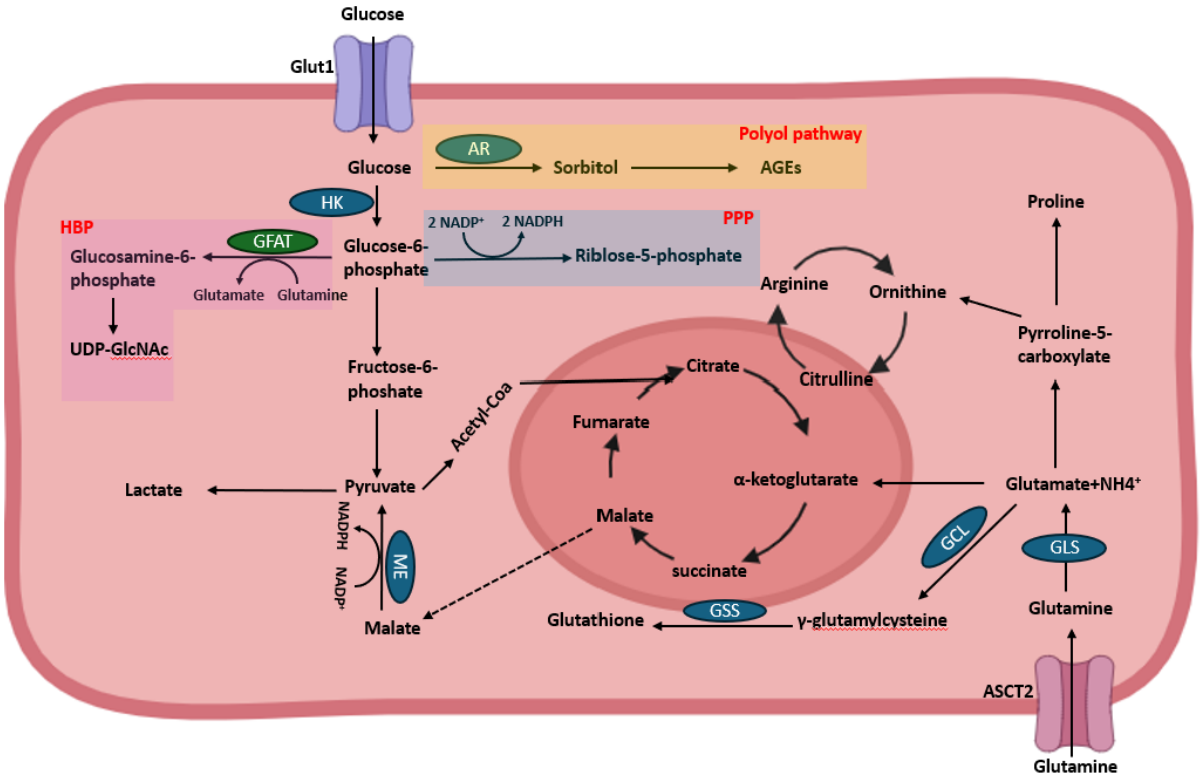

Figure 1-1: Overview of endothelial cell glucose and glutamine metabolism. *Glucose and glutamine supply interconnected pathways regulating energy production, redox homeostasis, and amino acid metabolism, including glycolysis, the polyol, pentose phosphate and hexosamine biosynthesis pathways, TCA cycle, glutathione synthesis, and arginine–citrulline cycling.*

1.5 Endothelial cell metabolism in health and hyperglycemia

1.5.1 Endothelial glucose metabolism

Healthy ECs rely mainly on glycolysis for their energy production, converting the majority of glucose taken up by glucose transporters (GLUT1) into lactate rather than oxidizing it in the form of pyruvate in mitochondria (Figure 1-1)[70,71]. For example, in cultured quiescent aortic ECs, almost 99% of glucose was converted to lactate[72] . Only a small fraction is delivered into glycolytic side branches, including the polyol pathway, pentose phosphate pathway (PPP), and hexosamine biosynthesis pathway (HBP). In a study by Moiz *et al.* using stable isotope assisted metabolic flux

analysis in untreated HUVECs, their model showed that only 11% percent of glucose flux was incorporated into the PPP [73].

Despite their overall dependence on glucose metabolism, in specific situations ECs also metabolize fatty acids and glutamine. Fatty acids are taken up by transporters like FATP3 or CD36 and then transported to the mitochondria by carnitine palmitoyltransferase 1A, where they undergo β-oxidation and are cleaved into acyl-CoAs. These acyl-CoAs then enter the TCA cycle to generate dNTPs for biomass formation [74]. Glutamine metabolism, a primary focus of this thesis, is discussed in detail in the next section. Thus, in EC glucose metabolism provides rapid ATP via glycolysis while fatty acids and glutamine are essential for TCA cycle, macromolecule synthesis and redox balance [71,74].

1.5.2 Endothelial glutamine metabolism

Glutamine, the most abundant amino acid in the body, becomes conditionally essential during stress or injury as it is important for many cellular metabolic and signaling pathways. Specifically, glutamine serves as a precursor for non-essential amino acids (e.g., glutamate, arginine, asparagine) and nucleotide and protein synthesis. Glutamine also supports redox balance by serving as a precursor to antioxidants (Figure 1-1)[75].

Glutamine is taken into the cell via the alanine-serine-cysteine transporter 2 (ASCT2)[76]. It is then deaminated to glutamate and NH_4^+ by the enzyme glutaminase (GLS). Glutamate can then enter the TCA cycle after converting to α-ketoglutarate (α-KG). Most of the α-KG provides carbons for oxidative phosphorylation, while a portion of α-KG can undergo reductive carboxylation (reverse TCA cycle) to citrate for lipid and biomass synthesis[77].

Glutamine entry into the TCA cycle is crucial for EC proliferation and angiogenic growth, as demonstrated by genetic, pharmacological, and metabolic flux approaches [77,78]. By incubating human umbilical vein endothelial cells (HUVECs) with 2 mM ^{13}C-glutamine for 24 hours, Kim *et al.* showed that glutamine supplies ~70% of TCA cycle carbons. Genetic knockdown or pharmacological inhibition of GLS1 depleted TCA intermediates, leading to suppression of EC proliferation and increased apoptosis while migration remained intact. Importantly, supplementation with cell permeable α-KG restored TCA intermediates and fully rescued EC proliferation and survival, directly demonstrating that glutamine supports proliferation primarily through maintenance of TCA cycle flux and biosynthetic capacity. They also extended these findings *in vivo* and showed that endothelial-specific GLS1 deletion impaired retinal angiogenesis by reducing EC proliferation and vessel sprouting[77].

In parallel, Huang *et al*. showed that glutamine deprivation or GLS1 inhibition impaired EC sprouting both *in vitro* and *in vivo* but revealed an additional, nitrogen-dependent mechanism underlying the proliferative defect. While glutamine withdrawal did not induce an energetic crisis, it disrupted TCA anaplerosis, reduced non-essential amino acid pools, impaired nucleotide and protein synthesis, and activated endoplasmic reticulum stress pathways. Notably, replenishing TCA intermediates alone was insufficient to restore proliferation; full rescue required combined supplementation with α-KG and asparagine, identifying glutamine-derived nitrogen flux through asparagine synthetase as a critical parallel pathway supporting biomass synthesis and mTOR signaling during angiogenesis[78]. Together, these studies established that glutamine metabolism fuels endothelial proliferation and angiogenesis through TCA cycle metabolism to support biosynthesis and maintaining nitrogen balance for amino acid and macromolecule production.

Beyond fueling growth, glutamine-derived glutamate in combination with glycine and cysteine forms glutathione (GSH) in a two-step enzymatic reaction, making glutamate rate limiting for GSH formation [79]. In the first step, glutamate–cysteine ligase (GCL) catalyzes the formation of γ-glutamylcysteine from glutamate and cysteine[80]. In the second step, glutathione synthetase (GSS) catalyzes the ATP-dependent addition of glycine to γ-glutamylcysteine to form GSH [81]. Glutamine also contributes to the formation of NADPH, an important cofactor to keep GSH reduced and in its active form. Glutamine is metabolized to malate in the TCA cycle, after which it enters the cytosol where it is metabolized by malic enzyme (ME) to produce NADPH and pyruvate (Figure 1-1) [75,82,83] . Hence, glutamine is important for maintaining EC redox balance. Additionally, glutamine activates other EC antioxidant responses like heme oxygenase (HO-1), an enzyme with cytoprotective and anti-inflammatory functions. Glutamine deamination by GLS produces ammonia (NH_3), which activates the Nrf2 pathway in ECs to induce HO-1 expression. Consequently, HO-1 produces carbon monoxide and bilirubin to overcome oxidative stress [84]. Consistent with this, Peyton *et al.* cultured human ECs from different sources (umbilical vein, aorta, microvascular) in glutamine depleted conditions or with GLS inhibition for 24 hours. Oxidative stress increased by nearly 3 fold and HO-1 decreased by about 60% relative to cells incubated with glutamine [85].

Additionally, glutamine serves as a precursor to other amino acids. For example, the amide nitrogen of glutamine is used by asparagine synthetase (ASNS) together with aspartate to make asparagine[86]. Glutamate is cyclized via pyrroline-5-carboxylate synthase to pyrroline-5-carboxylate which then can be reduced to proline by pyrroline-5-carboxylate reductase (PYCR1) or to ornithine by ornithine aminotransferase (OAT). This process links glutamine metabolism to

ornithine cycle in which L-arginine, which is essential for NO production, can be regenerated from L-citrulline (Figure 1-1)[87,88].

Glucose and glutamine metabolism are highly interconnected. Specifically, glutamine enters the TCA cycle, intersecting with glucose-derived pyruvate that also fuels TCA cycle activity.Glutamine metabolism intersects with the HBP as well. The amide nitrogen of glutamine is used by the enzyme GFAT to convert glucose-derived fructose-6-phosphate into glucosamine-6-phosphate and eventually UDP-GlcNAc, which causes protein O-GlcNAcylation [86,87]. O-GlcNAcylation is dynamically regulated by two enzymes: O-GlcNAc transferase (OGT), which adds GlcNAc to serine/threonine residues, and O-GlcNAcase (OGA), which removes it[89]. O-GlcNAcylation has both protective and toxic effects on vascular function. Multiple studies *in vitro* have shown that glutamine increases eNOS O-GlcNAcylation, leading to decreased eNOS activity and reduced NO[90,91] . For example, Wu *et al.* cultured bovine venular ECs with 0.2 to 2 mM L-glutamine for 24 hours. They measured a ~ 38% decrease in NO production and a ~10 fold increase in UDP-GlcNAc at 2 mM glutamine compared to 0.2 mM glutamine. Indeed, GFAT inhibition using the chemical inhibitor azaserine prevented glutamine's inhibitory effect on NO[90] . On the other hand, *in vivo* studies have shown that glutamine increases endothelium-dependent vasodilation. Addabbo *et al*. induced EC dysfunction by feeding 0.5 mg/mL L-NMMA (NOS inhibitor) to mice who were cotreated with 0, 0.5, or 1% L-glutamine in drinking water for 2 months. L-NMMA impaired vasodilation by 60% in aortic rings, but 1%glutamine restored vasodilation so that it was comparable to untreated aortic rings [92]. Additionally, a recent *in vivo* study in rats showed that glutamine perfusion before and after myocardial ischemia improved cardiac function, linking this beneficial impact to a significant increase in O-GlcNAc [93]. Therefore, there are conflicting data on whether glutamine improves or reduces vasodilation via increasing

O-GlcNAc. In order to better understand glutamine's role in endothelial function, more detailed mechanistic research is required. Indeed, under hyperglycemic conditions, glutamine may have beneficial effects on ECs, like reducing oxidative damage and inflammation; however, the precise mechanisms are not well defined.

1.5.3 Altered endothelial metabolism in hyperglycemia

In hyperglycemia, the endothelial metabolic balance is perturbed. As glucose concentration increases, cytosolic glycolysis increases, which produces NADH and pyruvate. Pyruvate can enter the TCA cycle where it produces additional NADH and $FADH_2$. Increased flux of these electron donors to the mitochondrial electron transport chain (ETC) increases proton pumping across the inner mitochondrial membrane, generating high mitochondrial membrane potential ($\Delta\Psi$). Under conditions in which electron input is higher than cellular ATP demand, proton re-entry through ATP synthase (Complex V) becomes limiting, leading to abnormally high $\Delta\Psi$. At complex I and III, elevated mitochondrial membrane potential prolongs the reduced state of flavin and ubiquinone intermediates, enabling the one-electron reduction of molecular oxygen to form superoxide. (Figure1-1)[94]. The increased oxidative stress depletes NAD^+, a required cofactor for functionality of the glycolytic regulatory enzyme glyceraldehyde-3-phosphate dehydrogenase (GAPDH). GAPDH activity in bovine aortic endothelial cells incubated in 30 mM glucose was reduced by 66%, which caused upstream glycolytic metabolites to accumulate [95]. The excess metabolites increased flux down glycolytic side branch pathways such as the polyol pathway[96] and the hexosamine biosynthetic pathway (HBP)[97] while decreasing flux in the pentose phosphate pathway (PPP)[98].

In the polyol pathway, excess intracellular glucose is diverted away from glycolysis and instead reduced to sorbitol by the enzyme aldose reductase. This reaction consumes NADPH and generates $NADP^+$. NADPH consumption by aldose reductase diminishes its availability to regenerate GSH from GSSG, depleting antioxidant capacity in hypergycemia[96,99]. In addition, advanced glycation end product (AGE) formation is increased as fructose generated by the polyol pathway can get phosphorylated to fructose-3-phosphate (F3P) which is then broken down to 3-deoxyglucosone, producing glycation agents. AGEs accumulate on long-lived extracellular matrix and plasma proteins, increasing vessel stiffness and basement membrane thickness [100]. Additionally, in the polyol pathway sorbitol dehydrogenase produces NADH which may feed NADH oxidase and produce ROS[101]. Therefore, polyol pathway activation in hyperglycemia increases AGEs and disturbs redox homeostasis by decreasing NADPH and increasing NADH.

Under chronic hyperglycemia, more fructose-6-phosphate is diverted into the HBP where it is converted to glucosamine-6-phosphate by glutamine:fructose-6-phosphate amidotransferase (GFAT). Glucosamine-6-phosphate then generates UDP-N-acetylglucosamine (UDP-GlcNAc), which is involved in protein post-translational modifications (O-GlcNAcylation). O-GlcNac can modify more than 1500 different intracellular proteins, regulating functions that are required for regulation of transcription, metabolism, stress signaling, protein hemostasis, and cell survival [93]. When eNOS is O-GlcNAcylated, it cannot be activated by phosphorylation at ser1177, and therefore NO production is reduced [97,102]. Bovine aortic endothelial cells lost about 65% of eNOS activity in hyperglycemia via increased eNOS-GlcNAcylation[103]. Thus, the metabolic reprogramming towards the HBP induced by hyperglycemia results in reduced NO synthesis, ultimately contributing to EC dysfunction.

Normally, NADPH is replenished by the PPP[98]; however, glucose flux in the PPP is reduced in hyperglycemia by lowered glucose-6-phosphate dehydrogenase (G6P) activity[98]. In bovine aortic endothelial cells, high glucose (10-25 mM) increased intracellular cAMP stimulated by adenylate cyclase activity. This increase in cAMP activated cAMP-dependent protein kinase A (PKA), which then induced phosphorylation of G6PD, decreasing its activity[104]. This reduction in G6PD activity and PPP flux is critical in diabetic pathology because it decreases NADPH and reduces defense against oxidative stress and cell death.

Therefore, hyperglycemia alters endothelial metabolism to increase oxidative stress and alter flux down glycolytic side branch pathways, which contributes to endothelial dysfunction. This pathophysiological sequence links diabetes to CVD, emphasizing the need for a deeper understanding of endothelial dysfunction induced by hyperglycemia to prevent diabetic cardiovascular complications.

1.6 Red blood cell metabolism in health and hyperglycemia

1.6.1 Red blood cell glucose metabolism

Healthy RBCs primarily rely on glucose for ATP production, as they don't have mitochondria[105]. In RBCs, up to 90% of glucose is metabolized through glycolysis, and about 10% shuttles into the PPP [105]. Although only ~10% of glucose goes through the PPP, this pathway is critical to RBC function (Figure 1-2). Without NADPH generated in the PPP, RBC cannot regenerate reduced glutathione, and oxidative stress will stiffen and damage the cell.

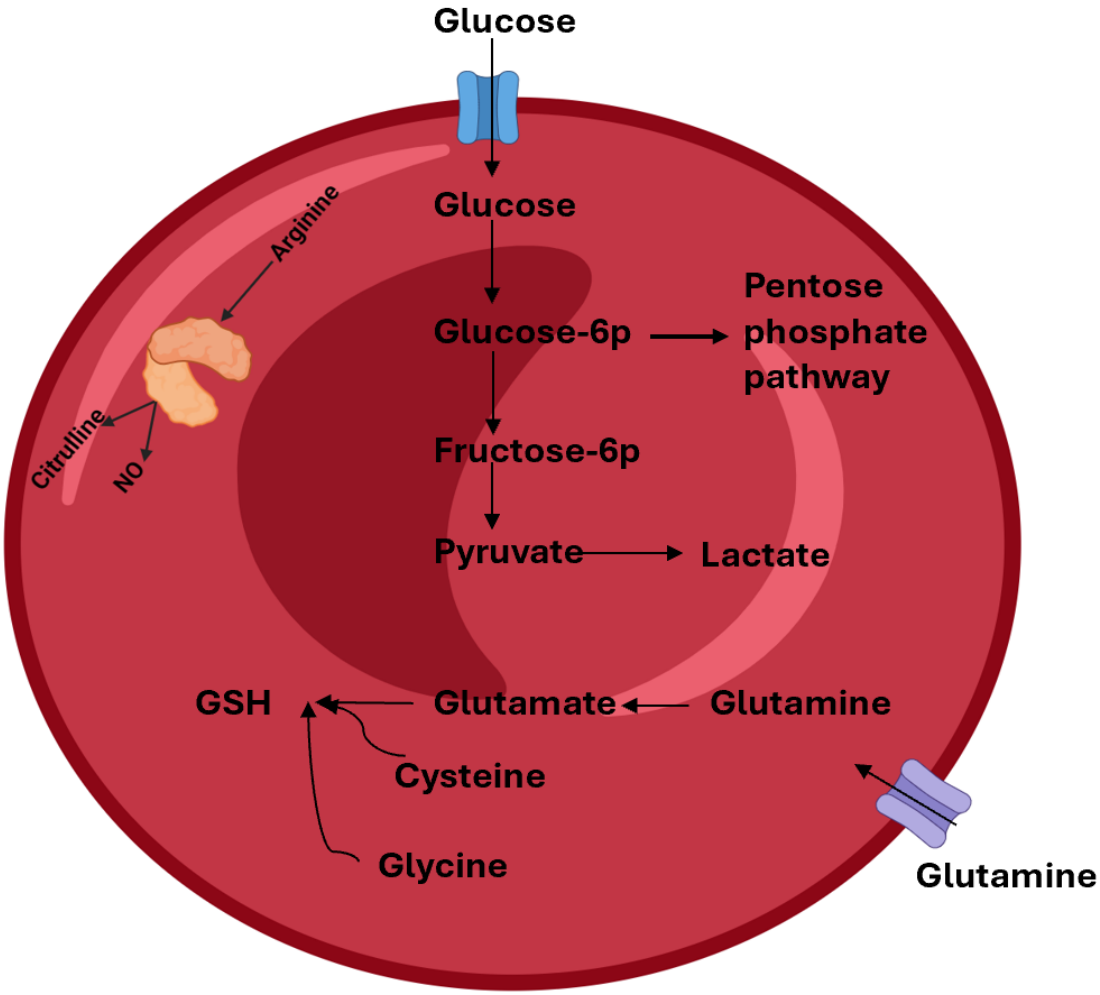

Figure 1-2 Schematic of glucose and glutamine metabolism in red blood cells. Glucose and glutamine are taken up by RBCs via appropriate transporter and metabolized to produce ATP and antioxidant GSH, respectively. RBCs contain functional eNOS that can generate NO and help vascular tone.

1.6.2 Red blood cell glutamine metabolism

While RBCs lack mitochondria, they do contain mitochondrial enzymes to enable glutamine metabolism. The RBC membrane is impermeable to glutamate[106], the building block for GSH, so RBCs need to take up glutamine for oxidative defense in a hemoglobin-rich environment (Figure 1-2)[107]. In sickle cell disease, RBCs depleted of glutamine had perturbed glutathione

metabolism and higher oxidative stress [108]. A phase 3 clinical trial found that glutamine oral supplementation improved RBC oxidative balance in sickle cell patients, making the RBC less prone to hemolysis and reducing pain crises and hospitalization [109]. Additionally, glutamine treatment in sickle cell disease decreased RBC adhesion to the endothelium, improved flow, and reduced hemolysis, suggesting less RBC damage [110] . Although glutamine is an FDA approved drug for sickle cell disease [109], another study showed that glutamine alone is less efficient in controlling oxidative stress compared to when glycine and cysteine, two other glutathione building blocks, are added as well [111] . RBCs under malaria-like conditions were treated with glutamine alone (1 mM) or glutamine mixed with glycine and cysteine (1 mM). Glutamine alone failed to reduce ROS in malaria conditioned RBCs, while the glutamine:glycine:cysteine mix reduced ROS in RBCs by ~20% and doubled GSH [111].

In RBCs, glutamine may also increase NO bioavailability, not only through decreased oxidative stress, but also through the citrulline-arginine pathway which produces the substrate for eNOS. Glutamine is a precursor to citrulline, which in the ornithine cycle regenerates L-arginine, the substrate for eNOS-catalyzed NO production [107]; however, whether glutamine supplementation directly increases NO production in RBCs has not yet been experimentally demonstrated and more research is needed to understand role of glutamine on RBC derived NO.

1.6.3 Altered red blood cell metabolism in hyperglycemia

Glucose uptake by RBCs increases proportional to blood glucose, and the excess glucose disturbs healthy RBC metabolism by changing fluxes into glycolytic side branches to increase ROS as described in ECs[36]. For example, Travis *et al.* incubated human RBCs for 2 hours in 5 or 50 mM glucose, and they reported increased sorbitol and fructose at 50 mM [112]. Cuinchi *et al.*

measured sorbitol and GSH inside the RBCs of healthy patients and people with diabetes. They reported ~67% higher sorbitol and ~34% lower GSH in T2D RBCs compared to healthy RBCs [113] . Both of these studies confirm polyol pathway upregulation in T2D RBCs, along with reduced oxidative defense capacity. Increased oxidative stress subsequently reduces NO availability by uncoupling eNOS and reacting with NO to form peroxynitrite [49,56,114,115]. RBCs also contain active NADPH oxidase (NOX), which transfers electrons from intracellular NADPH to molecular oxygen, generating superoxide. In a healthy environment, RBC oxidative balance is maintained by enzymes like superoxide dismutase (SOD) and catalase along with GSH; however, when the oxidative defense mechanism is compromised in diabetes, NOX may further contribute to increased ROS not only by increasing superoxide formation but by reducing NADPH required for GSH regeneration [116].

1.7 Glutamine supplementation in disease

Glutamine metabolism has been extensively investigated in diseases like cancer[117], sickle cell disease[118], and cardiovascular conditions[119]. In cancer, inhibiting glutamine metabolism reduced cancer cell viability[120]. In sickle cell disease, glutamine supplementation reduced RBC oxidative stress[118]. In diabetes, glutamine may be depleted because of chronic hyperglycemia. Yu *et al*. showed *in vivo* that both diabetic patients and diabetic mice have lower glutamine in their aqueous humor compared to healthy controls[121]. Circulating glutamine is reduced in the plasma of patients with type 2 diabetes relative to healthy individuals[99,122,123]. Alterations in glutamine levels in diabetes may reflect metabolic interactions between glucose and glutamine pathways. In a study by Zhoa *et al.*, human umbilical vein endothelial cells (HUVECs) were cultured in 25 mM glucose for 48 hours or cardiac microvascular endothelial cells were isolated from the hearts of diabetic mice. GLS1 protein and mRNA were downregulated in hyperglycemia and diabetes, leading to

reduced proliferation and angiogenic capacity[124]. Such glutamine depletion or metabolic disruption in diabetes can contribute to endothelial dysfunction, suggesting that maintaining sufficient glutamine levels can ameliorate vascular health. Various *in vivo*, *ex vivo,* and *in vitro* studies support that glutamine supplementation can reduce oxidative stress and vascular damage.

In vitro studies: In cultured human endothelial cells exposed to high glucose, glutamine has shown cytoprotective effects. In a study by Safi *et al*. using HUVECs in high glucose (20 mM) culture, addition of glutamine reduced cell death, increased IL-10, suppressed TNF-α, and maintained mitochondrial integrity, suggesting cytoprotective effects[125]. Similarly, in H9c2 cardiac cells exposed to high glucose plus hypoxia-reoxygenation, glutamine supplementation increased both cytosolic and mitochondrial GSH to GSSG ratio and lowered intracellular ROS, which was associated with less cytochrome c release, reduced caspase-3 activation, and a significant decrease in apoptosis[126]. This *in vitro* evidence suggests that glutamine can boost antioxidant defense capacity and cell survival under stress conditions like diabetes.

Animal models: *In vivo* studies further support glutamine's importance and protective vascular effects. In mice, GLS deletion in ECs prevented new blood vessel formation[127]. When streptozotocin-induced diabetic mice were supplemented with glutamine, the activity of key antioxidant enzymes like catalase, glutathione peroxidase (GPx), glutathione reductase and superoxide dismutase (SOD) increased. The GSH:GSSG ratio also increased, favoring more antioxidant capacity[123]. The impact of glutamine on vascular function was also studied using a mouse model of high-fat diet-induced obesity with hind limb ischemia. Replacing 25% of protein nitrogen with glutamine improved physiological response to ischemic injury through mechanisms like increased SOD activity, increased GSH, and lower pro-inflammatory cytokines like IL-6 and

TNF-α[128]. These animal model studies emphasize that glutamine availability and metabolism are essential in maintaining vascular function.

Clinical studies: Glutamine is approved by the United States Food and Drug Administration (FDA) to treat sickle cell disease [110] . Although not extensively investigated, early clinical research suggests that glutamine may confer cardiometabolic benefits in diabetic patients as well. Mansour *et al.* conducted a randomized trial in patients with type 2 diabetes, in which the treatment group received ~30 g of glutamine daily for 6 weeks. Glutamine supplementation significantly improved glycemic control and several cardiovascular risk factors. By the end of the trial, the glutamine group showed lower fasting blood glucose and HbA1c levels compared to placebo, as well as a reduction in systolic blood pressure [129]. These results suggest that short-term oral glutamine can improve metabolic profiles and body composition in diabetes[99]. The established treatment for sickle cell disease and preliminary clinical findings in diabetes are encouraging, suggesting that glutamine therapy, along with other diabetes medications, might help reduce oxidative stress and cardiovascular complications in this at-risk population.

Choosing glutamine over currently available cardioprotective drugs can be attractive for several reasons, including minimal side effects and toxicity, physiological compatibility, and broad tolerability [74,130]. Importantly, glutamine supplementation is not intended to replace established therapies such as semaglutide, which primarily target systemic glucose regulation and weight loss. Rather, glutamine may serve as a complementary approach that acts at the vascular level.

The gap in knowledge regarding glutamine's role in diabetic vascular health provides a strong motivation to research how glutamine supplementation might rescue the vascular system under pathological conditions like diabetes. By investigating the mechanism by which glutamine supports the endothelium and red blood cells, we can better determine the potential of targeting

and manipulating glutamine metabolism as a physiologically compatible strategy to prevent cardiovascular complications in diabetes.

1.8 Thesis Goal

The overall goal of this thesis is to understand how L-glutamine, the most abundant amino acid in the body, regulates endothelial cell and red blood cell metabolism and function in health and hyperglycemia. *I hypothesized that glutamine reduces hyperglycemic oxidative stress in both endothelial and red blood cells, and thereby reduces endothelial cell dysfunction.* In *Aim 1*, I showed that 0.5 (physiological) or 2 mM (supplemented) glutamine decreased endothelial cell oxidative stress in both normal (5.5 mM) and high (15 mM) glucose. Using a chemical inhibitor of glutaminase 1 (GLS 1), the rate-limiting enzyme in glutamine metabolism, I further demonstrated that glutamine regulates oxidative stress through the synthesis of the antioxidants glutathione and NADPH. I also showed that glutamine-treated isolated murine carotid arteries dilated more in response to acetylcholine, suggesting that glutamine-induced reductions in oxidative stress increase vasodilation. In *Aim 2*, I traced glutamine metabolism inside endothelial cells using heavy isotope-labeled glutamine and liquid chromatography - mass spectrometry to get detailed insight into how increasing media glutamine impacts its metabolism. I identified that glutamine metabolism in the forward direction of the TCA cycle increased as extracellular glutamine concentration increased, while no changes were observed in the reverse direction, referred to as reductive carboxylation. Interestingly, unlike other TCA metabolites, I observed reduced succinate with increasing media glutamine concentration, which may relate to elevated succinate dehydrogenase activity. I also identified that glutamine increased UDP-GlcNAc synthesis and ornithine cycle flux, while decreasing polyunsaturated fatty acids and one-carbon metabolites.. In *Aim 3*, I showed that glutamate and antioxidant capacity are reduced in red blood

cells (RBCs) of diabetic subjects. Unlike in endothelial cells, glutamine did not reduce oxidative stress and may even have further reduced RBC antioxidant capacity. Finally, I showed that RBC-EVs generated by stimulation of the mechanosensitive ion channel piezo1 were taken up by ECs but did not increase inflammation and may even have decreased oxidative stress.

1.9 Thesis Organization

This thesis is composed of five chapters.

Chapter 1 introduces the dissertation objectives and structure. It describes the clinical motivation for the study and reviews the relevant literature on endothelial and red blood cell metabolism in health and hyperglycemia, with focused discussion on glutamine metabolism and supplementation in physiological and pathological conditions.

Chapter 2 investigates the impact of altered glutamine concentrations on endothelial cell function under normal and hyperglycemic conditions. HCAECs were incubated with 0, 0.5, or 2 mM glutamine in 5.5 or 15 mM glucose. A fluorescence based reactive oxygen species (ROS) assay showed that glutamine decreases oxidative stress in both normal and hyperglycemic conditions, while a luminescence based assay showed that GSH and NADPH levels increase in both normal and hyperglycemic HCAECs. Using a chemical inhibitor of GLS1, I demonstrated that glutamine increases GSH and NADPH through GLS1 activity leading to decreased oxidative stress. Finally, *ex vivo* mice aortas were incubated in 0 or 2 mM glutamine, and using a pressure myograph, I showed that vasodilation increased in the presence of 2 mM glutamine compared to no glutamine.

Chapter 3 investigates systemic glutamine metabolism in endothelial cells. Endothelial cells were incubated in 0–10 mM glutamine for 24 hours. Using a YSI bioanalyzer, I showed that glutamine uptake increases with extracellular glutamine concentration, while glutamate secretion

plateaus at 2 mM glutamine. The impact of glutamine on mitochondrial activity was then assessed using a Seahorse Analyzer and isotope-assisted metabolomics via liquid chromatography-mass spectrometry. Glutamine increased flux through the forward TCA cycle but not the reverse TCA cycle. Isotope distribution analysis additionally showed increased amino acids and glutathione synthesis with increasing glutamine. Total metabolite abundance measured by LC-MS showed decreased succinate, unsaturated fatty acids, and one carbon metabolites, suggesting increased succinate dehydrogenase activity and enhanced one carbon metabolism.

Chapter 4 investigates the impact of diabetes and glutamine on red blood cell (RBC) oxidative stress. RBCs were obtained from diabetic and non-diabetic subjects. Using a YSI bioanalyzer, I showed that glutamate is significantly decreased in RBCs from diabetic subjects. Fluorescence based ROS measurements revealed no significant difference in baseline ROS between diabetic and non-diabetic subjects; however, antioxidant capacity was reduced in diabetic patients. Treatment of RBCs from both diabetic and non-diabetic subjects with glutamine showed no change in ROS and potentially a decrease in antioxidant capacity. Unlike endothelial cells, a luminescence based assay demonstrated no changes in RBC GSH with increasing glutamine.

Chapter 5 concludes the dissertation by highlighting the major discoveries, emphasizing my contributions to the field, and discussing future directions for this work.

Chapter 2: Impact of glutamine supplementation on EC function

This chapter is based on the published article:

Kheradmand M, Sangha G, Sissons CM, et al. Glutamine enhances endothelial cell survival and vasodilation by increasing glutathione to reduce oxidative stress. *Physiol Rep*. 2026;14(2):e70737. doi:10.14814/phy2.70737

2.1 Introduction:

Hyperglycemia, which is a characteristic of both type 1 and type 2 diabetes, plays a critical role in endothelial dysfunction, a key initiating step in CVD. Hyperglycemia induced metabolic alterations to glycolytic side branches and mitochondrial respiration lead to increased oxidative stress. Specifically, when more glucose-derived pyruvate is oxidized in the mitochondrial TCA cycle, more superoxide is produced which, in turn, can activate other superoxide production pathways [103,131]. Many aspects of endothelial cell dysfunction observed in hyperglycemic conditions and diabetes are linked to elevated oxidative stress.

Glutamine metabolism in ECs has the potential to ameliorate endothelial dysfunction induced by hyperglycemia. As described in detail in chapter 1, glutamine is first metabolized by glutaminase 1 (GLS1), which converts glutamine to glutamate and ammonia. Glutamate can then be converted to α-ketoglutarate and enter the TCA cycle, or glutamate can be converted to the antioxidant glutathione (GSH) [78,132–134]. Glutamine is required for endothelial cell proliferation, survival and oxidative hemostasis[78,132,133]. However, reported effects of glutamine on NO and vasodilation *in vitro* and *in vivo* are contradictory. *In vitro,* glutamine impairs recycling of L-arginine, a key substrate for nitric oxide production by endothelial nitric oxide synthase (eNOS). Glutamine also increases HBP flux, which can lead to eNOS O-GlcNAcylation and subsequent impaired activation through phosphorylation at serine 1177 [133,135–138]. *In vivo,* glutamine increases vasodilation in most animal and human studies. For example, glutamine supplementation partially

restored vasodilation in mice with induced endothelial dysfunction, and six months of glutamine supplementation enhanced flow-mediated vasodilation in older adults [92,139].

Several studies have shown the potential of glutamine as a therapeutic for diabetic CVD. Glutamine levels are reduced in the blood of people with diabetes [134,140]. Reduced GLS1 expression was found in skin wounds and cardiac endothelial cells from diabetic patients [134]. *In vitro,* glutamine reduced mitochondrial dysfunction in human umbilical vein endothelial cells cultured in high glucose, while supplementation with α-ketoglutarate and nonessential amino acids restored proliferation and tube formation in endothelial cells cultured in both high glucose and high fat [134,141]. *In vivo,* oral glutamine supplementation significantly improved CVD risk factors in patients with type 2 diabetes, including those linked to endothelial dysfunction such as systolic blood pressure [140].

Glutamine supplementation has therapeutic potential to ameliorate endothelial dysfunction caused by high glucose. However, the mechanisms by which glutamine impacts hyperglycemia-induced endothelial dysfunction are not well understood. I hypothesized that glutamine promotes endothelial cell survival and vasodilation by increasing the biosynthesis and recycling of the antioxidant glutathione to reduce hyperglycemia-induced oxidative stress. To investigate this hypothesis, I first measured proliferation, oxidative stress, and survival when primary human coronary artery endothelial cells were cultured in varied glutamine levels in normal and high glucose. I further measured vasodilation *ex vivo* in murine carotid arteries and nitric oxide production in endothelial cells *in vitro* in the presence or absence of glutamine. I then measured the antioxidant glutathione and the reducing agent NADPH in cells cultured in varied glutamine levels in normal and high glucose. Finally, I chemically inhibited GLS1 to determine if glutamine conversion to glutamate enhanced endothelial cell survival by regulating oxidative stress through

glutathione. These studies deepen our understanding of how glutamine metabolism impacts oxidative stress and nitric oxide in endothelial cells in high glucose, revealing new strategies to reduce CVD in diabetic patients.

2.2 Materials and methods

2.2.1 Cell culture:

Primary human coronary artery endothelial cells (HCAEC, passage 5-9) were purchased from Lifeline Cell Technology. HCAECs were cultured in Endothelial Growth Medium-2 (EGM-2; Lonza) supplemented with 1% penicillin-streptomycin (PS; ThermoFisher, 15140163), 10% fetal bovine serum (FBS; Cytiva, SH30088) and 10 mM glutamine (Fisher Scientific, 25-030-081) until 90% confluent. The growth medium was then removed, cells were rinsed with phosphate buffered saline (PBS, ThermoFisher, 70011069), and Dulbecco's Modified Eagle Medium (DMEM without phenol red, glucose, or glutamine, Gibco, A1443001) supplemented with EGM-2 Endothelial SingleQuots (Lonza, CC-4176), 5.5 or 15 mM D-glucose (Sigma-Aldrich, G8270), and 0, 0.5, or 2 mM glutamine was added for 24 hours. These glucose and glutamine concentrations were selected to model physiologically relevant and common experimental conditions. Specifically, 5.5 mM glucose represents normal plasma glucose, whereas 15 mM glucose represents hyperglycemia. 0 mM glutamine represents glutamine depletion, 0.5 mM glutamine represents physiological plasma glutamine, and 2 mM glutamine represents supplemented endothelial cell culture media [142–144]. Media with no glutamine and L-glucose (Sigma-Aldrich, G5500) at 2 or 11.5 mM was the osmotic control (OC) for glutamine in 5.5 mM glucose media and glucose and glutamine in 15 mM glucose media, respectively. Bis-2-(5-phenylacetamido-1,2,4-thiadiazol-2-yl)ethyl sulfide (BPTES, Sigma-Aldrich, SML0601, 10 μM) was used to inhibit

glutamine metabolism to glutamate. BPTES binds to an allosteric site on glutaminase 1 (GLS1) to keep it in an inactive confirmation, thereby inhibiting glutamine hydrolysis [145].

2.2.2 Cell viability:

Endothelial cell viability was assessed using ethidium homodimer (EthD-1, ThermoFisher, E1169), which enters permeabilized dead cells and fluoresces red after it binds to DNA. I used Hoechst to count the total number of cells (live and dead), since the live cell label Calcein AM fluoresced even in dead cells due to ROS [146]. To assess viability in response to stress, cells were cultured in varied glucose and glutamine media for 24 hours and then stressed with 50 μM tert-butyl hydroperoxide (tBHP; Sigma-Aldrich, 458139), an inducer of oxidative stress [147] for another 24 hours. After a PBS wash, 2 μM EthD-1 and Hoechst (ThermoFisher, 62249, 1:2000) were added in DMEM supplemented with 10% FBS and 1% PS for 30 minutes at room temperature. 50% methanol was added for 10 minutes to some wells as a positive control for cell death. After washing with PBS, cells were imaged using a Nikon Eclipse Ti2 spinning disk confocal microscope at 10× magnification. Nuclei (blue) and dead (red) cells were quantified using NIS software, and the percentage of dead cells was calculated as: $\frac{\boldsymbol{number\ of\ dead\ cells}}{\boldsymbol{total\ number\ of\ nuclei}} \times \mathbf{100}$.

2.2.3 Cell proliferation:

Cell proliferation was assessed by labeling for Ki67, a protein found in the nucleus of actively dividing cells, as well as cell counts. For Ki67 labeling, HCAECs were seeded at 75,000 cells per well on glass coverslips in 12-well plates and allowed to adhere overnight. Cells were serum-starved in EBM-2 with 1% PS for 24 hours, followed by treatment with varied glucose and glutamine media. Human fibroblast growth factor-2 (hFGF-2; Peprotech, 100-18B) at 1 ng/mL

served as a positive control. After 24 hours, cells were fixed in 4% paraformaldehyde (Millipore Sigma, P6148) for 15 minutes and then permeabilized and blocked in 0.2% Triton X-100 (Alfa Aesar, A16046) with 0.5% BSA (Sigma-Aldrich, A7906) in PBS for 40 minutes. A Ki67 primary antibody (Abcam, ab15580) was applied overnight at 4°C (1:200 in 0.2% Triton X-100 with 0.5% BSA in PBS). The next day, cells were incubated for 1 hour with donkey anti-rabbit IgG Alexa Fluor 488-conjugated secondary antibody (ThermoFisher, A-21206, 1:1000) and DAPI (ThermoFisher, 62248, 1:2000). Samples were rinsed with PBS and coverslips were mounted and imaged on a Revolve microscope (ECHO) at 20× magnification. Ki67 co-localization with nuclei was quantified using a custom Python script. The percentage of Ki67-positive cells was calculated as: $\frac{\boldsymbol{\#\ of\ ki67\ positive\ nuclei}}{\boldsymbol{total\ \#\ of\ nuclei}} \times 100$.

For cell counts, HCAECs were seeded at 50,000 cells per well in a 24-well plate in varied glucose and glutamine media. After two days, cells were detached using trypsin (ThermoFisher, 25300120) and counted using a Countess II FL (ThermoFisher). hFGF-2 (1 ng/mL) was included as a positive control.

2.2.4 Reactive oxygen species (ROS):

5-(and-6)-chloromethyl-2′,7′-dichlorodihydrofluorescein diacetate, acetyl ester (CM-H_2DCFDA, Invitrogen, C6827), which becomes fluorescent after oxidation by intracellular ROS, was used as a general ROS indicator. HCAEC cultured in varied levels of glucose and glutamine for 24 hours were treated with 2 μM CM-H_2DCFDA and Hoescht (1:2000, to visualize nuclei) in DMEM for 1 hour at 37°C. Cells treated with 0.5 mM tBHP in EGM-2 media for 1 hour were the positive control. Cells were then washed with PBS and imaged on a Nikon Eclipse Ti2 spinning disk confocal microscope with a 10x objective. After rolling ball background subtraction, mean fluorescence intensity was quantified in ImageJ and normalized to number of nuclei.

2.2.5 Glutathione:

Intracellular glutathione was measured using a GSH/GSSG Glo assay (Promega, V6612) and liquid chromatography-mass spectrometry (LC-MS). For the Glo assay, HCAEC were seeded in a white bottom 96-well polystyrene plate (Sigma-Aldrich, CLS3917) at 50,000 cells/well. The next day, cells were treated with varied glucose and glutamine media for 24 hours. On the day of the assay, cells were rinsed with Hanks' Balanced Salt solution (HBSS, Millipore Sigma, 55037C) and then lysed for 30 minutes at room temperature in the presence of luciferin NT substrate and glutathione S-transferase enzyme. Luciferin detection reagent was then added for 15 minutes, after which luminescence was measured using a Spark multimode plate reader. Glutathione concentration was determined using a standard curve.

For LC-MS, metabolites were extracted from confluent HCAECs treated with varied glucose and glutamine media for 24 hours using 80% HPLC grade methanol (Sigma-Aldrich, G6025-11VL) and 20% HPLC grade water (Midland Scientific, Wooo6-4L) at -80°C for 15 minutes. Cells were then scraped, transferred to 1.5 mL centrifuge tubes (Cell Treat, 229443), and centrifuged at 17,000 *xg* for 10 minutes. The supernatant was transferred to a new 1.5 mL tube, and the cell pellet was stored at -80°C for protein concentration measurement. The supernatant was dried using a CentriVap Vacuum Concentrator (Labconco), resuspended in 200 µL 5% methanol and 95% water, and transferred to mass spectrometry vials (Waters, 600000670). Quality control samples were prepared by adding 50 µL of each sample to a separate vial. Reduced L-Glutathione (GSH, Sigma-Aldrich, G4251) was used to establish a standard curve. 3 µL of each sample was analyzed in duplicate using a Shimadzu LCMS-8045 CL Triple Quad LC-MS/MS with an attached Nexera HPLC/UHPLC Pump (LC-20AD XR) and a Luna Omega Polar C18 reverse-phase column (2.1 × 50 mm, 1.6 µm; Phenomenex). Mobile phases consisted of HPLC

grade water with 1% formic acid (mobile phase A) and HPLC grade acetonitrile with 1% formic acid (mobile phase B). The flow rate was maintained at 0.45 mL/min. A gradient elution was applied as follows: 5% B for 0.6 min, linearly increased to 20% B at 1.80 min, ramped to 50% B at 1.81 min, and then linearly increased to 100% B from 3.00 to 5.00 min. The column was re-equilibrated with 5% B from 6.00 to 8.00 min. Mass spectrometry was performed in positive electrospray ionization mode (ESI+) with a capillary voltage of 4 kV. Nebulizing gas and drying gas flows were set to 3 L/min and 10 L/min, respectively. Desolvation and interface temperatures were set to 250°C and 300°C. GSH was quantified using multiple reaction monitoring (MRM) with a mass transition of m/z 307.9 → 179. Data were processed in Skyline Software for peak identification and ion count integration.

2.2.6 NADPH/NADP+ ratio:

The NADP/NADPH-Glo assay (Promega, G9082) was used to measure the NADPH/NADP+ ratio, which is one indication of intracellular reducing capacity. Briefly, confluent HCAECs in a white bottom 96-well polystyrene plate were treated with varied glucose and glutamine media. After 24 hours, the cells were lysed in 1% dodecyl trimethyl azanium bromide (Sigma, D-8638-25). 50 µL cell lysate was then transferred to an empty well and treated with 25 µl 0.4 N HCl to measure $NADP^+$, while the base only wells were used to measure NADPH. Each group was mixed with equal volume of NADP/NADPH-Glo detection reagents. After 30 minutes, luminescence was recorded using a Spark multimode plate reader, and the $NADPH/NADP^+$ ratio was calculated.

2.2.7 Pressure myography:

The animal protocol was approved by the University of Maryland Institutional Animal Care and Use Committee (IRBNet ID: 1932985-6). Twelve-week-old male (n=5) and female (n=5) C57BL/6J mice were obtained from Jackson Laboratory (Bar Harbor, ME) and allowed to acclimate for three days. Standard chow diet was provided ad libitum. Mice were euthanized by exsanguination. The carotid arteries were excised and placed in cold HEPES physiological saline solution (HEPES-PSS) supplemented with either 0 or 2 mM glutamine for 24 hours at 4°C.

For pressure myography, the carotid artery was cannulated with stainless steel micropipettes in a pressure myograph chamber (114P; DMT) containing cold HEPES-PSS. The myograph chamber was slowly warmed to 37°C and aerated with carbogen (5% CO_2, 95% O_2). Arterial pressure was increased from 0 to 40 mmHg at increments of 10 mmHg every 5 minutes. The carotid artery was then equilibrated at 50 mmHg for an additional 15 minutes. Vessel viability was confirmed by superfusing arteries with high potassium PSS (KPSS) for 5 minutes. Carotid arteries were considered viable if at least 10% constriction was achieved. Carotid arteries were then submaximally constricted 10-15% using 10^{-5} M phenylephrine (61-76-7; Acros Organics) prior to vasodilation experiments. Vasodilation was measured by treating carotid arteries with 10^{-9} M to 10^{-5} M acetylcholine (A6625; Sigma-Aldrich). Endothelial-independent vasodilation was measured by pre-incubating carotid arteries with eNOS inhibitor NG-Nitroarginine methyl ester hydrochloride (L-NAME, 10^{-5}M; HY-18729A; Med Chem Express) for 1 hour. Vasodilation to acetylcholine was then measured as previously described.

2.2.8 Nitrate/Nitrite:

Nitrates and nitrites in endothelial cell media were measured as a nitric oxide byproduct using the Nitrate/Nitrite Colorimetric Assay Kit (Cayman Chemical, 780001) as per manufacturer instructions. Confluent HCAECs were treated with varied glucose and glutamine media. After 24 hours, 40 μL media from each condition was added to a 96-well plate in duplicate and mixed with nitrate reductase to convert nitrates into nitrites. Plates were incubated for 2 hours at room temperature, followed by addition of Griess reagents for 10 minutes. Absorbance was measured at 550 nm using a Spark multimode plate reader (TECAN), and a standard curve was used to obtain nitrite concentration.

2.2.9 Statistical analysis:

GraphPad Prism 10 was used to analyze all data. Due to small sample sizes ($n < 30$), I assumed non-normal distributions for all datasets and used non-parametric statistical tests. When two conditions were compared, a Mann-Whitney non-parametric test was used to determine statistical significance. When the same vessel was measured multiple times during pressure myography, a repeated measured ANOVA was used. In all other cases, a two-way ANOVA with post-hoc Tukey test was used to determine statistical significance. A ROUT method outlier test (5% aggressive) was used to identify and exclude outliers. The specific test used is indicated in each figure caption. All data are represented as mean ± standard deviation. Statistical significance was determined at $p < 0.05$.

2.3 Results

2.3.1 Glutamine enhanced endothelial cell proliferation in normal and high glucose.

I first determined the effect of glutamine on endothelial cell proliferation in normal and high glucose culture, since previous studies showed that glutamine increases endothelial cell proliferation in normal glucose culture [133]. Phase contrast microscopy images showed similar morphology for HCAECs cultured in 5.5 mM or 15 mM glucose with 0, 0.5, or 2 mM glutamine (Figure 2-1 A). However, glutamine significantly increased endothelial cell proliferation. A two-way ANOVA showed a significant main effect of glutamine ($p<0.0001$) and interaction between glutamine and glucose ($p=0.0251$) on proliferation, with no significant main effect of glucose ($p=0.4826$). 0.5 and 2 mM glutamine increased proliferating $Ki67^+$ cells by ~2.5 fold compared to 0 mM glutamine in normal glucose culture ($p=0.0023$ and $p=0.0091$, respectively; Figure 2-1 B, C). In high glucose culture, $Ki67^+$ cells increased by more than 3.5 fold ($p=0.0005$) only at 2 mM glutamine relative to 0 mM glutamine (Figure 2-1 B, C). Furthermore, there were twice as many $Ki67^+$ cells in normal glucose at 0.5 mM glutamine as compared to in high glucose (Figure 2-1 B, C). To confirm glutamine effects on endothelial cell proliferation, I quantified cell number over two days in cells cultured with 0, 0.5, or 2 mM glutamine in normal and high glucose. Two-way ANOVA only showed a significant main effect of glutamine ($p<0.0001$) on cell number, with no significant effect of glucose ($p=0.4752$) or interaction ($p=0.9565$). I observed approximately 50% more cells in both normal and high glucose in 2 mM as compared to 0 mM glutamine (Figure 2-1 D; $p=0.0182$ in 5 mM glucose, and $p=0.0036$ in 15 mM glucose). These data suggest that although endothelial cells maintained their morphology and adhesion in normal and high glucose culture without glutamine, glutamine was required for endothelial cell proliferation in both normal and high glucose.

2.3.2 Glutamine decreased endothelial cell oxidative stress in normal and high glucose.

Glutamine has previously been shown to decrease endothelial cell oxidative stress in normal glucose [85]. To evaluate how glutamine impacts endothelial cell oxidative stress in high glucose, I measured ROS in HCAECs cultured with 0, 0.5, and 2 mM glutamine in normal or high glucose. Two way ANOVA indicated a significant main effect of glutamine ($p<0.0001$) on oxidative stress with no significant effect of glucose ($p=0.6570$) or interaction ($p=0.1548$; Figure 2-2). HCAECs in 0 mM glutamine showed significantly elevated ROS, with more than 2-fold higher H_2DCFDA fluorescence compared to HCAECs cultured in 0.5 mM glutamine ($p<0.0001$) and more than 3-fold higher compared to HCAECs cultured in 2 mM glutamine ($p<0.0001$; Figure 2-2 A,B). No significant differences in ROS were observed between HCAEC in normal and high glucose. Thus, these data support the possibility that glutamine reduces endothelial cell oxidative stress in both normal and high glucose conditions.

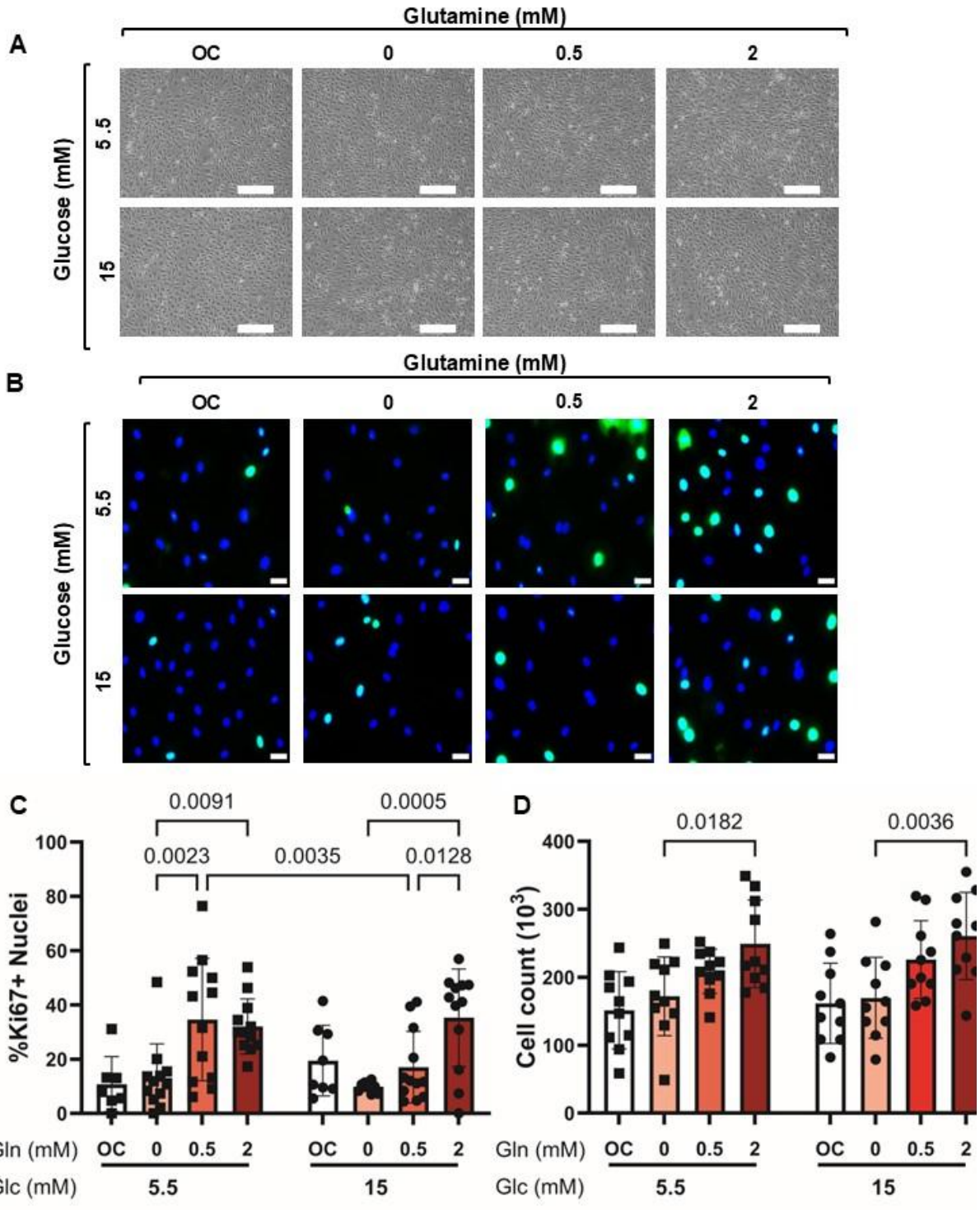

Figure 2-1: Glutamine increased HCAEC proliferation in normal and high glucose. HCAECs were cultured with 0, 0.5, or 2 mM L-glutamine in 5.5 and 15 mM glucose for 24 h. L-glucose at 2 mM (for glutamine in normal glucose) or 11.5 mM (for glutamine and glucose in high glucose) was included as osmotic control (OC). A) Representative phase contrast images. Scale bar = 500 µm, B) Representative fluorescent microscopy images (20x). Green = Ki67, blue = nuclei. Scale bar = 100 µm. C) Quantification of % Ki67+ nuclei. n = 12 samples. D) Cell count after 2 days of incubation in varied glucose and glutamine media. n=10 samples. Data shown as mean ± standard deviation. Statistical significance determined by two-way ANOVA followed by Tukey's post hoc test.

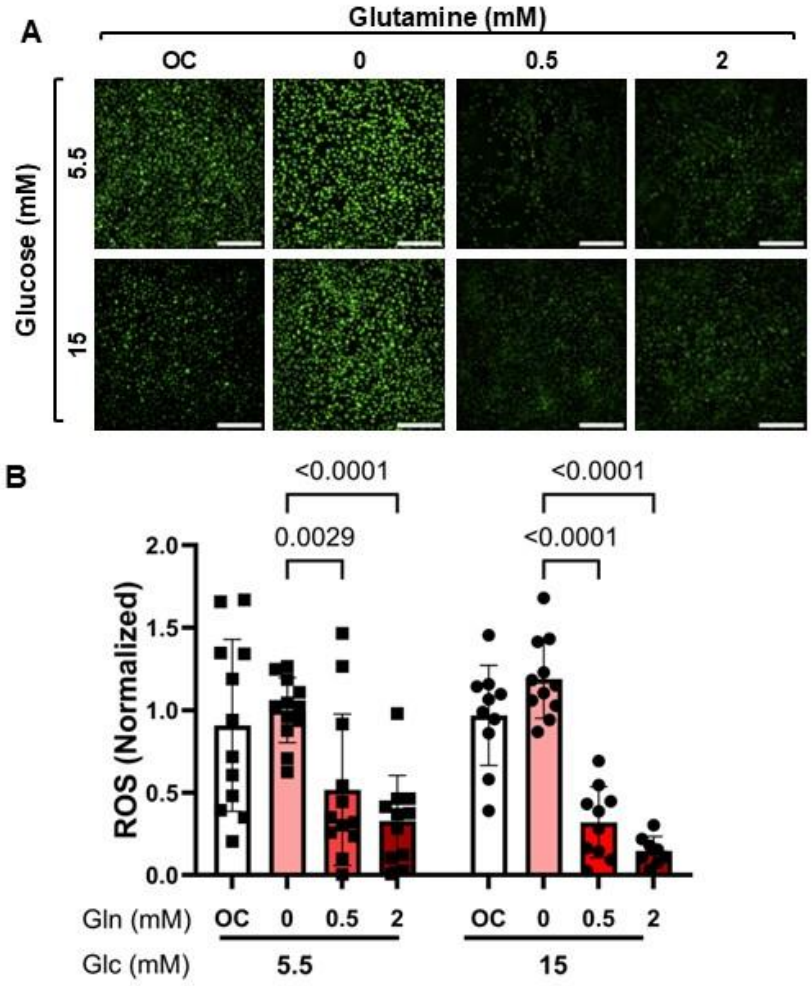

Figure 2-2: Glutamine decreased oxidative stress. HCAECs were cultured with 0, 0.5, or 2 mM L-glutamine in 5.5 and 15 mM glucose for 24 h. L-glucose at 2 mM (for glutamine in normal glucose) or 11.5 mM (for glutamine and glucose in high glucose) was included as osmotic control (OC). A) Representative confocal microscopy images of HCAEC labeled with 2 μM CM-H_2DCFDA (green) with B) quantification of mean fluorescent intensity. All samples were normalized to 0 mM glutamine in 5.5 mM glucose. n = 12 samples, scale bar = 500 μm. Data shown as mean ± standard deviation. Statistical significance determined by two-way ANOVA followed by Tukey's post hoc test.

2.3.3 Glutamine increased endothelial cell survival in oxidative stress in normal and high glucose.

I then measured how glutamine impacted endothelial cell survival under oxidative stress. I used 50 μM tBHP to induce oxidative stress in HCAECs cultured with 0, 0.5, and 2 mM glutamine in normal and high glucose. Two way ANOVA indicated significant main effects of glutamine ($p<0.0001$) and glucose ($p=0.0283$) on cell survival but no significant interaction ($p=0.1743$; Figure 2-3). Endothelial cells in 0 mM glutamine showed around 15-fold higher cell death compared to those treated with 0.5 or 2 mM glutamine ($p<0.0001$; Figure 2-3 A,B) and this effect was independent of glucose conditions. However, there were statistically significantly more dead cells with 0 mM glutamine in 15 mM glucose culture as compared to 5.5 mM glucose culture ($p=0.0018$; Figure2-3 A,B). These data suggest that glutamine is essential for endothelial cell survival during oxidative stress in both normal and high glucose.

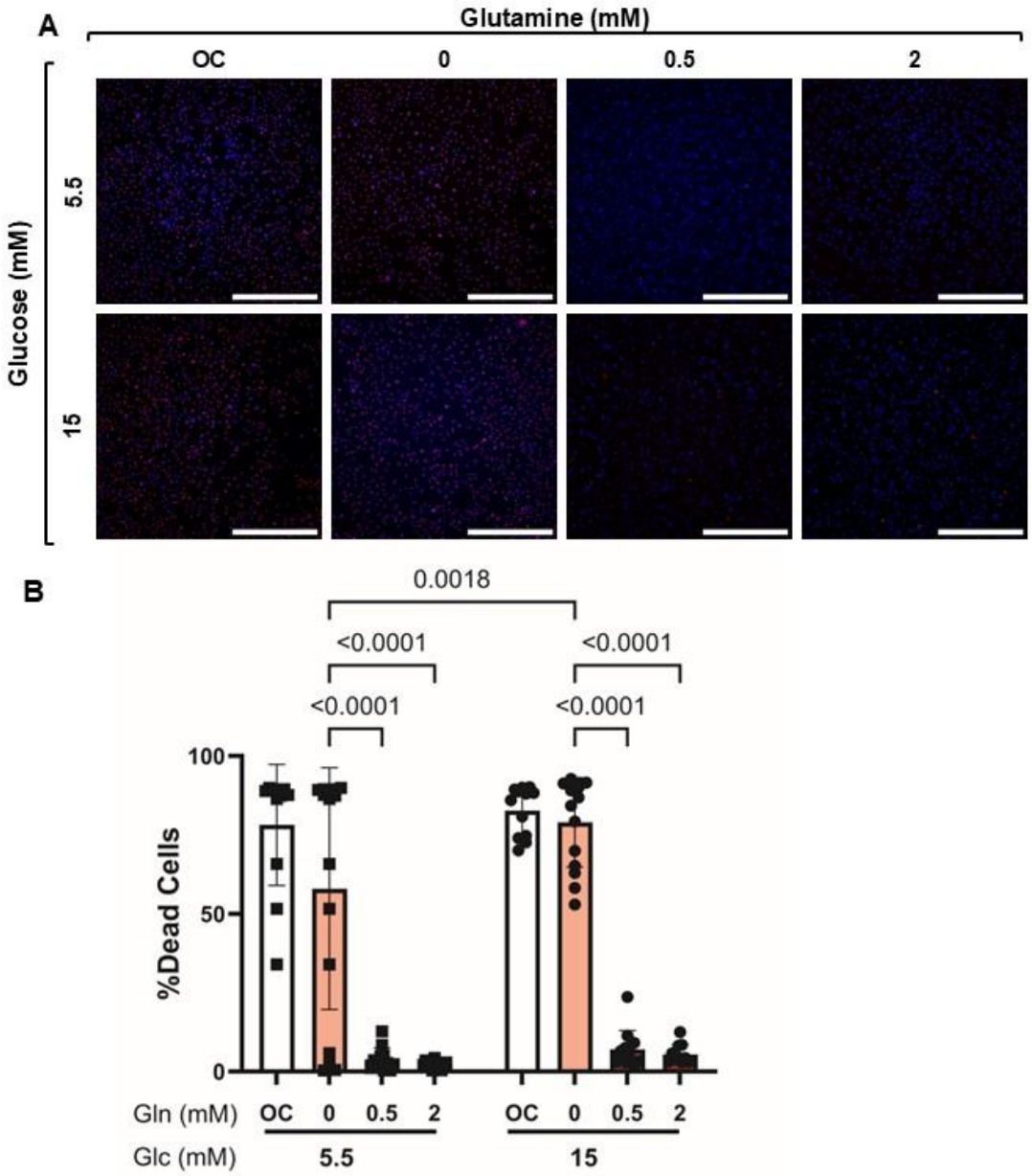

Figure 2-3: Glutamine increased HCAEC survival in moderate oxidative stress. HCAECs were cultured with 0, 0.5, or 2 mM L-glutamine in 5.5 and 15 mM glucose for 24 h. L-glucose at 2 mM (for glutamine in normal glucose) or 11.5 mM (for glutamine and glucose in high glucose) was included as osmotic control (OC). Oxidative stress was induced by adding 50 μM tBHP for 24 hours. A) Representative confocal microscopy images of HCAEC labeled with DAPI (nuclei, blue) and ethidium homodimer-1 (EthD-1, dead cells, red). Scale bar = 500 μm. B) Percentage of dead cells. n = 12 samples. Data shown as mean ± standard deviation. Statistical significance determined by two-way ANOVA followed by Tukey's post hoc test.

2.3.4 Glutamine increased vasodilation without changing eNOS phosphorylation.

ROS can scavenge vasodilatory nitric oxide produced by endothelial cells. I therefore evaluated the impact of glutamine on murine carotid artery vasodilation in response to acetylcholine using pressure myography. Male and female carotid arteries that were incubated with 2 mM glutamine for 24 hours showed elevated vasodilation in response to acetylcholine as compared to carotid arteries incubated with 0 mM glutamine by repeated measures ANOVA ($p=0.035$; Figure 2-4A and Figure 2-5 A,B). This change was likely nitric oxide dependent, since carotid arteries incubated in both 0 and 2 mM glutamine did not vasodilate when pre-treated with the eNOS inhibitor L-NAME (Figure 2-5 C). However, when I measured eNOS phosphorylation in endothelial cells cultured with 0 and 2 mM glutamine in normal glucose, I did not observe any significant changes ($p=0.7045$; Figure 2-4 B). Two-way ANOVA indicated a significant effect of glucose on nitrites ($p=0.0281$; Figure 2-4 C), with nitrites trending lower in 15 mM glucose media at 2 mM glutamine as compared to 5.5 mM glucose media ($p=0.0510$). However, there was no significant effect of glutamine ($p=0.2360$) or interaction ($p=0.7220$) between glucose and glutamine. Thus, glutamine may increase vasodilation without changing eNOS activation or nitric oxide production.

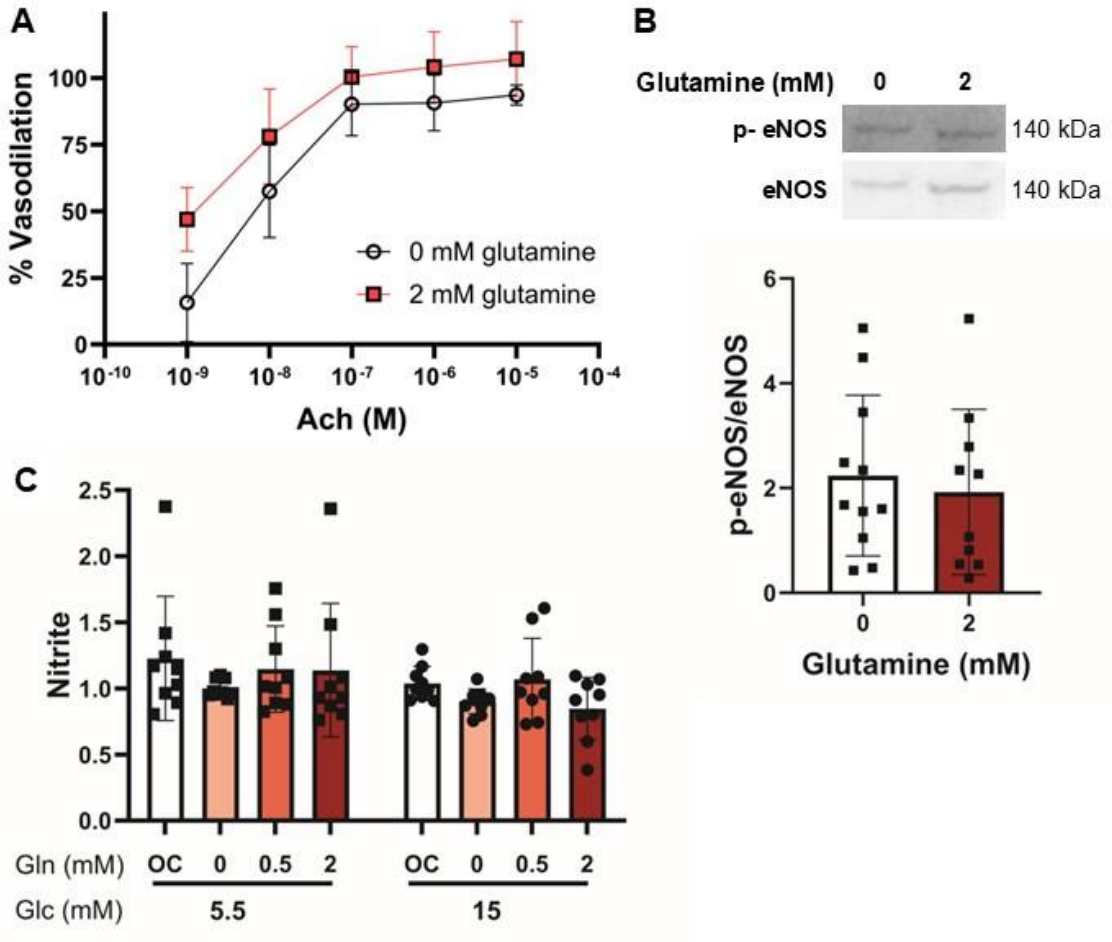

Figure 2- 4: Glutamine increased vasodilation *ex vivo* but did not impact eNOS phosphorylation or nitric oxide *in vitro.* A) Mouse carotid artery vasodilation in response to acetylcholine with an intact endothelium. Isolated mouse carotid arteries were incubated at 4°C overnight in physiological saline containing either 0 or 2 mM glutamine. Vasodilation was measured the following day by pressure myography. n=4-5 arteries per condition. B) representative Western blot with quantification of eNOS and p-eNOS in HCAEC cultured in 0 and 2 mM glutamine. n=10-11 samples per condition. C) HCAECs were treated with 0, 0.5, and 2 mM glutamine in 5.5 and 15 mM glucose. L-glucose at 2 mM and 11.5 mM was included as positive control for glutamine and glucose respectively. After 24 hours cells were treated with 20 µM of yoda1 and then the nitrites in the culture media was measured using a Griess assay. n = 9 samples. Data shown as mean ± standard deviation. Statistical significance determined by repeated measures ANOVA (A), Mann-Whitney non-parametric test (B), and two-way ANOVA followed by Tukey's post hoc test.

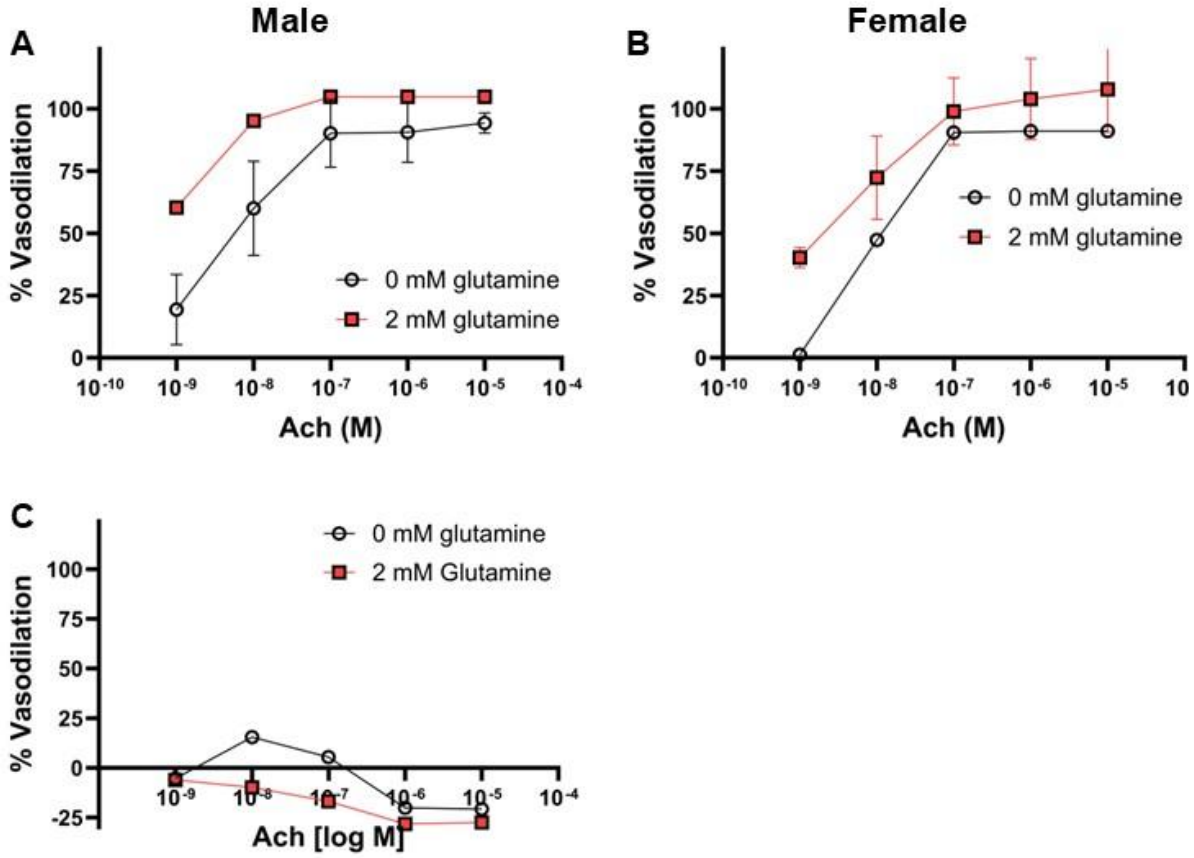

Figure 2-5. Glutamine increased vasodilation in male and female arteries and in an NO-dependent manner. Mouse carotid artery vasodilation in response to acetylcholine with an intact endothelium. Isolated male (A) and female (B) mouse carotid arteries were incubated at 4°C overnight in physiological saline containing either 0 or 2 mM glutamine. For male mice, 0 mM glutamine: n = 4 arteries; 2 mM glutamine: n = 1 artery. For female mice, 0 mM glutamine: n = 1 artery; 2 mM glutamine: n = 4 arteries. Vasodilation was measured the following day by pressure myography. C) Mouse carotid artery vasodilation in response to acetylcholine after eNOS was inhibited using 10^{-5} M L-NAME, as measured by pressure myography. n = 1 artery per condition.

2.3.5 Glutamine increased total endothelial cell glutathione and NADPH in normal and high glucose.

The antioxidant glutathione can be derived from glutamine after it is converted to glutamate by GLS1. I therefore measured glutathione in endothelial cells cultured with and without glutamine in normal and high glucose using a GSH/GSSG Glo assay. Two-way ANOVA indicated a

significant effect of glutamine ($p<0.0001$) and interaction between glucose and glutamine ($p=0.0025$) on glutathione but no significant effect of glucose ($p=0.5301$; Figure 2-6 A). In HCAECs cultured under normal glucose, total glutathione increased by more than 2 fold with both 0.5 mM and 2 mM glutamine compared to 0 mM glutamine ($p < 0.0001$; Figure 2-6 A). In HCAEC cultured in high glucose, total glutathione was 25% higher with 0.5 and 2 mM glutamine as compared to 0 mM glutamine ($p=0.0124$ for 0.5 mM; Figure 2-6 A). I further found that glutathione was statistically significantly lower in HCAECs cultured in 15 mM glucose and 2 mM glutamine as compared to 5.5 mM glucose ($p=0.0205$). I validated these findings using LC-MS. Glutathione trended 5 to 6.5-fold higher in HCAEC cultured with 0.5 and 2 mM glutamine ($p=0.0543$) in normal glucose as compared to cells cultured without glutamine (Figure 2-6 B). Similarly, glutathione trended 6 to 8.5-fold higher in cells cultured with 0.5 and 2 mM glutamine in high glucose compared to cells cultured without glutamine ($p=0.0111$ and $p=0.0566$, respectively; Figure 2-6 B). Notably, while the increase in intracellular glutathione was modest, it was biologically meaningful. Around 2 fold GSH increase (from ~1 μM to ~2 μM) was sufficient to significantly reduce oxidative stress (Fig. 2-2 and Fig. 2-6), suggesting that relatively small changes in glutathione availability can have substantial functional impact on endothelial redox balance.

Since NADPH is a key cofactor for regenerating glutathione from its oxidized form, I measured NADPH in HCAECs cultured in normal and high glucose and varied glutamine. Two-way ANOVA indicated a significant effect of glutamine ($p<0.0001$) and glucose ($p=0.0015$) on NADPH but no interaction ($p=0.7069$; Figure 2-6 C). NADPH increased 30-60% in HCAEC cultured with glutamine in both normal and high glucose ($p=0.0059$ and $p=0.0005$ for 0.5 and 2 mM glutamine in normal glucose; $p=0.0002$ and $p<0.0001$ for 0.5 and 2 mM glutamine in high

glucose). NADPH was also statistically significantly higher in HCAEC cultured without glutamine in 5.5 mM glucose as compared to 15 mM glucose ($p=0.0170$; Figure 2-6 C). I also calculated the $NADPH/NADP^+$ ratio, an indicator for cell reducing capacity [148]. Two-way ANOVA indicated a significant effect of glutamine ($p<0.0001$) but no effects of glucose ($p=0.8575$) and interaction ($p=0.7143$; Figure 2-6 D). Glutamine increased the NADPH/NADP+ ratio by more than 50% in cells cultured in both normal and high glucose as compared to 0 mM glutamine (Figure 2-6 D). These results suggest that glutamine increases glutathione and NADPH to enhance ROS scavenging and cellular reducing power in both normal and high glucose.

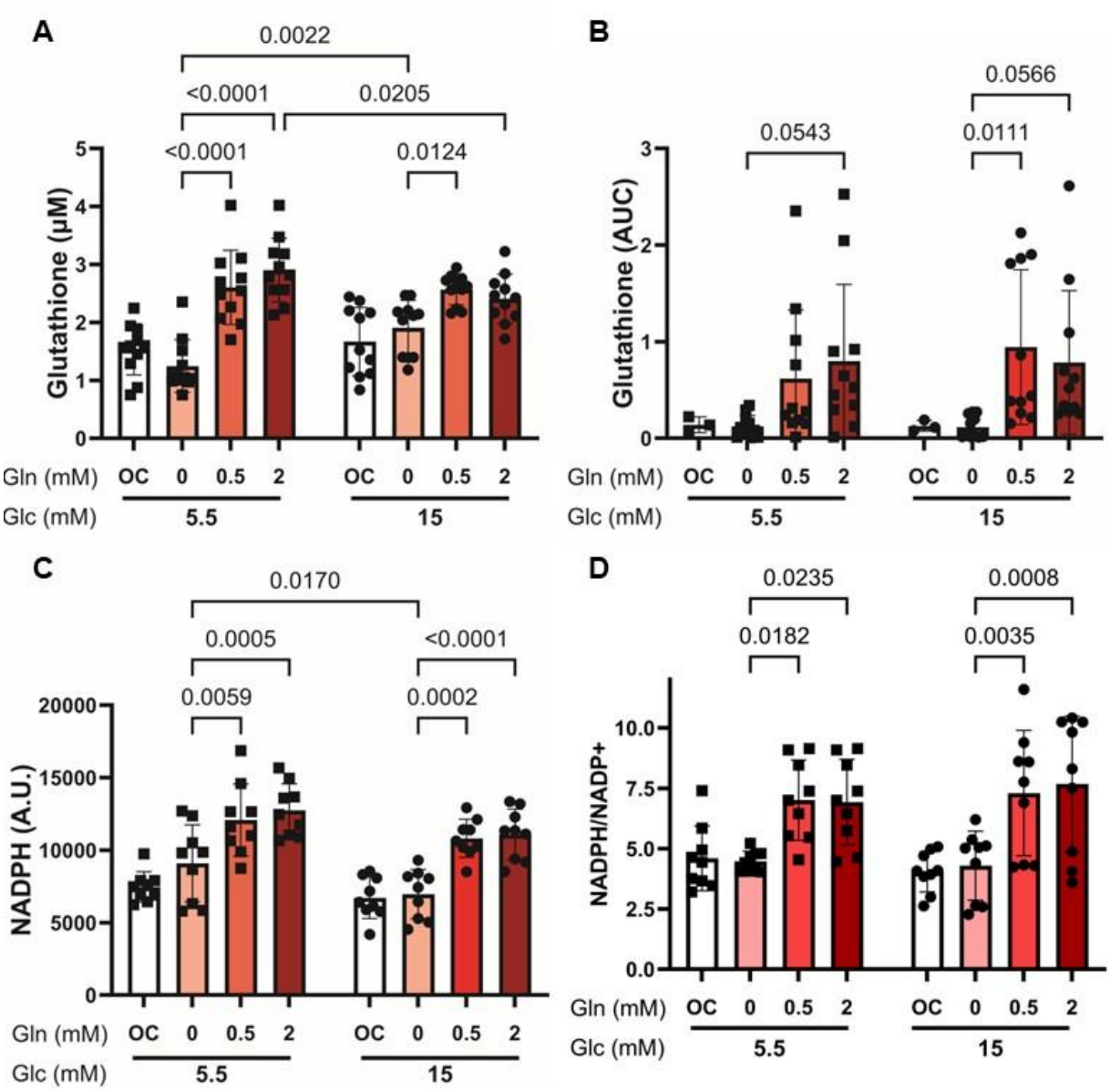

Figure 2-6: Glutamine increased endothelial cell antioxidants, including glutathione and NADPH. HCAECs were cultured in 5.5 and 15 mM glucose with 0, 0.5, or 2 mM L-glutamine for 24 h. L-glucose at 2 mM (for glutamine in normal glucose) or 11.5 mM (for glucose and glutamine in high glucose) was included as osmotic control (OC). A) Total glutathione concentration measured using GSH-GSSG Glo assay (n=11 samples). B) Glutathione area under the curve (AUC) measured by LC-MS (n= 11 samples). C) NADPH measured using NADPH/NADP+ Glo assay (n=12 samples). D) NADPH/NADP+ ratio was calculated and normalized to its value at 5.5 mM glucose and no glutamine for each experiment (n= 12 samples). Data shown as mean ± standard deviation. Statistical significance determined by two-way ANOVA followed by Tukey's post hoc test.

2.3.6 Glutaminase-induced glutathione production regulates endothelial cell oxidative stress and survival in normal and high glucose.

To determine how glutamine metabolism to glutathione through GLS1 contributes to reduced oxidative stress and enhanced cell survival and vasodilation, I inhibited GLS1 using BPTES [149]. 10 μM BPTES effectively decreased glutamine uptake, glutamate secretion, and glutathione concentration. BPTES also reduced HCAEC reducing capacity. Two-way ANOVA indicated a significant effect of BPTES treatment on NAPDH ($p<0.0001$), a significant effect of glucose ($p=0.0031$), and no interaction ($p=0.3330$; Figure 2-7 A). HCAEC NADPH in 2 mM glutamine with BPTES in both normal and high glucose was comparable to NADPH in HCAEC in 0 mM glutamine. BPTES also attenuated glutamine's antioxidant effects. Two-way ANOVA indicated a significant effect of BPTES treatment ($p<0.0001$) and glucose ($p=0.0427$) but no significant interaction ($p=0.0833$; Figure2-7 B,C). Glutaminase inhibition in HCAEC cultured in 2 mM glutamine increased ROS to a comparable level as HCAEC cultured in 0 mM glutamine. Finally, the percent of dead cells for HCAEC in 2 mM glutamine and BPTES was comparable to that of HCAEC in 0 mM glutamine in both normal and high glucose (Figure 2-7 D,E). Cell death was higher in BPTES treated cells in 15 mM glucose as compared to 5.5 mM glucose ($p=0.0028$). Thus, glutamine metabolism to glutamate may regulate NADPH and ROS in endothelial cells and improves their survival under moderate oxidative stress, especially in high glucose.

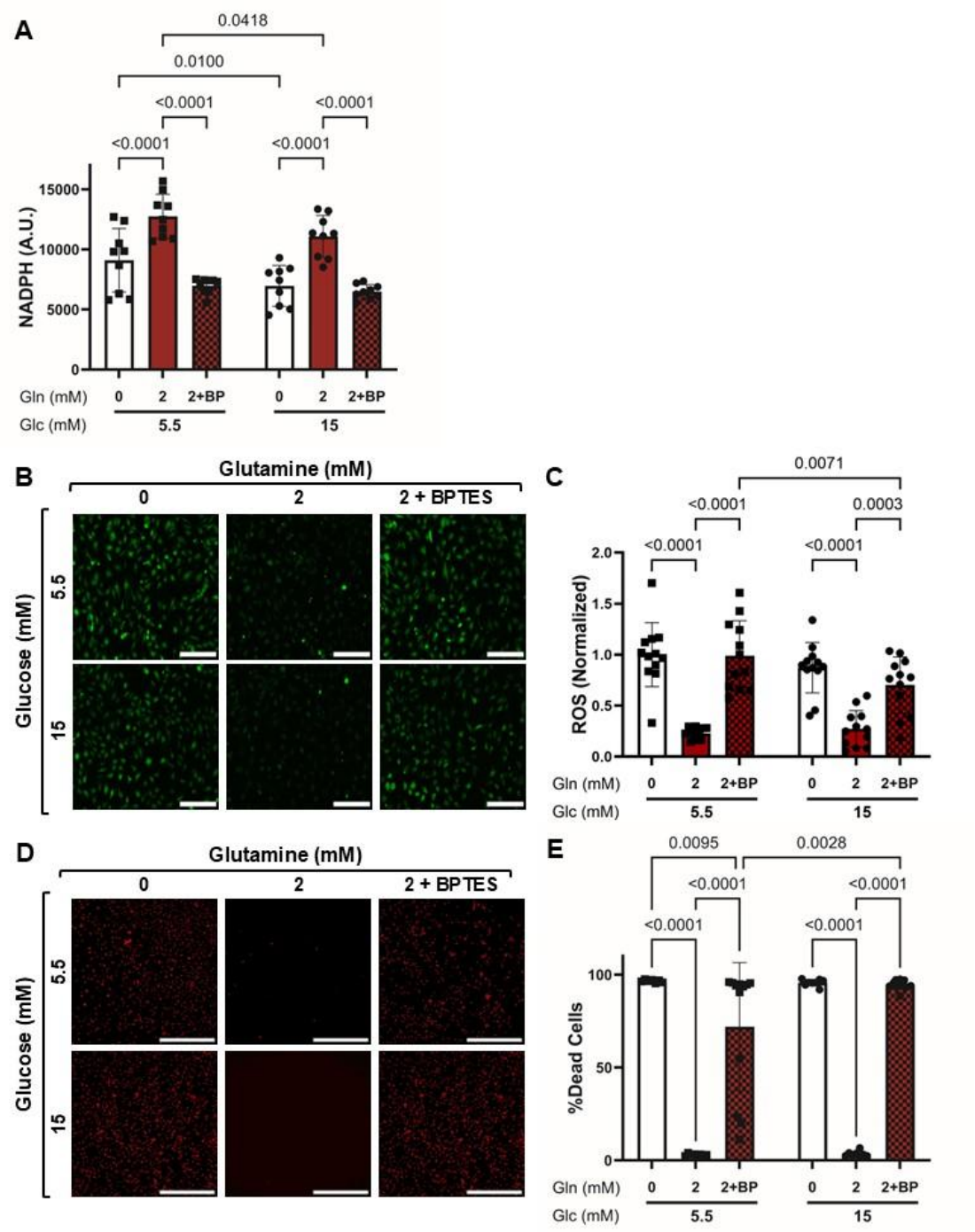

Figure 2-7: Glutamine-derived glutathione regulates endothelial reducing capacity, oxidative stress, and survival. HCAECs were cultured 0 or 2 mM glutamine in 5.5 or 15 mM glucose for 24 h. Some cells in 2 mM glutamine were also treated with the glutaminase inhibitor BPTES (BP, 10 μM). A) NADPH measured using NADPH/NADP+ Glo assay. n=9 samples. B) Representative confocal microscopy images of HCAECs labeled with ROS indicator CM-H_2DCFDA (green). Scale bar = 500 μM. C) Quantification of ROS mean fluorescence intensity normalized to normal glucose samples cultured with 0 mM glutamine. n=12 samples. D) Representative confocal microscopy images of HCAECs labeled with DAPI (nuclei, blue) and ethidium homodimer-1 (EthD-1, dead cells, red). Scale bar = 500 μm. E) Percentage of dead cells. n = 12 samples. Data shown as mean ± standard deviation. Data were analyzed using ordinary Two-way ANOVA followed by Tukey's post hoc test.

2.4. Discussion:

Glutamine is known to reduce oxidative stress *in vitro* and *in vivo* [150,151]; however, its effect on hyperglycemia-induced oxidative stress in the vasculature, which contributes to cardiovascular complications in diabetes, was not known. I therefore investigated how glutamine impacted endothelial cells cultured in normal and high glucose. Our data suggest that glutamine is required for endothelial cell proliferation and reduces endothelial cell oxidative stress in both normal and high glucose conditions. Glutamine enhanced endothelial cell survival under moderate oxidative stress by increasing intracellular glutathione and NADPH through glutamine deamination to glutamate by GLS1. Glutamine also improved endothelium-dependent vasodilation *ex vivo*, likely by reducing oxidative stress. These findings highlight glutamine metabolism, particularly GLS1-mediated glutathione synthesis, as a critical regulator of endothelial redox balance, which in turn may improve vasodilation by reducing nitric oxide scavenging. Glutamine metabolism may offer a therapeutic strategy to maintain endothelial redox balance under stressful conditions, which could reduce cardiovascular complications associated with diabetes.

Our data expand upon prior studies by supporting that glutamine promotes endothelial cell proliferation in both normal and high glucose. Although endothelial cells are highly glycolytic, most TCA cycle carbons come from glutamine. Both glutamine deprivation and glutaminase inhibition reduced human umbilical vein endothelial cell proliferation *in vitro* and murine angiogenesis *in vivo* by preventing the formation of TCA cycle intermediates and non-essential amino acids such as asparagine [78,132]. Peyton et al. further showed that glutamine-derived asparagine was essential for cyclin A expression and cell cycle progression in human umbilical vein, aortic, and microvascular endothelial cells in normal glucose[133]. Our findings extend these

observations to primary human coronary artery endothelial cells and suggest that glutamine is essential for endothelial cell proliferation even under conditions of excess glucose.

Our data also indicate that glutamine reduced oxidative stress in both normal and high glucose conditions and that this effect was mediated through glutamine deamination by GLS1 into glutamate and ammonia. Others had previously shown that glutamine deprivation and GLS1 inhibition increased endothelial oxidative stress via reduced ammonia, which then decreased expression of antioxidant heme-oxygenase-1 (HO-1) [133,152]. However, the other product of glutamine deamination, glutamate, is converted to the antioxidant glutathione by glutamate-cysteine ligase (GCL) and glutathione synthetase (GS) [153]. Our data demonstrate that glutamine deprivation and glutaminase inhibition also decrease glutathione. Interestingly, both HO-1 and glutathione are regulated by the transcription factor nuclear factor erythroid 2-related factor 2 (Nrf2). Nrf2 binds to antioxidant response elements in the HO-1 promoter to upregulate its transcription, and it additionally increases GCL transcription [154,155].

I also measured decreased NADPH in endothelial cells deprived of glutamine or with inhibited GLS1. NADPH acts as a reducing agent for glutathione reductase, which converts oxidized glutathione back to its reduced form. Glutamine can increase NADPH formation in several ways. After its initial conversion to glutamate, glutamine can be converted to α-ketoglutarate and eventually to malate in the mitochondrial TCA cycle. This malate is then transported to the cytosol, where malic enzyme 1 (ME1) catalyzes its conversion to pyruvate, a reaction that reduces $NADP^+$ to NADPH. Glutaminase inhibition with BPTES decreased NADPH regeneration in control cells but did not impact ME1 knockout cells, linking glutamine metabolism via ME1 to NADPH production [156]. Alternatively, glutamine-derived α-ketoglutarate can be converted to citrate and then isocitrate in the reverse TCA cycle. Isocitrate is then exported to the

cytosol, where isocitrate dehydrogenase 1 (IDH1) regenerates α-ketoglutarate while producing NADPH[156]. Nrf2 can also increase NADPH-related gene expression, including ME1 and IDH1 [157]. Thus, Nrf2 may be a common pathway by which glutamine enhances endothelial antioxidant capacity.

In addition to increasing cell survival, glutamine enhanced acetylcholine-mediated vasodilation of murine carotid arteries. Glutamine has previously been shown to enhance vasodilation in both animals and humans. In mice with endothelial-dysfunction induced by L-Nω-methyarginine (L-NMMA), supplementation with glutamine for 2 months reversed impaired aortic ring vasorelaxation [92]. Similarly, 6 months of β-hydroxy-β-methylbutyrate, glutamine and arginine supplementation increased flow mediated vasodilation by 27% in older adults [139]. Epidemiological studies further report that higher plasma glutamine concentration or a higher glutamine:glutamate ratio is associated with reduced CVD incidence and mortality[158,159]. Our data support these studies and indicate that glutamine supplementation improves vascular function even in a healthy mouse model.

Intriguingly, glutamine enhanced vasodilation but did not impact eNOS phosphorylation (p-eNOS) or nitric oxide production in cultured endothelial cells. Prior studies showed that glutamine decreased endothelial cell nitric oxide synthesis, in part by increasing glucose flux through the HBP to O-GlcNAcylate eNOS and prevent its phosphorylation at Ser-1177 [90,160–163]. Our different results could come from a change in cell type or culture conditions. In our hands, without a change in eNOS or nitric oxide *in vitro,* our *ex vivo* increase in vasorelaxation is likely to have resulted from decreased ROS scavenging nitric oxide.

Interestingly, I did not detect an increase in ROS with high glucose culture alone, which has been shown in other studies including those from our laboratory [164,165]. Our observations may

reflect different experimental conditions (e.g., cell type, media, glucose concentration) or ROS assay sensitivity. I hypothesize that the high glucose conditions I used (15 mM), while physiologically relevant, were not high enough to induce oxidative stress in our cells over short-term culture, as compared to other studies that used extremely high glucose concentrations (> 25 mM). I did observe some detrimental effects of our high glucose culture on the endothelial cells, including decreased cell proliferation, increased cell death, and decreased glutathione and NAPDH at specific glutamine concentrations. Therefore, even though 15.5 mM glucose did not increase endothelial oxidative stress, it did have negative effects on endothelial cell function and oxidative capacity.

2.5 Limitations:

While our study suggests that glutamine regulates ROS in both normo- and hyperglycemia and may have cardiovascular protective effects, it is not without limitations. We studied hyperglycemic conditions on the order of days, although diabetes is a chronic condition. Short-term supraphysiological high glucose exposure is commonly used *in vitro* to model key early molecular events associated with hyperglycemia in diabetes, including increased oxidative stress, mitochondrial dysfunction, and reduced nitric oxide bioavailability. However, this study, only modeled hyperglycemia and did not incorporate hemodynamic stimuli on the endothelial cells (e.g., shear stress) or other vascular changes in diabetes such as increased inflammatory cytokines and free fatty acids[166,167]. Prior to clinical translation, these data would need to be validated in a more complex diabetic model to confirm the beneficial impact of glutamine.

2.6. Conclusions:

This chapter expands upon previous work by suggesting that GLS1-dependent glutamate production from glutamine supports endothelial cell glutathione biosynthesis and NADPH generation, which is essential for maintaining endothelial viability and potentially improve vasodilation in both normo- and hyperglycemic conditions. While these findings establish a critical role for glutamine metabolism via GLS1 in redox homeostasis, the broader metabolic network reprogramming in cells induced by changes in glutamine concentration remains poorly defined. In the following chapter, I investigated how extracellular glutamine concentration rewires endothelial cell metabolism at a systems level, with a specific focus on the TCA cycle, amino acid metabolism, and fatty acid pathways, and how these changes may contribute to metabolic disorders.

Chapter 3: Glutamine systematically changes endothelial cell metabolism

3.1 Introduction

Endothelial cell dysfunction is a hallmark of cardiovascular disease (CVD), the leading cause of mortality among subjects with diabetes [67]. Endothelial dysfunction is characterized by an imbalance between vasodilation and vasoconstriction, driven by reduced bioavailability of nitric oxide (NO) as well as increased oxidative stress [168]. Endothelial dysfunction promotes atherosclerotic plaque formation through increased permeability and inflammation [169]. Hyperglycemia causes endothelial cell dysfunction in diabetes. Even when glycemic control is achieved through appropriate medication in diabetic subjects, they still experience higher risk of cardiovascular disease.

Endothelial function is tightly linked to metabolic activity. Endothelial cells rely on glycolysis for up to 85% of their ATP production, even in the presence of oxygen [78]. However, glutamine metabolism is crucial for endothelial biomass production during processes such as vascular sprouting and for maintaining redox homeostasis [170,171]. Glutamine is transported into endothelial cells through specific transporters, including SLC1A5 (ASCT2) as well as SLC38A1 and SLC38A2 [172]. SLC1A5 is a Na^+-dependent transporter that functions as an exchanger, trading extracellular glutamine for intracellular neutral amino acids. In contrast, SLC38A1 and SLC38A2 belong to the System A transporter family and are Na^+-coupled symporters. Rather than exchanging glutamine, they use the inward sodium electrochemical gradient to power net glutamine uptake into the cell [173–175]. Once glutamine enters the cell, it can serve as an exchange substrate for SLC7A5 (LAT1), a Na^+-independent obligate antiporter that exports intracellular glutamine in exchange for extracellular essential amino acids such as leucine [172].

Glutaminase 1 (GLS-1) hydrolyzes glutamine into glutamate and ammonia [78,87]. Glutamate is further metabolized into alpha-ketoglutarate (α-KG) either through glutamate dehydrogenase (GLUD1) or via transamination reactions. α-KG then enters the tricarboxylic acid (TCA) cycle for ATP and macromolecule production [176]. Glutamine-derived glutamate contributes to the formation of other amino acids, including asparagine via asparagine synthetase and proline from pyrroline-5-carboxylate (P5C) via P5C reductase [87] . Glutamine-derived glutamate is also essential for glutathione (GSH) synthesis for antioxidant defense. Glutamate, through the enzyme glutamate–cysteine ligase (GCL), conjugates with cysteine to form the dipeptide γ-glutamylcysteine. Glutathione synthetase (GS) then adds glycine to γ-glutamylcysteine, resulting in the final tripeptide, γ-L-glutamyl-L-cysteinylglycine, known as GSH [80] .

Glutamine metabolic pathways are highly interconnected with additional biosynthetic networks, including the hexosamine biosynthetic pathway (HBP), ornithine cycle, and one carbon (1C) metabolism among others. The HBP integrates glucose and glutamine metabolism to generate UDP-N-acetylglucosamine (UDP-GlcNAc), a substrate required for protein O-GlcNAcylation and regulation of cellular signaling. [178]Glutamine availability directly impacts the production of UDP-GlcNAc by providing the essential amide group required for the activity of glutamine:fructose-6-phosphate aminotransferase (GFAT). Glutamine also provides other carbon substrates necessary for UDP-GlcNAc synthesis, including acetyl-CoA and UTP [177]. In the HBP, glucosamine-6-phosphate is acetylated using acetyl-CoA to form N-acetylglucosamine-6-phosphate. After conversion to N-acetylglucosamine-1-phosphate, UTP is incorporated by UDP-GlcNAc pyrophosphorylase to generate UDP-GlcNAc[178]. UDP-GlcNAc influences cell signaling through post-translational protein modification via GlcNAcylation, which often occurs at the same serine and threonine residues targeted by phosphorylation. Increased O-GlcNAcylation of endothelial

nitric oxide synthase (eNOS) has been shown to decrease NO synthesis and impair vasodilation [138,160,162].

Glutamine can also contribute to the ornithine cycle, which serves as a pathway for synthesizing several essential molecules including polyamines and citrulline that regulate cell growth, structural integrity, and detoxification cycle [179] . Glutamine-derived glutamate can be converted into Δ^1-pyrroline-5-carboxylate (P5C) by the enzyme P5C synthase, and subsequently into ornithine by ornithine aminotransferase (OAT) [87]. Ornithine is a substrate for production of polyamines, which are indispensable for cell proliferation. Ornithine can also increase proline synthesis by converting back to P5C. Proline is essential for collagen synthesis and integrity of vascular extracellular matrix [90,180], Wu_2000]. So glutamine can regulate ornithine metabolism to impact proliferation and structural integrity in endothelial cells.

1C metabolism, mediated by the folate cofactor, activates and transfers one carbon units for essential biological processes involved in cellular defense, amino acid homeostasis, and purine and thymidine biosynthesis[181]. 1C metabolism and glutamine availability are interconnected through biosynthetic pathways, cellular stress responses, and redox homeostasis. It has been shown in cancer cells that under conditions of glutamine deprivation or inhibition of glutamine metabolism, cells activate 1C metabolism as a compensatory survival strategy[182].

Glutamine supplementation may protect against cardiovascular disease and related complications through metabolic and anti-inflammatory mechanisms. In pulmonary artery endothelial cells, glutamine supplementation reduced hydrogen peroxide–induced injury, helping to maintain cellular ATP and viability during high oxidative stress[183]. In animal models of endotoxin shock and severe injury, glutamine supplementation improved survival rates, enhanced immune function, and supported gut barrier integrity [184]. However, inconsistent reports exist for

the effects of glutamine on endothelial function, as glutamine has been shown to reduce NO and vasodilation in certain contexts while improving vasodilation in others. Results vary based on the experimental model [139,161,162]. For instance, *in vitro*, 0.2 to 2 mM glutamine in cultured bovine aortic and venular endothelial cells significantly reduced the release of endothelium-derived relaxing factor while in a mouse model of chronic endothelial dysfunction, glutamine supplementation improved acetylcholine-induced relation of aortic rings [92,162].

Although glutamine supplementation is used clinically to enhance vascular health, the precise metabolic adaptations that occur in endothelial cells in response to altered glutamine are not fully understood. In this study, I therefore examined how physiological and supplemented glutamine affected endothelial metabolism. I hypothesized that increasing glutamine concentration will increase TCA cycle flux in the forward and reverse directions, and also amino acid synthesis and HBP pathway flux. I supplemented endothelial cell culture media with 0–10 mM glutamine and measured changes in glutamine and glutamate levels over 24 hours. I then used a Seahorse Mito Stress Test to measure oxidative respiration and a glutamine isotope-labeled tracer to track glutamine-derived carbon flow to determine how increased glutamine concentrations influence endothelial cell metabolic activity. Understanding how glutamine systematically impacts endothelial cell metabolism may help identify novel metabolic targets for the prevention of cardiovascular disease.

3.2 Materials and methods

3.2.1 Endothelial cell culture

Primary human coronary artery endothelial cells (HCAEC, passage 5-9) were purchased from Lifeline Cell Technology. HCAECs were cultured in 100 mM dishes in Endothelial Growth

Medium-2 (EGM-2; Lonza) supplemented with 1% penicillin-streptomycin (PS; Thermo Fisher Scientific, 15140163), 10% fetal bovine serum (FBS; Cytiva, SH30088) and 1% glutamine (Fisher Scientific, 25-030-081) until confluent. At confluency, cells were passaged into the appropriate well plates and incubated in EGM-2 media until 90% confluent. Cells were then switched to Dulbecco's Modified Eagle Medium (DMEM) without phenol red, glucose, or glutamine (Gibco, A1443001) supplemented with Endothelial SingleQuots (Lonza, CC-4176), 5.5 or 15 mM D-glucose (Sigma-Aldrich, G8270), and 0, 0.5, 1, 2, 5, or 10 mM glutamine for 24 hours.

3.2.2 Glutamine uptake and glutamate secretion

A YSI 2950 Biochemistry Analyzer (Yellow Springs Instruments, 527690) was used to measure media glucose, lactate, glutamine, and glutamate concentration. At 0 and 24 hours of glutamine treatment, 150 µL media was collected and placed in a 96 well-plate (CELLTREAT; 229196) for analysis by YSI. Glucose and glutamine uptake and lactate and glutamate secretion were calculated as the difference between the 0 and 24 hour concentrations.

3.2.3 Glutaminase analysis

A Western blot was used to detect changes in HCAEC glutaminase. After glutamine treatment, cells were washed with phosphate buffered saline (PBS; Thermo Fisher Scientific; 70011069) and lysed with RIPA buffer (Thermo Fisher Scientific; 89901) containing Halt protease and phosphatase inhibitor cocktail (Thermo Fisher Scientific; 78440) and ethylenediaminetetraacetic acid (EDTA; Sigma-Aldrich; E9884). The cell lysate was centrifuged for 15 minutes at 17,000 × g at 4°C to remove cellular debris. The supernatant was collected, and

the protein concentration was quantified using a BCA assay (Thermo Fisher Scientific; 23225). 3.5 μg protein was loaded into each well of a NuPAGE 4%-12% Bis-Tris gel (Thermo Fisher Scientific; NP0323BOX) for separation by SDS-PAGE. Proteins were then transferred to a polyvinylidene difluoride membrane (Thermo Fisher Scientific; IB34001X3) using an iBlot 3 (Thermo Fisher Scientific). Membranes were blocked in 5% bovine serum albumin (BSA; Sigma-Aldrich; A7906) in tris buffered saline (TBS; Fisher Scientific; BP24711) with 0.5% Tween (TBS-T; Thermo Fisher Scientific; 85115) for 1 hour at room temperature. Blots were then incubated with primary antibodies in 1% BSA in TBS-T overnight at 4°C. Primary antibodies included glutaminase-1 (1:1000; Abcam; EP7212) and β-actin (1:1000; Santa Cruz Biotechnology; sc-47778). The next day, membranes were washed with TBS-T and incubated with the appropriate anti-rabbit (Promega; W4011) or anti-mouse (Promega; W4021) secondary antibodies (1:2000) for 2 hours. Protein bands were visualized by SuperSignal West Pico PLUS Chemiluminescent Substrate kit (Thermo Fisher Scientific; 34578) and imaged using an Alpha Innotech Fluorchem Imager. AlphaView SA 3.4.0 was used to quantify band intensity.

3.2.4 Oxidative respiration

HCAEC oxidative respiration was measured using a Seahorse Mito Stress test (Agilent; 103015). HCAEC were seeded at 50,000 cells/well in Seahorse XF96 cell culture plates and incubated overnight to allow cells to adhere to the plate. The next day, DMEM with 0, 0.5, and 2 mM glutamine and 5.5 or 15 mM glucose was added to the appropriate wells. After 24 hours, the assay was performed on a Seahorse XFe96 (Agilent) according to the manufacturer's protocols. Wave software (Agilent) was used to calculate basal respiration, maximal respiration, spare

capacity, and non-mitochondrial oxygen consumption from the measured oxygen consumption rate (OCR).

3.2.5 Isotope tracing via liquid chromatography-tandem mass spectrometry (LC-MS/MS)

To gain detailed insights into glutamine metabolism, we designed a parallel isotope-labeling experiment. 1-^{13}C-glutamine was used to trace glutamine entry into the reductive (reverse) carboxylation pathway, as the C1 label is released as CO_2 during forward TCA cycle flux. 5-^{13}C-glutamine was used to identify forward TCA–derived metabolites. 0, 1, 2, or 5 mM 1-^{13}C-glutamine (CLM-3612, Cambridge Isotope Laboratory) or 5-^{13}C-glutamine (CLM-1166, Cambridge Isotope Laboratory) were added to confluent HCAECs in 6 well plates in supplemented DMEM (5.5 mM glucose) for 24 hours. Endothelial cells were previously determined to reach isotopic steady state by this time [73]. Metabolites were then extracted in 500 µL ice-cold 80:20 methanol:water at -80°C for 15 minutes. Cell lysates were scraped in the extraction solvent, transferred to 1.7 mL micro centrifuge tubes, and centrifuged at 17,000 × g for 15 minutes at 4°C to pellet cell proteins. The supernatant was collected, stored at -80°C and analyzed by LC-MS/MS in the University of Colorado School of Medicine Metabolomics Core. Finally, the pellet was lysed in 50 µL RIPA buffer, and protein concentration was measured by BCA and used for normalization.

3.2.6 Mass spectrometry data analysis

Natural abundance correction, multivariate analysis, and univariate analysis were performed in RStudio. The IsoCorrector 1.22.0 package was first used to correct the isotopologue

natural abundance for each metabolite from the LC–MS/MS raw data. The mixOmics 6.28.0 package was then applied to conduct multivariate analyses, including principal component analysis (PCA). Univariate analyses, including the Kruskal–Wallis test and post-hoc pairwise Wilcoxon tests, were also performed in RStudio. The p-values obtained from these statistical analyses were adjusted using the Benjamini–Hochberg (BH) method. Score and loading plot for PCA was generated using the ggplot2 package in RStudio, and stackplots and barplots were created using GraphPad Prism 10.

After correction, the labeled fraction was calculated by dividing the signal from labeled metabolites by the total signal (labeled + unlabeled).

3.2.7 Media succinate

Media was collected from HCAEC cultured in 5.5 mM glucose DMEM with 0 or 5 mM glutamine for 24 hours. Media was centrifuged for 10 minutes at 17,000 × g at 4°C to remove cell debris. 200 µL of supernatant was added to 800 µL of ice cold 100% HPLC grade methanol, vortexed and centrifuged at 17,000 × g at 4°C for 15 minutes. The supernatant was transferred to a new tube and dried overnight using a CentriVap Vacuum Concentrator (Labconco). Samples were resuspended in 100 µL 80% methanol (Sigma-Aldrich, G6025-11VL) and transferred to mass spectrometry vials (Waters, 600000670). Extracellular succinate was analyzed using a Bruker maXis-II QTOF mass spectrometer (Bruker Daltonics) coupled to a Waters ACQUITY UPLC system. Chromatographic separation was performed on an Atlantis BEH C18 AX column (2.1 × 100 mm, 1.7 µm; Waters) maintained at 30°C, with the sample manager held at 6°C. A 5 µL injection volume was used. The mobile phases consisted of solvent A: water containing 0.1% formic acid and solvent B: acetonitrile containing 0.1% formic acid. The flow rate was 0.25

mL/min. The gradient program was as follows: 0–2 min, 2% A; 2–11 min, linear increase to 90% A; 11–16 min, hold at 90% A; 16–17 min, return to 2% A; 17–20 min, re-equilibration at 2% A. Mass spectrometric detection was performed in negative electrospray ionization (ESI−) mode with a capillary voltage of 4,500 V. Data were acquired in full scan mode over an m/z range of 80–400 without MS/MS fragmentation. A 10 µM sodium succinate dibasic hexahydrate standard (Sigma-Aldrich; S2378-100MG) was injected at the beginning of each sequence to confirm both mass and retention time prior to sample analysis. Succinate was identified based on accurate mass and retention time relative to the standard. Extracted ion chromatograms were generated at m/z 116.9967 ± 0.02 Da, and the succinate peak eluted at 1.4 min.

3.2.8 Succinate dehydrogenase activity assay

Succinate dehydrogenase (SDH) activity was measured using a commercially available SDH Activity Assay Kit (Abcam; ab228560) according to the manufacturer's instructions. HCAECs were seeded in 100 mm culture dishes and grown in EGM-2 medium to approximately 90% confluence. Cells were rinsed with PBS and then switched to DMEM supplemented with 1% PS, 10% FBS, 5.5 mM glucose, and either 0 or 5 mM glutamine for 24 hours. Following treatment, cells were detached using trypsin, washed with cold PBS, and resuspended in 100 µL SDH assay buffer supplemented with 1% protease inhibitor cocktail and EDTA. Cells were lysed using a D1000 homogenizer (Benchmark Scientific), incubated on ice for 10 minutes, and then centrifuged at 10,000 × g for 5 minutes at 4°C. The supernatant was collected for analysis. Protein concentration was determined using a BCA assay. 75 µg protein for each sample was loaded into a 96-well plate and adjusted to a final volume of 50 µL. The standard curve and reaction mixture were prepared according to the manufacturer's protocol and added to the designated wells.

Absorbance was measured at 600 nm in kinetic mode for 60 minutes at 2 minute intervals using a Spark multimode plate reader (TECAN). SDH activity was calculated according to the manufacturer's instructions using the linear portion of the kinetic curve.

3.2.9 Statistical analysis

All statistical analyses were performed using GraphPad Prism 10. Data are presented as mean ± standard deviation (SD) unless otherwise indicated. The number of biological replicates (n) for each experiment is specified in the corresponding figure legends. For experiments comparing multiple glutamine concentrations, statistical significance was determined using an ordinary one-way ANOVA followed by Tukey's post hoc multiple comparisons test. When comparisons were made against a single control group (e.g., 0 mM glutamine), a one-way ANOVA followed by Dunnett's multiple comparisons test was used. For comparisons between two groups with unequal variance (e.g., extracellular succinate measurements), a Mann Whitney non-parametric test was used. Principal component analysis (PCA) was performed on labeled fraction data to assess global metabolic differences among conditions. Statistical significance was defined as $p < 0.05$. The specific statistical test used for each dataset is indicated in the corresponding figure legend.

3.3 Results:

3.3.1 Glutamine uptake increased with glutamine concentration; however, glutamate secretion plateaued above 2 mM glutamine.

I first determined how HCAECs take up glutamine in both 5.5 mM (normal) and 15 mM (high) glucose by adding 0 to 10 mM glutamine to the cell culture media. HCAECs took up significantly more glutamine as media glutamine concentration increased in both normal and high glucose conditions, as analyzed by one-way ANOVA ($p<0.0001$; Figure 3-1A, D). In normal glucose, HCAECs took up 5 and 10 times more glutamine, respectively, at 5 and 10 mM glutamine than at the physiological level of 0.5 mM glutamine ($p<0.0001$; Figure 3-1A). Similarly, in high glucose, HCAEC took up more than 4 times more glutamine in 5 and 10 mM glutamine as compared to 0.5 mM glutamine ($p<0.001$; Figure 3-1D). Glutamine uptake was only statistically different between normal and high glucose at 10 mM glutamine, where glutamine uptake in high glucose was around half the uptake in normal glucose ($p=0.0280$; Figure 3-1G).

I then measured secretion of the primary glutamine-derived metabolite, glutamate, into the cell culture media. Glutamate secretion also increased with increasing media glutamine concentration in both normal and high glucose conditions ($p<0.0001$ by ANOVA; Figure 3-1B, E). In normal glucose, glutamate secretion was about 10 times higher for HCAEC in 0.5 mM as compared to 0 mM glutamine ($p=0.0001$) and about 2 times higher for HCAEC in 2, 5, or 10 mM glutamine as compared to 0.5 mM glutamine ($p=0.0004$, 0.0010, and <0.0001, respectively). In both normal and high glucose, HCAEC glutamate secretion did not change above 2 mM glutamine. There were no statistically significant differences in glutamate secretion for HCAEC in normal and high glucose at any glutamine concentration.

I calculated the ratio of glutamate secreted to glutamine uptake as a measure of glutaminolysis. From 0.2 to 2 mM glutamine, the glutamate:glutamine ratio remained statistically similar at around 0.7 for HCAEC in normal and high glucose. At 5 and 10 mM glutamine, the glutamate:glutamine ratio decreased to around 0.2 for HCAEC in normal glucose ($p<0.0001$; Figure 3-1C, F) and around 0.3 for HCAEC in high glucose ($p=0.0534$ at 5 mM and $p=0.0159$ for 10 mM glutamine). There were no statistically significant differences in the glutamate:glutamine ratio for HCAEC in normal and high glucose.

Glutaminase 1 (GLS-1) catalyzes the deamidation of glutamine to glutamate in endothelial cells. I therefore determined how extracellular glutamine concentration affected GLS-1 protein by Western blot (Figure 3-1H-J). As I did not observe significant changes in glutamate secretion at glutamine concentrations higher than 2 mM, I measured glutaminase protein levels at 0, 0.5 and 2 mM glutamine. HCAEC in normal glucose and 0.5 or 2 mM glutamine had twice as much GLS-1 compared to HCAEC in 0 mM glutamine ($p=0.0006$ and $p=0.0015$, respectively; Figure 3-1I). Similarly, HCAEC in high glucose and 0.5 or 2 mM glutamine had 50% more GLS-1 compared to HCAEC in 0 mM glutamine ($p=0.0088$ and $p=0.0289$, respectively; Figure 3-1J). GLS-1 protein did not increase above 0.5 mM glutamine for HCAEC in normal or high glucose. These data suggest that ECs take up more glutamine as extracellular glutamine concentration increases but reach a limit of glutamate secretion, possibly due to a lack of additional GLS-1.

Since endothelial cells are also dependent on glycolysis, I assessed glucose uptake and lactate secretion in HCAECs in increasing extracellular glutamine. Glutamine supplementation did not significantly alter glucose uptake (Figure 3-2A,C). Lactate secretion increased with extracellular glutamine for HCAEC in both normal and high glucose ($p=0.0007$ and $p<0.0001$ by ANOVA for normal and high glucose, respectively; Figure 3-2B, D). Lactate secretion at 10 mM

glutamine was about 25% higher for HCAEC in normal and high glucose as compared to HCAEC in 0.5 mM glutamine. These data show that extracellular glutamine did not significantly change glycolysis, suggesting that the two metabolic pathways remain distinct.

3.3.2 Glutamine increased oxidative respiration.

Glutamine is a primary carbon source for the endothelial TCA cycle. As I did not measure changes in glutamate secretion above 2 mM glutamine, I measured how 0, 0.5, or 2 mM extracellular glutamine impacted mitochondrial activity (Figure 3-3A) using a Seahorse Mito Stress test. HCAEC oxygen consumption rate (OCR), a measure of mitochondrial oxidative respiration, increased with glutamine ($p=0.0016$ for basal OCR and $p<0.0001$ for all others by ANOVA). Basal OCR was five time higher for cells in 0.5 and 2 mM glutamine compared to 0 mM glutamine ($p=0.0342$ and 0.0013, respectively; Figure 3-3B). Maximal respiration, which measures mitochondrial ability to meet increased energy demand[185] , and spare capacity, which is the difference between maximal and basal respiration, more than doubled for cells in 0.5 ($p=0.008$) and 2 mM ($p<0.0001$) glutamine relative to 0 mM glutamine (Figures 3-3C, D). Similarly, cells in 0.5 and 2 mM glutamine had double the non-mitochondrial oxygen consumption of cells in 0 mM glutamine ($p=0.0003$ and $p<0.0001$, respectively; Figure 3-3E), indicating increased cellular oxidase activity. Only spare respiratory capacity was statistically significantly higher for cells in 2 mM as compared to 0.5 mM glutamine ($p=0.0058$). I observed a similar OCR response to glutamine in HCAECs cultured in high glucose (Figure 3-4A-E). Taken together, these data support evidence in the literature that glutamine fuels endothelial mitochondrial activity, although the effect is limited at higher glutamine concentrations.

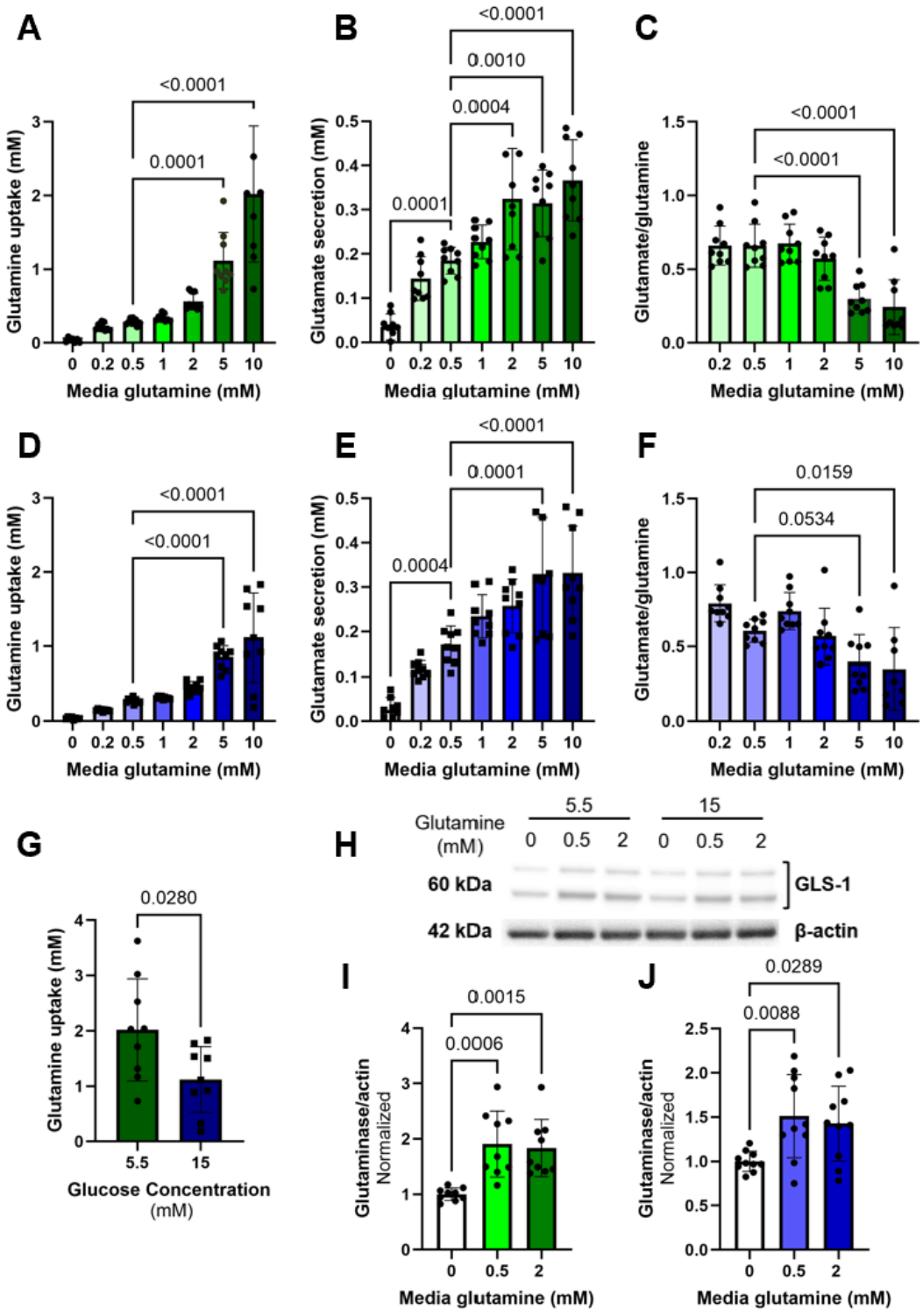

Figure 3-1: Glutamine uptake and glutamate secretion increased with glutamine concentration; however, glutamate secretion plateaued above 2 mM glutamine. HCAEC were incubated with 0-10 mM glutamine in normal (5.5) and high glucose (15 mM) for 24 hours. Glutamine uptake and glutamate secretion were measured in normal (A, B) and high (D, E) glucose using a YSI bioanalyzer. The glutamate:glutamine ratio was determined for each condition in (C) normal and (F) high glucose.(G) Comparison of glutamine uptake in normal vs high glucose at 10 mM glutamine. n=9 biological replicates. (H) Representative glutaminase-1 (GLS-1) and β-actin Western blots, with quantification of (I) normal glucose and (J) high glucose. n=9 biological replicates. Data were analyzed using an ordinary one-way ANOVA with a Dunnett post-hoc multiple comparisons test.

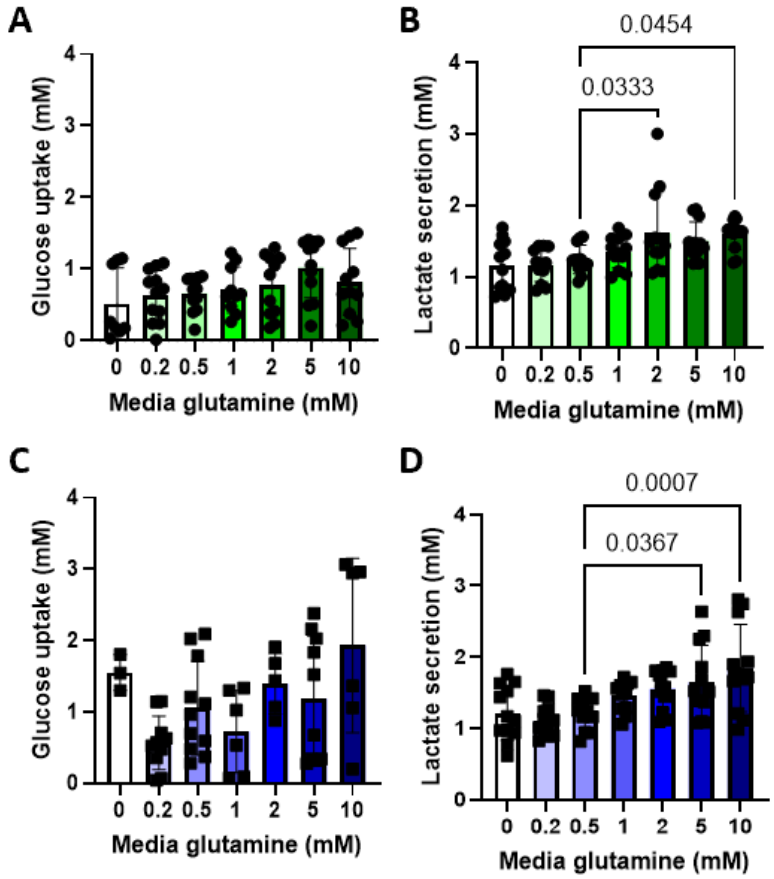

Figure 3-2: Extracellular glutamine increased lactate secretion without affecting glucose uptake. HCAEC were incubated with 0-10 mM glutamine in normal (5.5) and high glucose (15 mM) for 24 hours. Glucose uptake and lactate secretion were measured in normal (a, b) and high (d, e) glucose using a YSI bioanalyzer. n=3-12 biological replicates. Data were analyzed using an ordinary one-way ANOVA with a Dunnett post-hoc multiple comparisons test, following an ROT outlier test.

3.3.3 Increasing glutamine increased isotope enrichment through the forward TCA cycle with limited impact on reverse carboxylation.

Since extracellular glutamine increased endothelial TCA cycle activity, I used isotope-assisted tracing to get a more detailed understanding of how glutamine contributes to TCA cycle metabolites. Since I observed no TCA cycle differences for HCAEC in normal and high glucose, I conducted all labeling experiments in normal glucose. I used 1 mM glutamine instead of 0.5 mm glutamine to model physiological glutamine concentration due to concerns about our ability to detect isotope labeling at the lower concentration. I used 2 mM glutamine to model commonly

used endothelial cell culture media concentration and 5 mM glutamine to observe changes with additional glutamine. I used 1-^{13}C-glutamine and 5-^{13}C-glutamine parallel labeling to understand glutamine entry into the forward and reverse TCA cycle. In the forward TCA cycle, 1-^{13}C-glutamine loses its labelled first carbon when it is converted from α-KG to succinate while 5-^{13}C-glutamine retains its labelled fifth carbon, enabling us to trace forward glutamine movement. In the reverse TCA cycle (reverse carboxylation), 1-^{13}C-glutamine retains its labelled first carbon when it is converted from α-KG to citrate and therefore enables us to trace glutamine in the reverse TCA cycle.

Our LC-MS data (Figure 3-5) showed that nearly all intracellular glutamine was labeled in HCAEC treated with 1, 2, or 5 mM 1-^{13}C-glutamine or 5-^{13}C-glutamine. 5-^{13}C-glutamate enrichment increased from 69% to 76% and 5-^{13}C-α-KG enrichment increased from 64% to 71% with increasing extracellular glutamine. TCA metabolites in the forward TCA cycle also increased in a concentration dependent manner as extracellular glutamine increased from 1 to 5 mM, including succinate from 4% to 12%, fumarate from 31% to 50%, malate from 40% to 55%, and citrate from 39% to 49%. However, 1-^{13}C-citrate enrichment was less than 5% across all glutamine concentrations, indicating limited reverse carboxylation. Interestingly, succinate had the highest unlabeled pool among all TCA cycle metabolites, which could indicate a stable intracellular succinate pool or succinate generation from other carbon sources.

3.3.4 Increasing glutamine increased the total abundance of all TCA metabolites except for succinate, which decreased.

Next, I analyzed the total abundance of glutamine, glutamate, and TCA metabolites by determining the integrated peak area, which is proportional to the concentration. For HCAEC in 2 or 5 mM glutamine, intracellular glutamine total abundance was 2 and 5 times higher than for

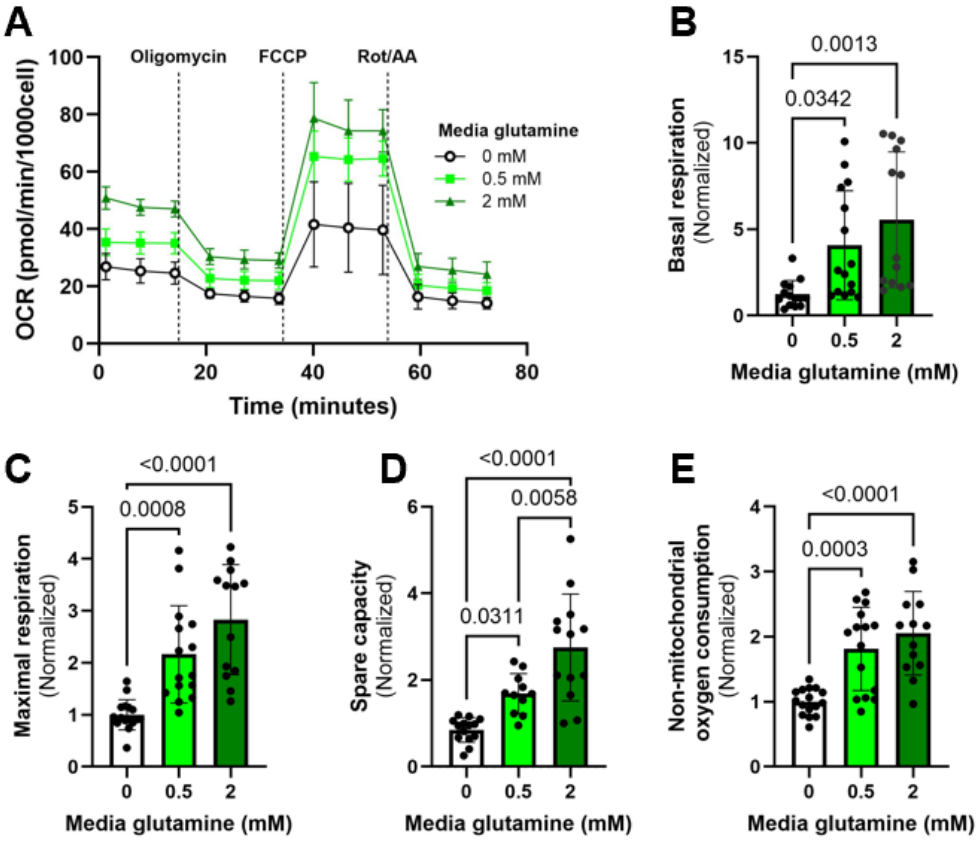

Figure 3-3: Glutamine increased endothelial oxidative respiration. HCAECs were incubated for 24 hours with 0, 0.5, or 2 mM glutamine in normal (5.5 mM) glucose culture. (A) Representative oxygen consumption rate (OCR) as measured by Seahorse Mito Stress test. (B) Basal respiration, (C) maximal respiration, (D) spare capacity, and (E) non-mitochondrial oxygen consumption from three experiments, normalized to the 0 mM glutamine condition. n=10-16 biological replicates. Data were analyzed using ordinary one-way ANOVA with a Tukey post-hoc multiple comparisons test.

HCAEC in 1 mM glutamine ($p=0.0056$ and $p<0.0001$, respectively; Figure 3-6A). Intracellular glutamate total abundance was 20 times higher for HCAEC cultured in 1 mM glutamine as compared to 0 mM glutamine ($p<0.0001$) and then an additional 50% higher for HCAEC in 5 mM glutamine as compared to 1 mM glutamine ($p<0.0001$; Figure 3-6B). The glutamate:glutamine ratio for HCAEC in 2 and 5 mM glutamine declined by 50% and 75%, respectively, as compared to the ratio for HCAEC in 1 mM glutamine ($p=0.0003$, and <0.0001, respectively; Figure 3-6C). These data confirm that the endothelial cells continued to take up more glutamine as extracellular

glutamine concentration increased but did not produce more glutamate, as previously shown (Figure 3-1).

Similar to the labeled fraction data, total TCA metabolite abundance increased in the presence of extracellular glutamine, except for succinate which decreased. α-KG, fumarate, citrate, and malate total abundance increased between 3 and 5 times for HCAEC cultured in 1 mM as compared to 0 mM glutamine (Figure 3-6D-G). While α-KG and citrate total abundance did not change at higher glutamine concentrations, malate and fumarate demonstrated small increases with glutamine concentration. Malate was 35% higher at 2 mM glutamine ($p=0.0024$) and 46% higher at 5 mM glutamine ($p=0.0001$) as compared to 1 mM glutamine, and fumarate was 29% higher at 2 mM glutamine ($p=0.0426$) and 51% higher at 5 mM glutamine ($p=0.0007$) as compared to 1 mM glutamine. In contrast to the other TCA metabolites, succinate total abundance decreased by 34%, 44%, and 56% in HCAEC cultured in 1, 2, and 5 mM glutamine compared to 0 mM glutamine ($p=0.0078$, 0.0002, and <0.0001, respectively; Figure 3-6H).

I then analyzed several mechanisms by which succinate concentration could decrease with increasing glutamine. Succinate accumulated inside the cells can get transported into the extracellular environment via MCT1 and OAT transporters[169,186] . Therefore, I examined whether glutamine increased succinate release from cells. However, when I measured succinate in the media by LC-MS after 24 hours of HCAEC incubation with 0 or 2 mM of glutamine, I did not observe any increase in extracellular succinate (Figure 3-6I). Glutamine deprivation has also been shown to cause deSUMOylation of succinate dehydrogenase (SDH), leading to reduced SDH activity and therefore reduced succinate oxidation to fumarate [187,188]. I therefore measured how increasing extracellular glutamine affected SDH activity. SDH activity was 24% higher in HCAEC in 5 mM and compared to 0 mM glutamine ($p=0.0117$; representative experiment in Figure 3-6J,

sum of three experiments in Figure 3-6K). These findings suggest that reduced intracellular succinate with increased extracellular glutamine may, at least in part, reflect enhanced SDH activity.

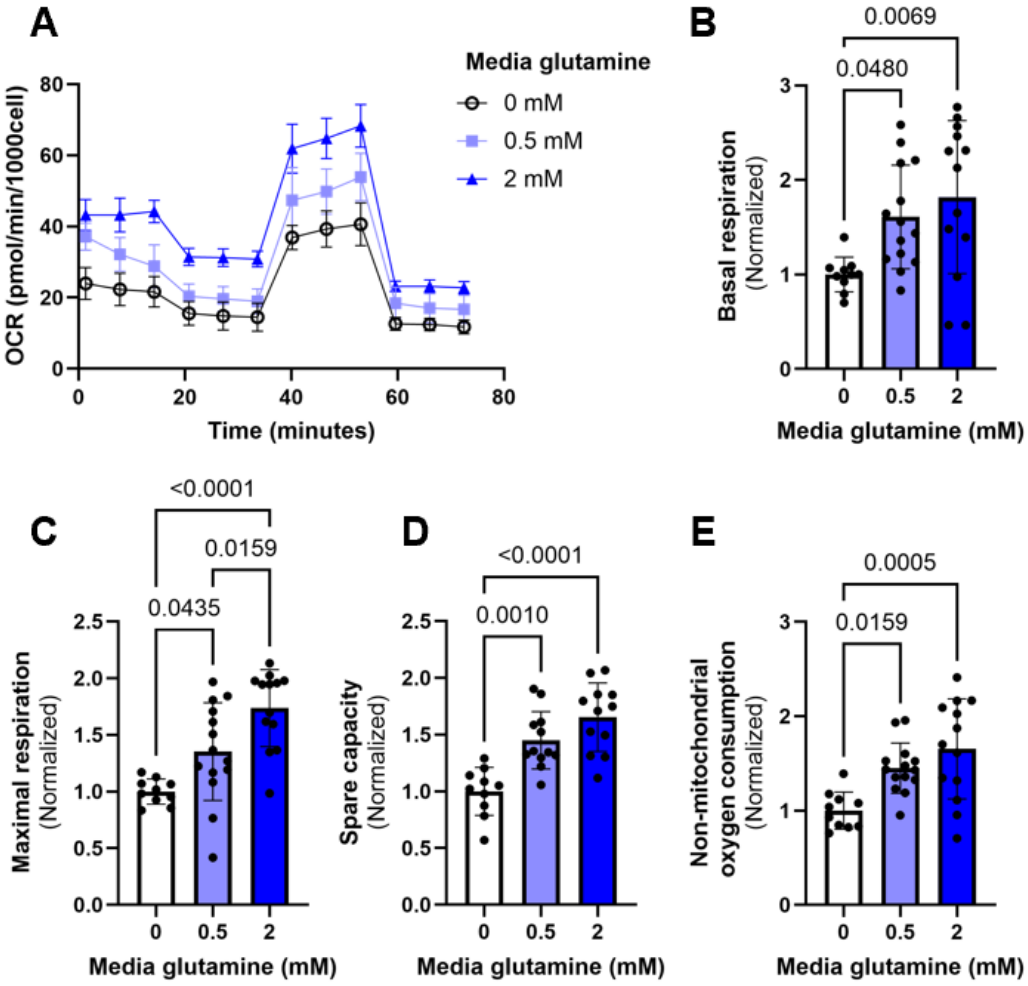

Figure 3-4: Glutamine increased endothelial oxidative respiration in high glucose. HCAECs were incubated for 24 hours with 0, 0.5, or 2 mM glutamine in high (15 mM) glucose culture.(a) Representative oxygen consumption rate (OCR) as measured by Seahorse Mito Stress test. (b) Basal respiration, (c) maximal respiration, (d) spare capacity, and (e) non-mitochondrial oxygen consumption from three experiments, normalized to the 0 mM glutamine. n=10-16 samples. Data were analyzed using an ordinary one-way ANOVA with a Tukey post-hoc multiple comparisons test.

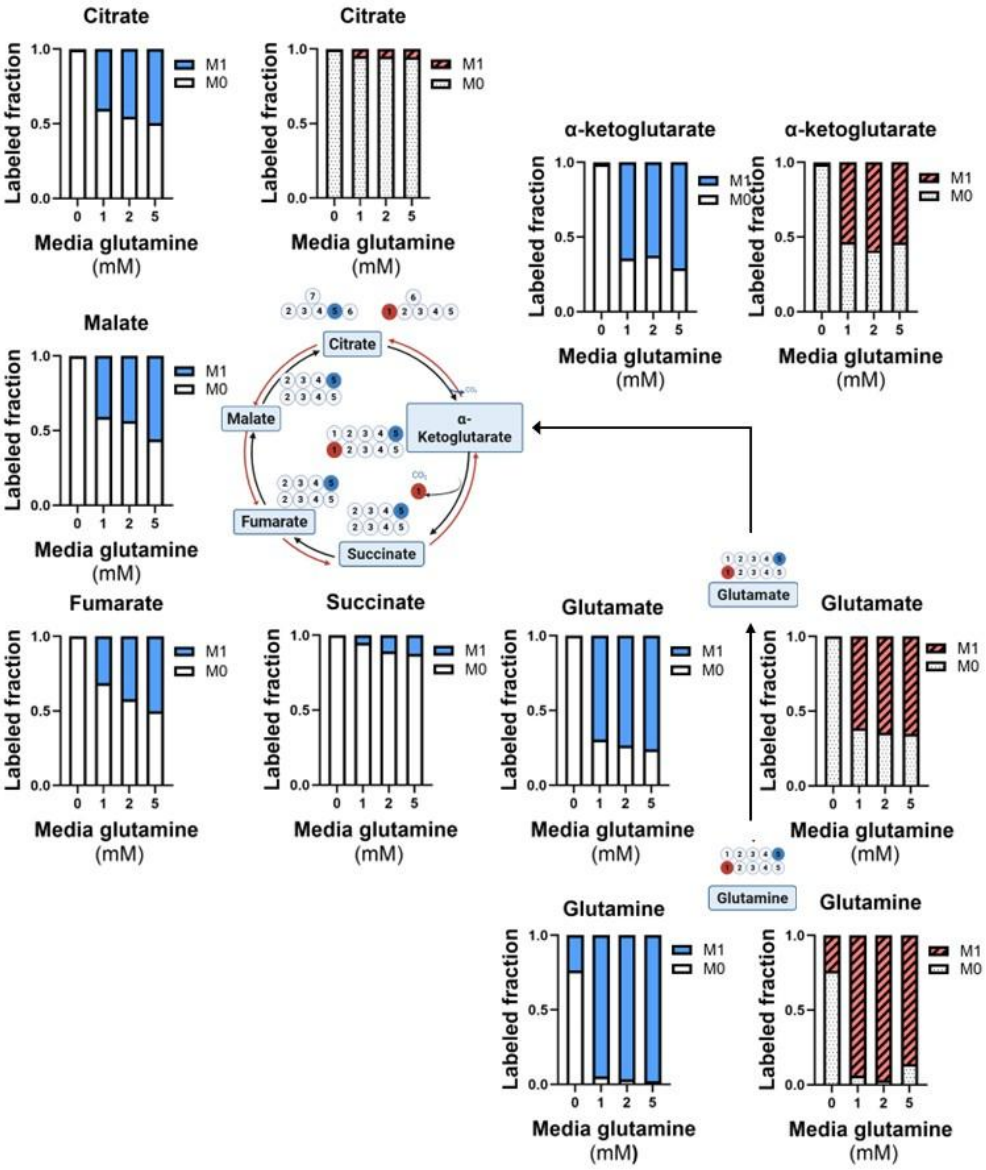

Figure 3-5: Increasing glutamine increased isotope enrichment through the forward TCA cycle; reverse carboxylation also increased with glutamine but was limited overall. HCAECs were cultured with 0, 1, 2, or 5 mM 1-^{13}C- or 5-^{13}C-glutamine for 24 hours, after which cells were collected and the isotope distribution was determined using LC-MS. Isotope labeled fractions for 5-^{13}C-glutamine metabolites are shown in blue. Isotope labeled fractions for 1-^{13}C-glutamine metabolites are shown in red with diagonal hatching. 5-^{13}C-glutamine was used to measure glutamine flux through the forward TCA cycle, since α-KG loses its first carbon as CO_2 when it converts to succinate, thereby retaining the M1 label. 1-^{13}C-glutamine was used to measure reverse carboxylation, since when α-KG is converted to citrate in the reverse TCA cycle, the first labeled carbon is preserved. n=3 biological replicates.

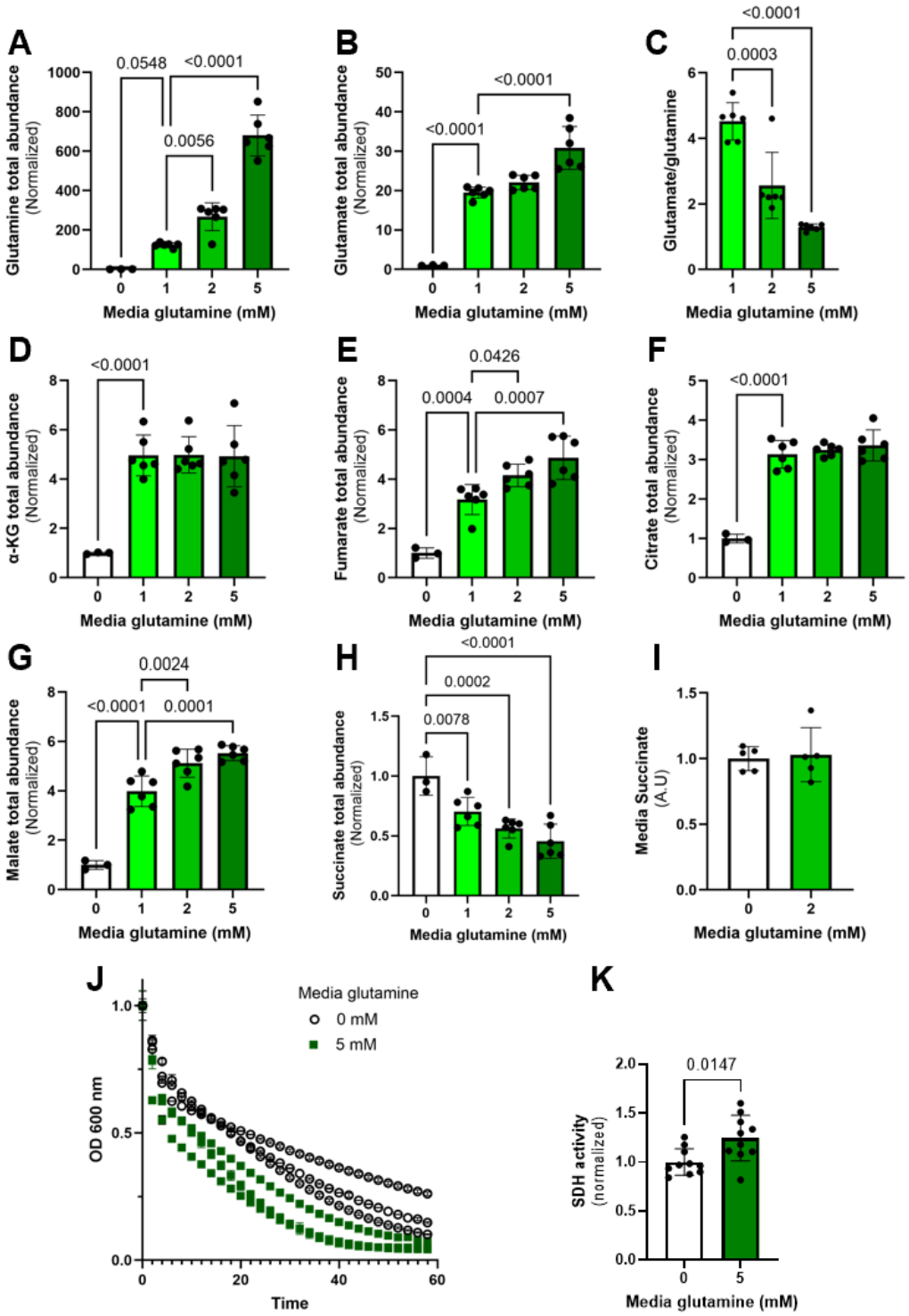

Figure 3-6: Increasing glutamine increased total abundance of all TCA metabolites except for succinate which decreased. HCAECs were treated with 0, 1, 2, or 5 mM of 1-^{13}C- or 5-^{13}C-glutamine for 24 hours and then analyzed by LC-MS. (A-C) Total abundance of L-glutamine, L-glutamate and glutamate:glutamine ratio. Total abundance of TCA cycle metabolites (D) α-KG, (E) fumarate, (F) citrate, (G) malate, and (H) succinate. n=6 samples for 1, 2, and 5 mM glutamine and n=3 for 0 mM glutamine. All data points were normalized to the average value at 0 mM glutamine. Data were analyzed using ordinary one-way ANOVA with a Dunnett post-hoc multiple comparisons test. (I) Succinate was measured in media by LC-MS after 24 hour HCAEC incubation with 0 or 2 mM glutamine. n= 5 biological replicates. (J) Representative curve and summation of (K) succinate dehydrogenase activity for HCAEC cultured in 0 and 5 mM glutamine for 24 hours. All data points were normalized to average value at 0 mM glutamine. n=10 biological replicates. Data were analyzed

3.3.5 Glutamine enriched amino acids and glutathione in addition to TCA metabolites.

Since our data showed that ECs took up more glutamine as extracellular concentration increased but did not secrete more glutamate or proportionally increase TCA metabolite labeling, I investigated where the extra glutamine is metabolized using our LC-MS data. A principal component analysis (PCA) score plot of the 5-^{13}C-glutamine metabolite labeled fractions revealed clear separation of samples along component 1 (PC1=51.6%), with the 0 mM glutamine condition clustering distinctly from glutamine-treated groups (Figure 3-7A). To identify the metabolites driving the separation observed in the PCA score plot, I next examined the PCA loading plot (Figure 3.7B). In addition to glutamine, glutamate, and TCA cycle metabolites, the amino acids L-proline, L-aspartate, and GABA along with the tripeptide glutathione were the metabolites that contributed the most to the separation of glutamine-treated cells (Figure 3-7B). A heatmap of the glutamine-labeled fractions of metabolites that most strongly contributed to the separation further indicated that HCAEC treated with 1, 2, or 5 mM glutamine are metabolically distinct from HCAEC treated with 0 mM glutamine but not different from each other (Figure 3-7C). The PCA score plot of the 1-^{13}C-glutamine metabolite labeled fractions also showed 0 mM glutamine condition clustering distinctly from glutamine-treated groups (Figure 3-8A) and the metabolites identified using PCA loading plot was similar to data from 5-^{13}C-glutamine metabolite (Figure 3-8B-C)

3.3.6 Glutathione and proline were enriched with glutamine-derived carbons.

HCAEC cultured with glutamine separated from HCAEC cultured without glutamine due to glutamine-derived glutamate contributing carbon to both glutathione and proline. Glutamate becomes part of glutathione through the ATP-dependent addition of cysteine and glycine,

catalyzed by glutamine-cysteine ligase (GCL) and glutathione synthetase (GS). Glutathione isotopic enrichment from 1-^{13}C-glutamine and 5-^{13}C-glutamine increased from no detectable enrichment at 0 mM glutamine to 63% enrichment at 1 mM glutamine, respectively (Figure 3-9B). Glutathione enrichment increased by an additional ~5% at 2 and 5 mM glutamine. Total glutathione abundance increased by more than 6 times when glutamine was increased from 0 mM to 1, 2, or 5 mM ($p < 0.0001$; Figure 3-9F); however, no differences in glutathione were observed among HCAEC cultured in 1, 2, or 5 mM glutamine.

Glutamate can also be metabolized to pyrroline-5-carboxylate (P5C), which can then be directed toward either proline synthesis or the ornithine cycle. Isotopic enrichment of proline increased by 36%, 43%, and 48% at 1, 2, and 5 mM 1-^{13}C-glutamine and 5-^{13}C-glutamine, respectively, compared to 0 mM glutamine (Figure 3-9B). Total proline abundance doubled in HCAEC cultured in 1 mM glutamine as compared to 0 mM glutamine (Figure 3-9G; $p = 0.0002$). Similar to glutathione, no difference in proline abundance was observed in HCAEC cultured in 1, 2, and 5 mM glutamine. In contrast, there was no detectable carbon enrichment in ornithine cycle metabolites (Figure 3-9C-E). However, total metabolite abundance in this pathway was altered by glutamine (Figure 3-9H-J). Increasing extracellular glutamine from 0 to 2 or 5 mM decreased total citrulline abundance by 47% ($p= 0.0153$) and 53% ($p=0.0039$), respectively. Similarly, increasing glutamine decreased total arginine abundance by 39% at 2 mM glutamine ($p= 0.0161$) and 46% at 5 mM glutamine ($p=0.0050$) compared to 0 mM glutamine. Total ornithine abundance remained unchanged across glutamine concentrations. Together, these data suggest that glutamine contributes carbon to glutathione and proline but not to ornithine cycle metabolites. Reduced arginine and citrulline abundance suggest that glutamine increased their utilization.

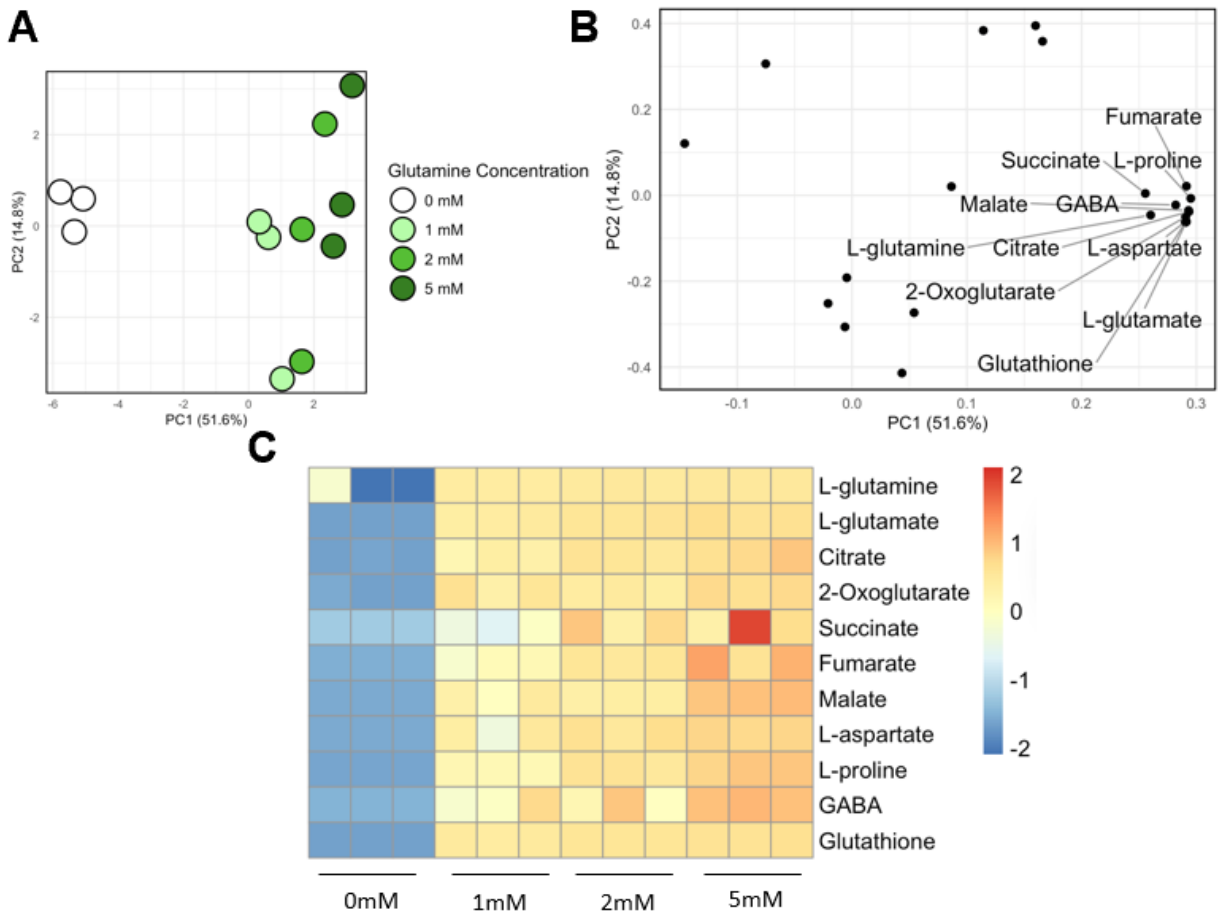

Figure 3-7: Glutamine carbons were incorporated into amino acids and glutathione in addition to TCA metabolites. HCAECs were cultured with 0, 1, 2, or 5 mM 5-^{13}C-glutamine for 24 hours, after which metabolites were extracted and profiled by LC–MS. (A) PCA score plot of the labeled fraction of each metabolite, showing a separation between cells cultured with versus without glutamine but minimal differences with increasing glutamine concentration. (B) PCA loading plot of the labeled fraction, with the top 11 loadings labeled. (C) Heatmap of metabolite labeled fractions.

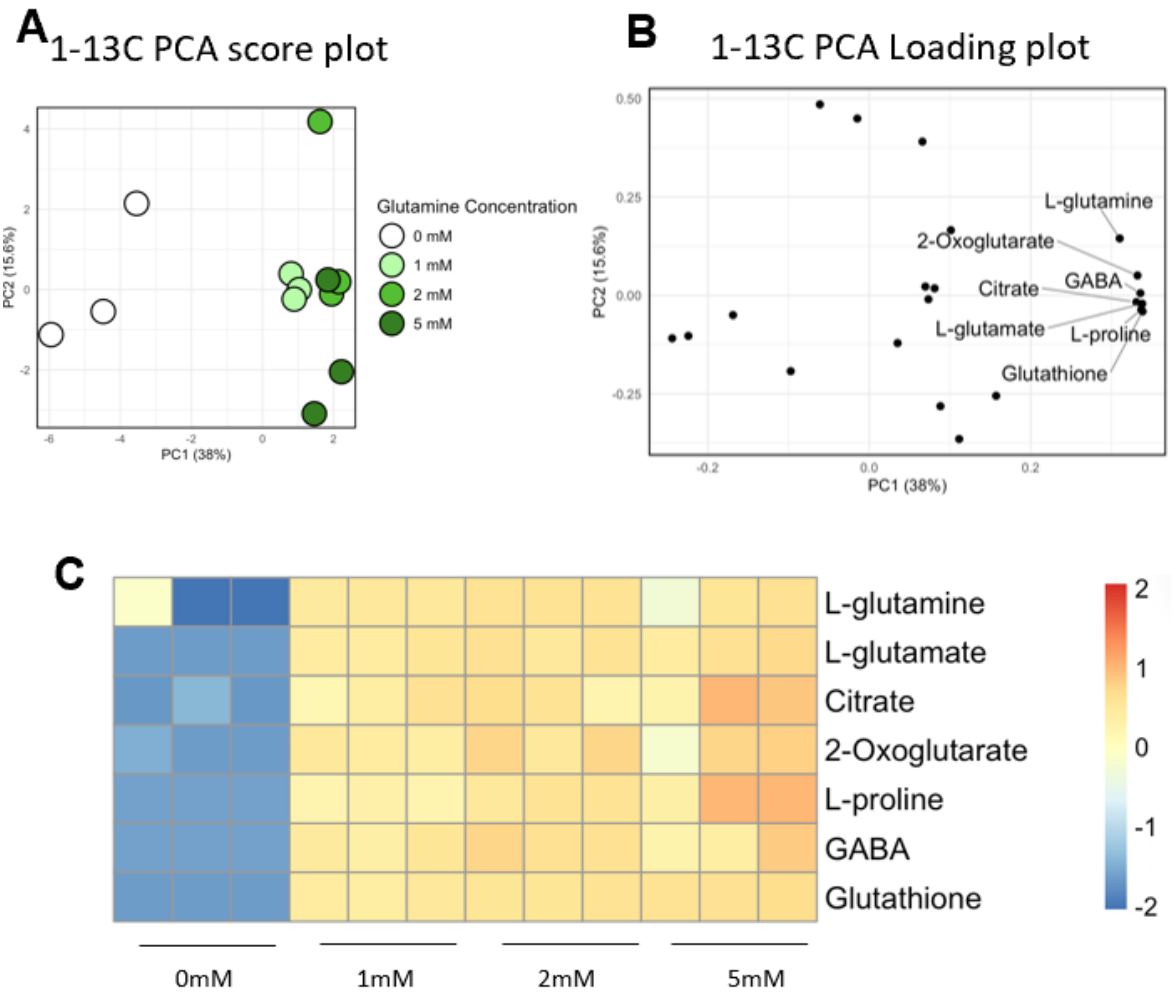

Figure 3-8: 1-^{13}C-glutamine carbons were incorporated into citrate through the reverse TCA cycle, as well as glutathione and L-proline. HCAECs were cultured with 0, 1, 2, or 5 mM 1-^{13}C-glutamine for 24 hours, after which metabolites were extracted and profiled by LC–MS. (A) PCA score plot of the labeled fraction of each metabolite, with the top 7 loadings labeled. (B) PCA loading plot of the labeled fraction. (C) Heatmap of metabolite labeled fractions. n=3 samples

3.3.7 Glutamine derived aspartate contributed carbons to UDP-GlcNAc.

Since I also observed isotope enrichment of aspartate, I next examined how increasing extracellular glutamine concentration impacts pathways downstream of aspartate such as UDP-GlcNAc synthesis. Glutamine-derived α-KG becomes oxaloacetate, which is then transaminated to form aspartate. Aspartate is incorporated into orotate, which becomes uridine triphosphate (UTP) and is then incorporated into UDP-GlcNAc (Figure 3-10). LC-MS analysis showed increased isotopic enrichment of aspartate from 5-^{13}C-glutamine, with enrichment increasing by

45%, 56%, and 60% at 1, 2, and 5 mM glutamine, respectively, compared to no glutamine (Figure 3-10A). Total aspartate abundance increased by 33-, 44-, and 70-fold as glutamine increased from 0 mM to 1, 2, and 5 mM, respectively ($p=0.0003$, <0.0001; Figure 3-10B). Isotopic distribution analysis from 5-^{13}C-glutamine revealed a progressive increase in labeled carbon incorporation into UDP-GlcNAc, with enrichment increasing by 7%, 9%, and 16% at 1, 2, and 5 mM glutamine, respectively (Figure 3-10C). In parallel, total UDP-GlcNAc abundance increased by around 50% as glutamine concentration increased from 0 to 2 or 5 mM glutamine ($p=0.0276$, and 0.0070, respectively; Figure 3-10D), with no differences observed between 2 and 5 mM glutamine. Collectively, these data suggest that glutamine enhanced UDP-GlcNAc synthesis through increased aspartate availability.

3.3.8 Glutamine altered fatty acid content and enhanced one-carbon metabolism.

Finally, I observed that the total abundance of poly unsaturated fatty acids (PUFA) eicosapentaenoic acid (EPA) and icosatrienoic acid decreased with increasing glutamine concentration. EPA abundance decreased by 70% for HCAEC in 1 mM glutamine as compared to 0 mM glutamine ($p<0.0001$, Figure 3-11A) and decreased an additional 12% for HCAEC in 5 mM glutamine ($p=0.0101$). Similarly, icosatrienoic acid abundance decreased by 48% for HCAEC in 1 mM glutamine as compared to 0 mM glutamine ($p=0.0034$, Figure 3-11A), with no additional decrease at higher glutamine concentrations.

I also observed significant alterations in metabolites associated with one-carbon (1C) metabolism, a process that supports purine biosynthesis, DNA and protein methylation, and redox homeostasis among others[181]. In the folate cycle, which supports one-carbon metabolism, the biologically active form of folate (tetrahydrofolate, THF) and its reduced form (5-methyl-THF)

serve as carriers for 1C units. New 1C units enter the folate cycle from the amino acids serine, glycine, and histidine among others. In our LC-MS data, increasing glutamine concentration from 0 to 2 mM decreased total folate abundance by 25% ($p=0.0078$), while increasing glutamine concentration from 0 to 5 mM decreased total folate abundance by 60% ($p=0.0001$, Figure 3-11B). Similarly, increasing glutamine concentration from 0 to 1, 2, or 5 mM decreased total histidine abundance by 51%, 61%, or 77% ($p<0.0001$ for all). Both glycine and serine showed smaller changes with increasing glutamine, with glycine 38% lower at 5 mM glutamine compared to 1 mM glutamine ($p=0.01870$). These data suggest that glutamine enhances 1C metabolism, perhaps to support endothelial cell proliferation.

3.4 Discussion:

Glutamine supplementation shows potential both *in vitro* and *in vivo* to preserve endothelial function under diverse stress conditions. However, how extracellular glutamine availability reprograms the endothelial cell metabolic network remains poorly defined. In this study, I systematically examined the metabolic fate of glutamine in human coronary artery endothelial cells over increasing concentrations (0 to 10 mM). I showed that endothelial cells continue to increase glutamine uptake as extracellular glutamine concentration increases, but glutamate secretion and oxidative respiration saturate above 2 mM glutamine, suggesting a limited capacity for glutaminolysis. Glutamine's carbons primarily enter the forward TCA cycle, with minimal contribution to reverse carboxylation, and support glutathione and non-essential amino acid synthesis. Although total TCA metabolite abundance increased with extracellular glutamine, succinate, PUFAs, and 1C metabolite levels declined. Together, these findings indicate that while

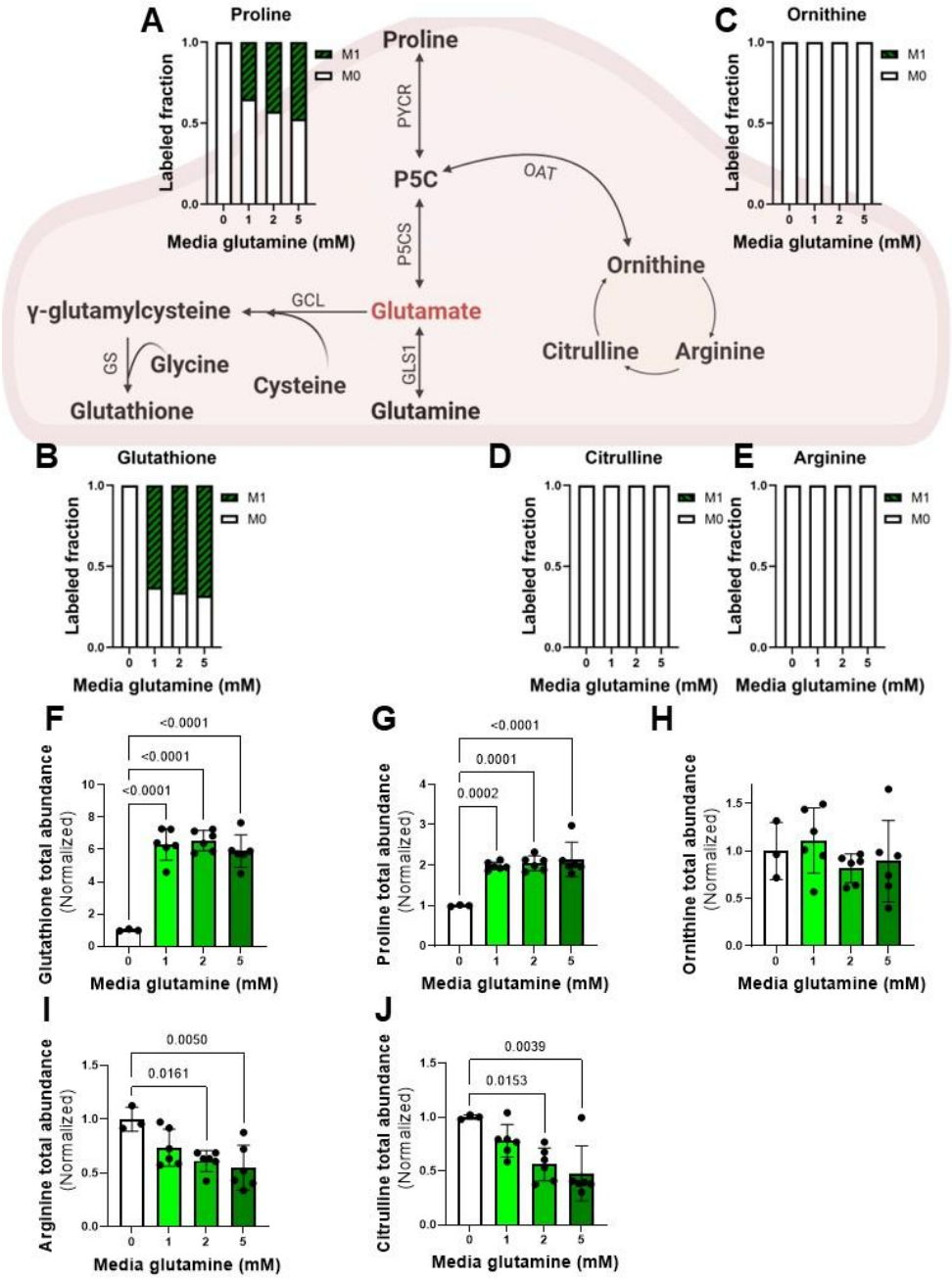

Figure 3-9: Glutathione and proline were enriched with glutamine-derived carbons. HCAECs were cultured with 0, 1, 2, or 5 mM 1-13C- or 5-13C-glutamine for 24 hours, after which cells were collected, and the isotope distribution and total abundance of metabolites were determined using LC-MS. (A-E) Glutathione, proline, ornithine, citrulline, and arginine isotope labeled fractions. n= 6 biological replicates. Quantification of total abundance of (F-J) proline, glutathione, ornithine, citrulline, and arginine. n=6 biologic replicates for 1,2,and 5 mM glutamine and n=3 biologic replicates for 0 mM glutamine. Data were analyzed using ordinary one-way ANOVA with a Tukey post-hoc multiple comparisons test.

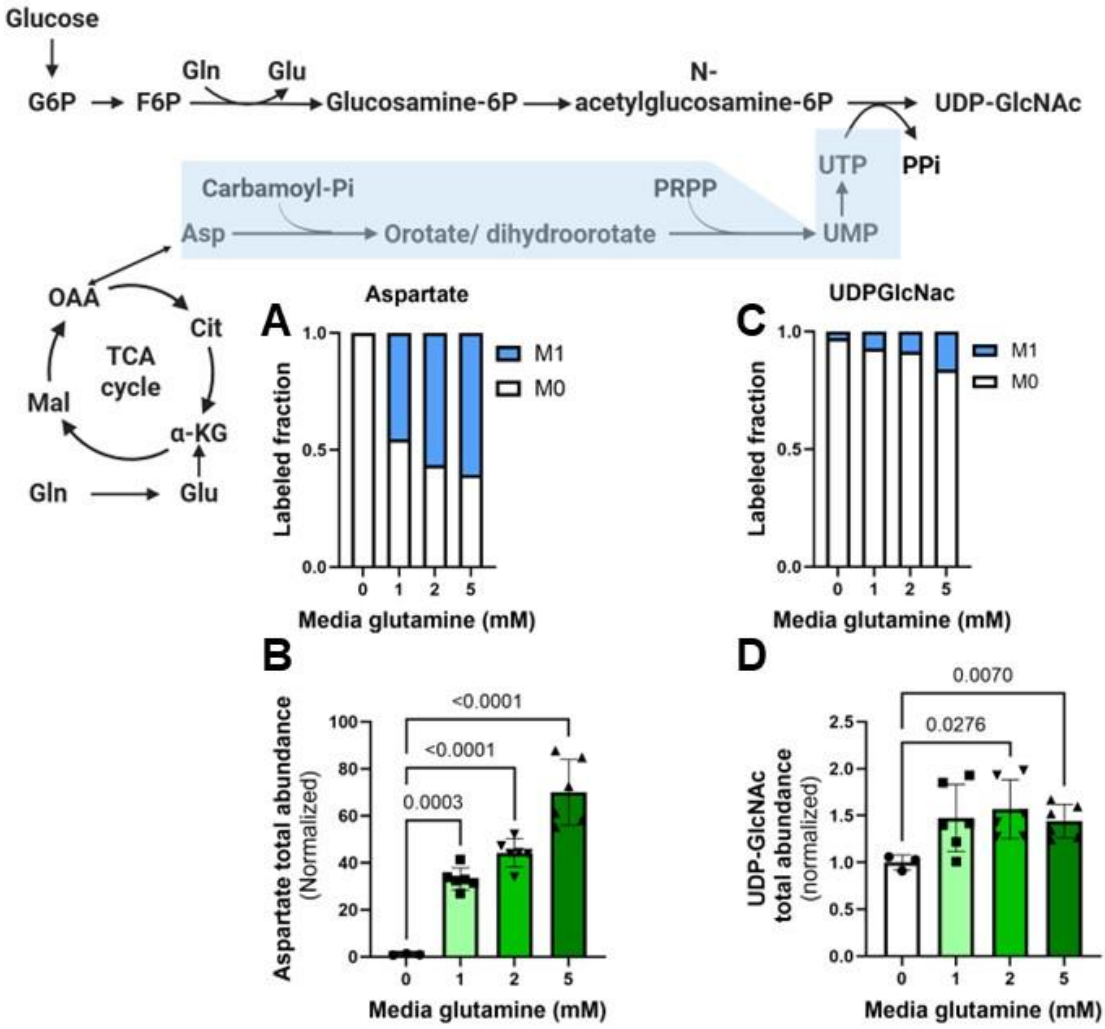

Figure 3-10: Glutamine derived aspartate contributed carbons to UDP-GlcNAc. Schematic of glutamine-derived aspartate incorporation into UDP-GlcNAc. Isotope enrichment from 5-^{13}C-glutamine into (A) aspartate, and (C) UDP-GlcNac. n=3 biological replicates. Quantification of total abundance of (B) aspartate, and (D) UDP-GlcNAc. n=6 biologic replicates for 1, 2, and 5 mM glutamine and n=3 biologic replicates for 0 mM glutamine. Data were analyzed using ordinary one-way ANOVA with a Tukey post-hoc multiple comparisons test.

endothelial cells take up more glutamine when it is available, excess glutamine is stored rather than metabolized. The presence of glutamine, but not its excess, sustains the TCA cycle, amino acid synthesis, redox balance, and 1C metabolism flux.

In both normal and high glucose conditions, glutamine uptake and intracellular glutamine increased with extracellular glutamine concentration. While others have shown that increasing extracellular glutamine from 0 to 2 mM increased intracellular glutamine, for example in bovine

venular endothelial cells [161] and in human diploid fibroblasts[189] , our study is the first to our knowledge to examine the extremely high glutamine concentrations often used in *in vitro* cell culture. Excess glutamine uptake would come at a cost to the endothelial cell, given that the primary glutamine importer ASCT2 (SLC1A5) imports sodium and exports a neutral amino acid (e.g., serine, threonine). Glutamine uptake would increase energy use, since the cell must use the Na^+/K^+ ATPase to maintain the sodium gradient. This excess energy likely comes from oxidative respiration, since I did not observe an increase in glycolysis. The net export of amino acids by ASCT2 would also need to be countered by amino acid import from system A and N transporters (SNAT1-5). It remains unclear why the endothelial cells take up excess glutamine.

In contrast, intracellular glutamate and glutamate secretion plateaued above 2 mM glutamine. Intracellular glutamate saturation may occur due to limitations in its production, while extracellular glutamate saturation may occur due to limitations in its export. Glutamine is metabolized to glutamate by GLS-1. I measured an increase in GLS-1 as glutamine increased from 0 to 0.5 mM but no further increase up to 2 mM glutamine. Furthermore, intracellular glutamate binds to and reduces GLS-1 activity [190]. Thus, GLS-1 availability and activity may limit glutamine conversion to glutamate despite continued glutamine uptake. The observed extracellular glutamate plateau may reflect limits in amino acid exchange. Glutamate export is functionally coupled to cystine uptake through the cystine–glutamate antiporter xCT. In human diploid fibroblasts, extracellular glutamate increased with extracellular cystine, indicating that extracellular cystine is essential for glutamate efflux [189]. Therefore, glutamine-derived intracellular glutamate could be exported in exchange for extracellular cystine up to the point at which cystine availability becomes limiting. These data suggest that glutamine supplementation alone may not be sufficient to fully

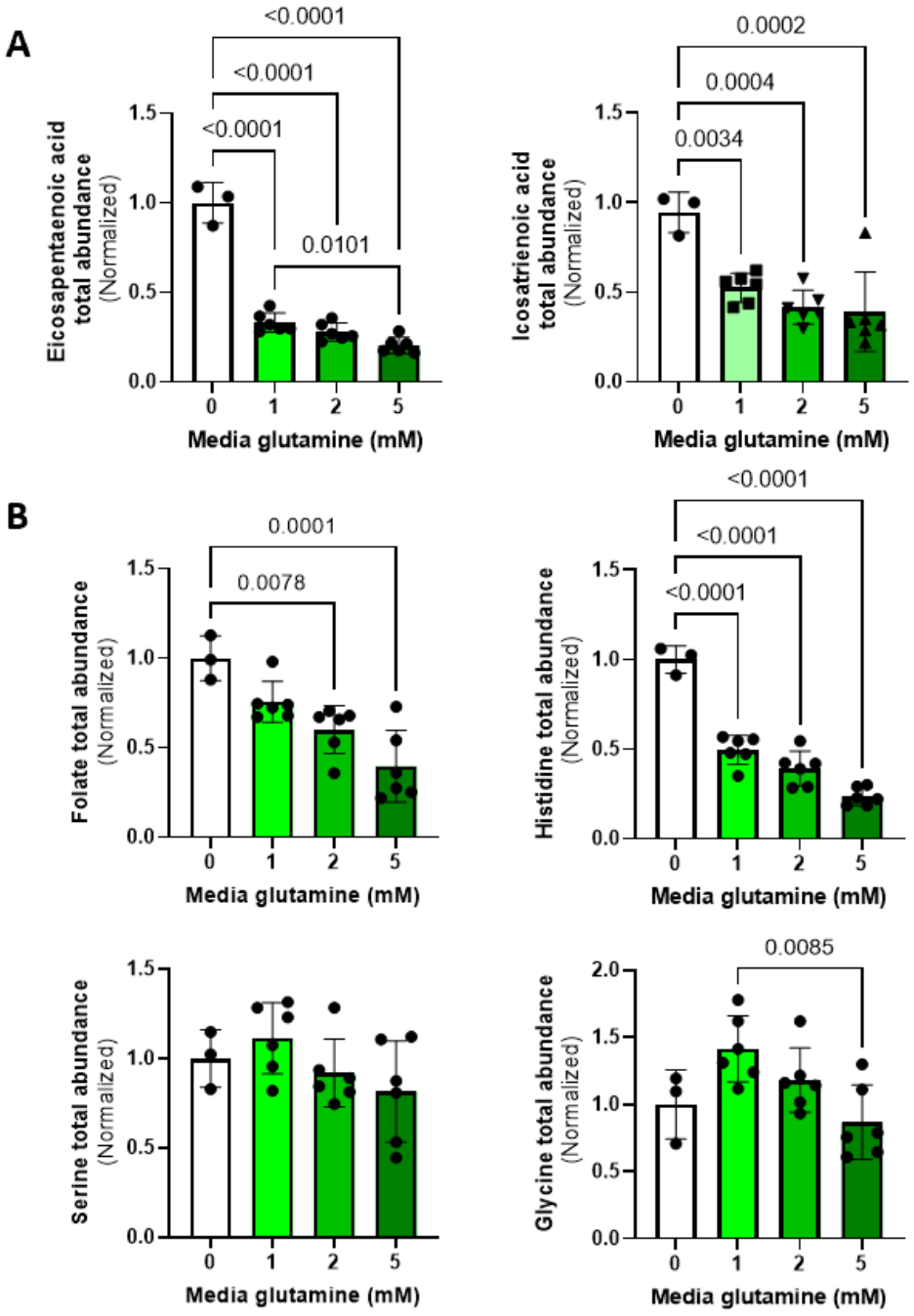

Figure 3-11:Glutamine decreased fatty acids and enhanced one-carbon metabolism. HCAECs were treated with 0, 1, 2, and 5 mM 1-^{13}C- or 5-^{13}C-glutamine for 24 hours, after which cells were collected, and the total metabolite abundance was determined using LC-MS. Total abundance for (A) eicosapentaenoic acid (EPA) and icosatrienoic acid and (B) one carbon metabolites (folate, histidine, serine, glycine). n=6 samples for 1, 2, and 5 mM glutamine and n=3 samples for 0 mM glutamine. Data were analyzed using ordinary one-way ANOVA with a Tukey post-hoc multiple comparisons test.

exploit the protective effects of glutamine, including enhanced antioxidant capacity and inflammation reduction [85,191–193]. Increasing GLS-1 expression or activity or promoting glutamate efflux through increased extracellular cystine may be required.

Our data confirm work by others showing that glutamine is a major mitochondrial substrate for endothelial cells, primarily in the forward TCA cycle but also in reductive carboxylation [77,171]. I measured lower glutamine reductive carboxylation than in other studies (5% vs. 13%) [77,171]. This difference could relate to variations in experimental conditions, including cell type (HUVEC vs. HCAEC) and culture conditions, specifically nutrient and oxygen availability. For example, in the A549 cell line cultured with glutamine conditions for 24 hours, reductive carboxylation increased from around 10% to 80% in hypoxia [194]. I also observed higher non-mitochondrial oxygen consumption with glutamine, which could indicate increased NOX activity [195]. I previously showed that glutamine increases HAEC NADPH production, providing more substrate for NOX [191] . Additionally, in rat neutrophils, 2 mM glutamine increased NOX activity by 74% [196]. Together, our data confirm that glutamine contributes carbons to the forward and reverse TCA cycle and increases non-mitochondrial oxygen consumption, likely through increased NADPH production and NOX activity.

In contrast to other TCA metabolites, which increased with extracellular glutamine, succinate decreased as glutamine concentration rose. I measured a large unlabeled intracellular succinate pool in our HCAEC, which is consistent with studies in HUVEC and iPSC-derived brain microvascular endothelial cells [73,197]. The large succinate pool suggests incomplete mitochondrial oxidation in endothelial cells, perhaps due to adequate energy production from glycolysis or a need to reduce oxidative stress generation from succinate oxidation [198]. In HepG2 cells, glutamine deprivation promoted deSUMOylation of succinate dehydrogenase substrate A (SDHA),

impairing SDH assembly and activity[188]. Consistent with this, our data showed that glutamine enhanced SDH activity, which likely increased succinate consumption and reduced the intracellular succinate pool. Intracellularly, succinate stabilizes HIF-1α and alters DNA and histone methylation, while extracellularly succinate activates SUCNR1 (GPR91) on endothelial and immune cells to promote angiogenesis and inflammation [199]. Indeed, elevated succinate has been linked to cardiometabolic disease [200,201]. I did not observe increased media succinate with glutamine, suggesting that glutamine does not reduce intracellular succinate via succinate release. However, glutamine could blunt succinate-induced inflammatory responses by reducing the intracellular succinate pool.

I and others demonstrated that glutamine reduces intracellular oxidative stress through glutathione (GSH) synthesis [133,191]. However, increasing glutamine above 1 mM did not further increase GSH concentration. The first step of GSH synthesis, in which glutamate and cysteine are combined in a reaction catalyzed by glutamate cysteine ligase (GCL), is rate-limiting and may explain the plateau in GSH production [153] . The glutamate concentration at which this reaction rate is half of its maximum velocity (K_m) is 1.8 mM, which is much lower than the estimated intracellular glutamate concentration (~21 mM in fibroblasts). Thus GCL is likely already saturated with glutamate, so additional glutamine-derived glutamate would not increase GSH production [189]. Furthermore, GSH itself binds to the glutamate site on GCL to inhibit its activity (K_i=2.3 mM), meaning that high GSH can also reduce GSH production [202]. Thus, high extracellular glutamine alone is not sufficient to increase endothelial GSH.

I also observed proline enrichment from glutamine-derived carbon, which aligns with endothelial ^{13}C-glutamine tracing by others[77] . Glutamate is converted to 1-pyrroline-5-carboxylate (P5C) and then reduced to proline via a reversible metabolic cycle. Proline is critical for synthesis

of collagen, an essential component of the vascular basement membrane and extracellular matrix [203]. ^{14}C-proline added to calf aortic endothelial cells resulted in 10% hydroxy-^{14}C-proline in collagen isolated from the culture medium [204]. Enhanced collagen synthesis capacity with glutamine could support vessel integrity and remodeling, as well as vessel stiffening in aging and disease. Proline can also be converted back to glutamate to support mitochondrial metabolism and redox balance. In this way, proline both in the extracellular matrix and inside the cells could serve as a carbon and redox reservoir.

Ornithine cycle metabolites were not labeled with glutamine-derived carbons, but both citrulline and arginine decreased in abundance with extracellular glutamine. Ornithine aminotransferase (OAT) catalyzes the reversible reaction between P5C and ornithine. Given the lack of ^{13}C labelled ornithine, this reaction appears to be primarily in the direction of P5C production from ornithine in our endothelial cells. Reduction of citrulline and arginine abundance can be explained by inhibited citrulline transport and reduced citrulline to arginine conversion. In bovine endothelial cells, extracellular glutamine reduced intracellular citrulline by inhibiting citrulline transport, likely because they share some of the same neutral amino acid transporters [205]. Furthermore, 2 mM glutamine inhibited arginine production from citrulline via argininosuccinate in bovine aortic endothelial cells [163]. Some studies also suggest that cultured endothelial cells do not have detectable carbamoyl-phosphate synthase I (CPS-I) activity, which is essential to transform ornithine into arginine [87].The decreased arginine with increasing glutamine may lead to decreased substrate availability for NO synthesis and impaired NO bioavailability. Thus, glutamine supplementation must be carefully titrated to maintain the endothelial cell arginine pool.

The observed increase in UDP-GlcNAc abundance and isotopic enrichment from 5-^{13}C-glutamine shows that glutamine and its carbons contribute to the endothelial cell HBP. Glutamine

provides a nitrogen to convert fructose-6-phosphate into glucosamine-6-phosphate early in the HBP [172], and glutamine abundance correlates with UDP-GlcNAc synthesis[206] . However, UDP-GlcNAc synthesis integrates many metabolic inputs, one of which is uridine supplied by pyrimidine nucleotide metabolism [181]. I observed increased aspartate total abundance and glutamine-derived isotopic enrichment, suggesting that glutamine-derived aspartate contributes to UDP-GlcNAc formation[207.] ıncreased endothelial UDP-GlcNAc can lead to eNOS O-GlcNAcylation reduced NO availability [90,138,160–162].

Increased extracellular glutamine decreased the long-chain polyunsaturated fatty acids (PUFAs) EPA and eicosatrienoic acid, which incorporate into cell membrane phospholipids to increase membrane fluidity. As the ω3 PUFA concentration increased for cultured HUVEC, polyunsaturated to saturated membrane fatty acid ratio increased by 33%, confirming PUFA incorporation into endothelial cell membranes [208]. Decreased PUFA quantity could relate to increased consumption or decreased uptake or liberation from membrane. PUFAs can be used for energy generation; however, this usually occurs compensatorily when other TCA metabolites such as glutamine are low [209]. PUFAs can be precursors for eicosanoids (e.g., prostaglandins, thromboxanes), which are essential vascular signaling molecules. Decreased PUFA quantity with glutamine could relate to increased eicosanoid synthesis. While additional experimental data are needed to determine the mechanism by which PUFA content decreased, as well as its effect on endothelial cell function, decreased endothelial PUFA content could reduce cell membrane fluidity and be detrimental for vascular health[168].

Finally, increasing glutamine decrease folate and histidine abundance, suggesting increased 1C metabolism flux. 1C metabolism is essential for nucleotide and amino acid biosynthesis, methylation reactions, and redox balance [181] . In the 1C pathway, folate serves as the

central carrier by accepting and transferring single-carbon units. Histidine and serine contribute 1C units to folate in the cytosol, while serine and glycine contribute 1C units to folate in mitochondria [181] . The increased 1C metabolism flux could relate to glutamine-induced enhanced cell proliferation via nucleotide synthesis [85] or to enhanced antioxidants [85,191]. Indeed, glutamine-derived aspartate activated mTORC1 signaling in HUVEC and human breast tumor endothelial cells, which then led to overexpression of 1C metabolism enzymes [210]. Additional experiments would be required to investigate this mechanism.

3.5 Limitations:

While our study shows the impact of glutamine on endothelial cells in culture, it is not without limitations. I treated endothelial cells near confluence, when endothelial cells are predominantly quiescent; however, I did not directly control and assess cell cycle phase. Because metabolic fluxes and isotopic labeling patterns differ between proliferating and quiescent endothelial cells [207], it would be interesting to compare glutamine metabolism across defined cell cycle states. In addition, while stable isotope tracing provided insight into glutamine carbon use in the forward and reverse TCA cycle, the use of single-position ^{13}C tracers limited our ability to resolve all possible carbon and nitrogen entry routes into downstream pathways. Finally, our analyses were performed at isotopic steady state following 24 hour incubations and therefore reflect net metabolic outcomes rather than dynamic flux changes. Dynamic tracing experiments would be useful to capture transient metabolic reprogramming with glutamine availability.

3.6. Conclusion:

In summary, our work expands upon prior studies to define how increasing extracellular glutamine reprograms endothelial metabolism across a higher than physiological range, including concentrations commonly used in cell culture media. Using functional and isotope assisted metabolomics, I show that endothelial cells increase glutamine uptake with increased availability, while glutamate secretion and glutaminolysis saturated above 2 mM glutamine. Glutamine increased most TCA cycle metabolites, glutathione, proline, aspartate, and UDP-GlcNAc, while reducing succinate, citrulline, arginine, PUFAs, folate, and histidine. Together, these findings highlight glutamine as a metabolic regulator that supports the endothelial TCA cycle, endothelial redox homeostasis, reduced inflammation, vascular stability, and proliferation; however, glutamine also could reduce endothelial NO and stiffen cell membranes. Thus, glutamine supplementation should be used in moderation, with a full understanding of its widespread effects.

Chapter 4: Impact of diabetes on red blood cells and their interaction with endothelial cells via extracellular vesicles.

4.1 Introduction

Diabetes increases oxidative stress [211], with diabetic subjects showing elevated oxidative damage to serum lipids and proteins [212]. While research into the effects of diabetic oxidative stress mainly focuses on vascular and immune cells, red blood cells (RBCs) have emerged as active regulators of vascular homeostasis [67,122,213]. Beyond their role as oxygen carriers, RBCs influence endothelial signaling through ATP release and regulation of nitric oxide (NO) bioavailability [47,67,122]. In diabetes, RBCs undergo significant pathological alterations, including increased oxidative stress, increased adhesiveness to the endothelium, and impaired deformability, which all together increase the risk of cardiovascular disease [214,215].

Under normal physiological conditions, RBCs generate reactive oxygen species (ROS) through non-enzymatic mechanisms such as hemoglobin auto-oxidation and enzymatic reactions like NADPH oxidase (NOX) [216,217]. In diabetes, increased intracellular glucose accelerates glycation of hemoglobin and other RBC proteins, increasing hemoglobin redox instability, altering membrane or cytosolic enzyme activities, and increasing the probability of heme/iron liberation and oxidative stress [213]. Additionally, hyperglycemia can directly increase ROS through the formation of advanced glycation end-products (AGEs). It has been shown that diabetic patients have higher AGE levels in their serum compared to non-diabetic controls [218]. Once AGE binds to its receptor, RAGE, it activates NOX, leading to further ROS production [219].

Thus diabetes alters enzyme activity and pro-oxidant signaling that can increase net ROS production, with clinical and ex vivo type 2 diabetes studies directly showing elevated RBC ROS and redox-mediated vascular effects [67,213,214].

RBCs possess a robust antioxidant defense system, including superoxide dismutase (SOD), catalase, and glutathione (GSH), which help maintain redox homeostasis[217]. However, in diabetes, the balance between ROS generation and scavenging by the antioxidant system is perturbed. In chronic hyperglycemia, glucose and its alpha-hydroxy aldehydes undergo auto-oxidation, leading to the generation of methylglyoxal, glyoxal, and 3-deoxyglucosone. These can glycate proteins such as SOD, resulting in its inactivation and impairment of the oxidative defense system [220]. Additionally, a significant reduction in GSH in diabetic patients has been reported [221]. GSH is a tripeptide composed of glutamate, cysteine, and glycine and represents one of the most abundant intracellular antioxidants. GSH serves as a critical reducing equivalent for enzymes such as glutathione peroxidase and glutaredoxin, and its regeneration from its oxidized form (GSSG) by glutathione reductase requires NADPH. Hyperglycemia also reduces NADPH availability for GSH regeneration through increased glucose flux into the polyol pathway, which consumes NADPH [220]. Thus, hyperglycemia in diabetes induces RBC oxidative stress by impairing antioxidant defense, contributing to the development of vascular complications.

One strategy to increase RBC GSH is to incubate RBC with extracellular glutamine. Glutamate is a major building block of GSH; however, the RBC membrane is impermeable to glutamate [222,223]. Consequently, RBCs must take up glutamine, which is then converted intracellularly to glutamate via glutaminase-1 (GLS-1). Reduced serum glutamine has been reported in diabetic subjects, which may impair RBCs ability to maintain GSH [129]. In sickle cell disease, oral L-glutamine supplementation is an FDA approved therapy that is hypothesized to

reduce oxidative stress by increasing intracellular NADPH and GSH regeneration [111,224]. However, whether such supplementation can restore antioxidant capacity in diabetic RBCs remains uncertain.

RBCs communicate with other cells in the vascular wall through extracellular vesicles (RBC-EVs) [67,225]. RBCs shed EVs under shear stress and oxidative conditions, and RBC-EVs carry bioactive cargo such as hemoglobin, heme, and pro-oxidant enzymes like arginase-1 that can be taken up by endothelial cells [46,67,69]. In diabetes, both the quantity and cargo of these EVs may be altered. A recent study suggests that RBC-EVs from diabetic subjects are internalized more by endothelial cells, where they induce ROS production and impair vascular relaxation by transferring arginase-1. However, in this study, RBC-EVs were generated through storage, which is not physiological [67]. There are multiple ways to generate EVs from RBCs *in vitro*, including storage, calcium ionophore treatment, and mechanical stimulation [46]. While storage derived EVs are often pathogenic, the impact of EVs generated under physiological shear stress remains less understood [46]. In this study, I determined the impact of RBC-EVs generated via a more physiologically relevant method (mechanical stimulation) on endothelial cell function *in vitro*.

In this chapter, I studied how glutamine supplementation impacted RBCs from non-diabetic and diabetic subjects. I also generated RBC-EVs from diabetic and non-diabetic subjects by stimulating the mechanosensitive ion channel Piezo1 and determined their internalization and impact on endothelial cell function. *I hypothesized that RBC glutamine supplementation would increase their antioxidant defense via increased GSH synthesis*. *I further hypothesized that RBC-EVs from diabetic subjects would carry more pro-oxidant and pro-inflammatory molecules compared to RBC-EVs from non-diabetic subjects, leading to increased endothelial cell inflammation and oxidative stress.*

4.2 Methods

4.2.1 Red blood cell isolation

Blood was collected from human subjects under protocols approved by the University of Maryland, Baltimore (UMB) Institutional Review Board (IRB) (IRB#: HP-00107788, and 1385293-7). All participants provided written informed consent prior to enrollment. Venous blood was collected from diabetic and non-diabetic men and women between 18 and 88 years of age. Participants were excluded if they had severe anemia (hemoglobin < 8 g/dL), blood dyscrasias, end-stage renal disease, cirrhosis, splenomegaly, active tobacco or nicotine use, body weight < 110 lbs, body mass index (BMI) > 40 kg/m², pregnancy, illicit drug use, or alcohol abuse. Men and women were recruited irrespective of race or socioeconomic status (Table 1). Blood was collected into ethylenediaminetetraacetic acid (EDTA) tubes (BD), gently inverted 10 times to prevent coagulation, and placed on ice until red blood cell (RBC) isolation on the same day. To collect RBC, whole blood was centrifuged at 600 ×g for 5 minutes at room temperature. Plasma was collected and stored at −80°C until further use. The buffy coat was removed, and the packed RBCs were then washed three times with Hank's Balanced Salt Solution (HBSS; MilliporeSigma, 55037C).

4.2.2 RBC-EV generation and isolation

RBCs were resuspended at 18% hematocrit (Hct) in HBSS. RBC-EVs were generated by treating RBCs with 10 μM of the Piezo-1 agonist Yoda1 (Sigma-Aldrich, SML1558) in a humidified 5% CO_2 incubator at 37°C for 30 minutes, as previously described[46]. Cell debris was removed by sequential differential centrifugation at 600 ×*g* for 20 minutes, 1,500 ×*g* for 15 minutes, and 3,200

×*g* for 15 minutes at room temperature, followed by centrifugation at 10,000 ×*g* for 30 minutes at 4°C. The resulting supernatant was passed through a 0.22 μm polyethersulfone syringe filter (Advangene, SD Filter-PES-0/22-30-S). The filtrate containing EV-rich HBSS was then ultracentrifuged at 100,000 ×*g* for 70 minutes. The final RBC-EV pellet was resuspended in 200 μL HBSS, aliquoted, and stored at −80°C until use.

4.2.3 RBC-EVs size and concentration

Tunable resistive pulse sensing (TRPS) was used to quantify RBC-EV concentration and size distribution (50–330 nm) using a qNano Gold (Izon Science) equipped with NP100 nanopore membranes (Izon, NP100). The system was calibrated using CPC100 beads with a known mean diameter of 100 nm (Izon, CPC100). Prior to analysis, RBC-EV samples were filtered through 0.22 μm Ultrafree-MC centrifugal filter unit (MilliporeSigma, UFC30GV) to remove large particles that could clog the nanopore. The TRPS voltage was set between 0.5–0.7 V to achieve a stable baseline current of approximately 130 nA. RBC-EVs were diluted 1:100 in measuring electrolyte (ME) solution (Izon, PK3). Particles were recorded when the root mean square (RMS) noise was below 10 pA and the particle rate was stable and linear. At least 500 particles were counted per sample at particle rates between 200–1,500 particles/min under applied pressures of 5 or 10 mbar.

4.2.4 Plasma and RBC intracellular metabolites

A YSI 2950 Bioanalyzer (Yellow Springs Instruments, 527690) was used to measure glucose, lactate, glutamine, and glutamate concentrations in plasma and RBC samples. For intracellular RBC metabolite measurements, isolated RBCs were lysed by mixing with deionized (DI) water at a 1:1 ratio (e.g., 300 μL RBCs with 300 μL DI water) and vortexed to ensure complete

lysis. 150 μL of the lysate was then loaded into individual wells of a 96-well plate (CELLTREAT,229196) for analysis. Plasma samples from each participant were similarly loaded into individual wells of a 96-well plate. Metabolite concentrations in plasma and RBC lysates were quantified using the YSI bioanalyzer according to the manufacturer's instructions.

4.2.5 RBC reactive oxygen species (ROS)

Intracellular ROS were measured using 5-(and-6)-chloromethyl-2′,7′-dichlorodihydrofluorescein diacetate, acetyl ester (CM-H_2DCFDA; Invitrogen, C6827), a general ROS-sensitive fluorescent probe that becomes fluorescent upon intracellular oxidation. Fluorescence was quantified using a plate reader or by flow cytometry. Isolated RBCs from each participant were resuspended in HBSS at 0.02% Hct (plate reader) or 1% Hct (flow cytometry). CM-H_2DCFDA was added at a final concentration of 1 μM, and cells were incubated for 30 minutes at 37°C. To assess antioxidant capacity, a subset of RBCs was pre-treated with 60 μM tert-butyl hydroperoxide (tBHP; Sigma-Aldrich, 458139) for 30 minutes at 37°C prior to addition of CM-H_2DCFDA. A positive control treated with 200 μM tBHP was included. Following incubation with CM-H_2DCFDA, RBCs were centrifuged at 600 ×g for 1 minute to remove excess dye, washed once with HBSS, and resuspended in an equal volume of HBSS.

For plate reader measurements, 200 μL of each sample was transferred to a black 96-well plate (Greiner Bio-One, 655090). Fluorescence was measured using a Spark multimode plate reader (TECAN) at 492–495 nm excitation and 517–527 nm emission. After fluorescence measurement, RBCs were lysed using RIPA buffer (Thermo Fisher Scientific, 89901) to determine protein concentration by bicinchoninic acid (BCA) assay (Thermo Fisher Scientific, 23225). Fluorescence intensity was normalized to total protein concentration for each sample.

For flow cytometry measurements, samples were transferred to 5 mL round-bottom polystyrene FACS tubes (Corning, 352008) and analyzed using a FACSCelesta flow cytometer (BD Biosciences). FITC fluorescence was excited with the 488-nm blue laser and detected using a 530/30 band-pass filter. Samples were acquired at a medium flow rate (35 µL/min) using sheath fluid according to the manufacturer's settings. To ensure single-cell analysis, RBCs were first identified based on FSC-A and SSC-A characteristics, and debris was excluded by gating the main RBC population. Doublets and aggregates were excluded using FSC-A vs FSC-H, and a gate was applied to include only linear events. For each condition, 10,000 single-cell events were collected. RBCs without CM-H_2DCFDA and RBCs treated with 200 µM TBHP were included as background and positive controls, respectively. The mean fluorescence intensity (MFI) of the gated single RBC population in the FITC channel was calculated and used as a quantitative measure of intracellular ROS levels.

4.2.6 RBC glutamine treatment

Isolated RBCs were resuspended at 10% Hct in HBSS supplemented with 1% PS, 5.5 mM D-glucose, and 0, 2, 10, or 20 mM glutamine. Cells were incubated at 37°C in a humidified 5% CO_2 incubator for 1 or 2 days. Following incubation, RBCs were diluted to 1% Hct for ROS and GSH measurements or lysed for YSI analysis as described. To determine the impact of glutamine on nicotinamide adenine dinucleotide phosphate (NADPH) oxidase (NOX) activity, RBCs were treated with diphenyleneiodonium chloride (DPI). DPI inhibits NOX by reacting with its flavin and heme prosthetic groups, forming stable adducts [226]. RBCs were incubated with 10 µM DPI for 1 hour at 37°C in a 5% CO_2 incubator.

4.2.7 Total glutathione analysis

RBCs were incubated with 0 or 2 mM glutamine, with or without 250 μM glycine and 25 μM L-cysteine hydrochloride monohydrate (Sigma-Aldrich, 30129), on an orbital shaker plate at 37°C in a humidified 5% CO_2 incubator for 24 hours. Total glutathione was measured using the GSH-GSSG Glo assay (Promega, V6612) according to the manufacturer's protocol for cells in suspension. Briefly, RBCs at 1% Hct were loaded into a white-bottom 96-well polystyrene plate (Sigma-Aldrich, CLS3917) and lysed for 5 minutes at room temperature. Following lysis, luciferin-NT substrate, glutathione S-transferase, and luciferin generation reagent were added, and samples were incubated for 30 minutes at room temperature. Luciferin detection reagent was then added, and samples were incubated for an additional 15 minutes before luminescence was measured using a Spark multimode plate reader. Glutathione concentration was determined using a standard curve generated according to the manufacturer's instructions.

4.2.8 Endothelial cell culture

Primary human coronary artery endothelial cells (HCAECs; passages 5–9) were purchased from Lifeline Cell Technology. HCAECs were cultured in Endothelial Growth Medium-2 (EGM-2; Lonza) supplemented with 1% penicillin-streptomycin (PS; ThermoFisher, 15140163), 10% fetal bovine serum (FBS; Cytiva, SH30088), and 1% glutamine (Fisher Scientific, 25-030-081) until approximately 90% confluent. HCAEC were rinsed with phosphate-buffered saline (PBS; Thermo Fisher Scientific, 70011069), and then 1×10^{10} RBC-EVs particles/mL in EBM-2 supplemented with 1% PS were added to the HCAEC monolayer and incubated for 24 hours at 37°C in a humidified 5% CO_2 incubator. To confirm that observed changes in HCAECs were due to RBC-EVs and not RBC-EV contents released into the extracellular media, 1×10^{10} RBC-EVs were incubated in EBM-2 supplemented with 1% PS for 24 hours at 37°C in a 5% CO_2 incubator.

The RBC-EV conditioned media (EV-CM) was then collected after ultracentrifugation at 100,000 × g to remove intact RBC-EVs.

4.2.9 Western blot

Western blot was used to detect EV-specific markers in isolated RBC-EVs and to assess the impact of RBC-EVs on HCAEC protein expression. For RBC-EV lysate preparation, RBC-EVs were adjusted to 2×10^{10} particles and brought to a final volume of 39 µL with PBS. Sample buffer (15 µL; Thermo Scientific, NP0008) and reducing agent (6 µL; Thermo Fisher Scientific, NP0009) were added, and samples were heated at 70°C for 5 minutes. Proteins were then loaded into each well of a Bolt™ 4–12% Bis-Tris gel (Thermo Fisher Scientific, NW04120BOX) and separated by SDS-PAGE.

For endothelial cell lysate preparation, HCAECs were washed with PBS after 24 hours of incubation with RBC-EVs and lysed in RIPA buffer (Thermo Fisher Scientific, 89901) containing Halt protease and phosphatase inhibitor cocktail (Thermo Fisher Scientific, 78440) and EDTA. Lysates were centrifuged at 17,000 ×*g* for 15 minutes at 4°C to remove cellular debris. The supernatant was collected, and protein concentration was determined using a BCA assay. 3.5 µg protein was loaded into each well of a NuPAGE 4–12% Bis-Tris gel (Thermo Fisher Scientific, NP0323BOX) for separation by SDS-PAGE.

Proteins were transferred to a polyvinylidene difluoride membrane (Thermo Fisher Scientific, IB34001X3) using an iBlot 3 (Thermo Fisher Scientific). Membranes were blocked in 5% bovine serum albumin (BSA; Sigma-Aldrich, A7906) in tris-buffered saline (TBS; Fisher Scientific, BP24711) containing 0.5% Tween (TBS-T; Thermo Fisher Scientific, 85115) for 1 hour at room temperature. Blots were incubated overnight at 4°C with primary antibodies diluted in 1% BSA in TBS-T. Primary antibodies included ALIX (Santa Cruz Biotechnology, sc-53538),

TSG101 (Santa Cruz Biotechnology, sc-7964), CD9 (Santa Cruz Biotechnology, sc-13118), band3 (Santa Cruz Biotechnology, sc-133190), hemoglobin-α (Santa Cruz Biotechnology, sc-514378), glutaminase-1 (Abcam, EP7212), HO-1 (Cell Signaling, 43966), GAPDH (Cell Signaling, 14C10), and β-Actin (Santa Cruz Biotechnology, sc-47778). Membranes were washed with TBS-T and incubated with appropriate anti-rabbit (Promega, W4011) or anti-mouse (Promega, W4021) secondary antibodies (1:2000) for 2 hours at room temperature. Protein bands were visualized using SuperSignal West Pico PLUS Chemiluminescent Substrate (Thermo Fisher Scientific, 34578) and imaged with an Alpha Innotech FluorChem SP Digital Imaging System. Band intensity was quantified using Fiji ImageJ by measuring mean gray intensity.

4.2.10 Viability

Endothelial cell viability after RBC-EV treatment was assessed using ethidium homodimer (EthD-1; ThermoFisher, E1169), which fluoresces red upon binding to DNA of permeabilized dead cells. Calcein AM (Thermo Fisher Scientific, C34852) was used as a live cell marker. Calcein AM is non-fluorescent and enters cells, where it generates green fluorescence following acetoxymethyl ester hydrolysis by intracellular esterases. After rinsing HCAECs with PBS, 5 μM EthD-1 and 10 μM Calcein AM were added in EBM-2 media supplemented with 1% PS and incubated for 30 minutes at room temperature. As a positive control for cell death, 50% methanol was added to selected wells for 10 minutes. Following washing with PBS, cells were imaged using a Revolve microscope (ECHO) at 20× magnification. Live (green) and dead (red) cells were quantified using ImageJ software. Percent viability was calculated as:

$$\text{Viability (\%)} = \frac{\text{Number of live cells}}{\text{Total number of live + dead cells}} \times 100$$

4.2.11 HCAEC ROS Measurement

HCAECs treated with RBC-EVs were rinsed once with PBS. 2 μM CM-H_2DCFDA and Hoechst (ThermoFisher, 62249; 1:2000) were added in EBM-2 supplemented with 1% PS and incubated for 1 hour at 37°C to assess intracellular ROS and visualize nuclei, respectively. 0.5 mM tBHP was added to designated wells as a positive control and incubated for 1 hour prior to the addition of CM-H_2DCFDA. After staining, cells were washed with PBS and imaged using a Revolve microscope (ECHO) at 20× magnification. Following rolling ball background subtraction, the mean fluorescence intensity of the green channel was quantified using ImageJ software and normalized to the number of nuclei for each treatment group.

4.2.12 Leukocyte adhesion assay

Leukocytes were used to assess HCAEC inflammation induced by RBC-EVs. Leukocytes were isolated from freshly drawn blood under IRB protocol 1385293-7 using Acrodisc WBC Syringe Filters (Cytiva, AP-4952). Isolated leukocytes were stained with Calcein AM (1:1000) in EGM-2 for 30 minutes at 37°C, washed, and resuspended at 2×10^6 cells/mL in EGM-2. HCAECs were washed with PBS and incubated with 2×10^6 leukocytes for 10 minutes at 37°C. After thorough washing to remove non-adherent cells, images were acquired using an ECHO Revolve microscope at 10× magnification. The number of adherent leukocytes was quantified using ImageJ.

4.2.13 Statistical analysis

GraphPad Prism 10 was used for all statistical analyses. When two independent groups were compared (e.g., non-diabetic vs diabetic), a Mann–Whitney non-parametric test was applied. Correlation analyses between intracellular metabolites and ROS measurements were assessed

using simple linear regression, and Pearson correlation coefficients (R) were reported. Outliers were identified using the ROUT method (Q = 5%) in GraphPad Prism and excluded from analysis when applicable. An ordinary two-way ANOVA was performed to assess the effects of group (ND vs DM) and treatment (−Gln vs +Gln), followed by Tukey's post hoc test for multiple comparisons. The specific statistical test used for each dataset is indicated in the corresponding figure legend. All data are presented as mean ± standard deviation. Each data point represents an individual biological replicate (patient or independent experiment). Statistical significance was defined as $p < 0.05$.

4.3 Results

4.3.1 Study population characteristics.

Characteristics of the diabetic and non-diabetic individuals participating in this study are shown in Table 4.1. Diabetic patients had higher glucose and HbA1c levels compared to non-diabetic controls; however this difference didn't reach statistical significance ($p=0.1349$, and $p=0.1310$, respectively). The non-diabetic subjects were on average over 15 years younger than the diabetic subjects ($p<0.001$). Systolic and diastolic blood pressure, weight, BMI, HDL, triglycerides, LDL, and total cholesterol were not significantly different between the diabetic and non-diabetic subjects.

Table 4-1. Study subject characteristics

Characteristics	Non-diabetic (F/M)	Diabetic (F/M)
	n = 14 (11/3)	n = 29 (16/13)
Age (years)**	39.67±11.91	56.17 ± 14.27
Glucose (mg/dL)	108.50 ± 3.54	150.38 ± 71.45
HbA1c (%)	6.00± 0.14	7.55 ± 2.28
Systolic blood pressure (mmHg)	120.67±10.50	127.34 ± 12.92
Diastolic blood pressure (mmHg)	78.33 ±5.03	79.34 ± 9.15
Weight (lb)	181.56 ±40.55	197.97 ± 31.76
BMI (kg/m^2)	30.19±5.07	31.76 ± 4.82
HDL (mg/dL)	70.67 ±21.73	53.00 ± 20.34
Triglycerides (mg/dL)	110.67 ±9.5	147.00 ± 104.88
LDL (mg/dL)	78.00±10.00	86.60 ± 35.01
Total cholesterol (mg/dL)	182.33 ±19.50	162.90± 42.86

Value is expressed as mean ± SD. Statistics were analyzed using Mann Whitney nonparametric test and ** is $p<0.01$ and *** is $p<0.001$. HbA1c, hemoglobin A1c; HDL, high density lipid; LDL, low density lipid.

4.3.2 Intracellular glutamate was significantly lower in RBC from diabetic subjects.

Plasma glutamine levels were reported to be lower in people with diabetes [129]. Therefore, we measured glutamine and its metabolite, glutamate, in both plasma and RBCs from diabetic and non-diabetic subjects. Median plasma glutamine was approximately 0.6 mM in both groups, while the median plasma glutamate was 0.017 mM in non-diabetic and 0.025 mM in diabetic subjects (Figure 4-1A, B). Similarly, median RBC glutamine was not statistically significantly lower in diabetic (1.12 mM) as compared to non-diabetic (0.98 mM) subjects. However, median RBC glutamate in diabetic subjects (0.11 mM) was less than half that of non-diabetic subjects (0.25 mM; $p=0.0060$; Figure 4-1E, F). Median glutamine and glutamate concentrations in RBCs were ~1.5 times and 5 times higher, respectively, than in plasma (Figure 4-1I, J; $p<0.0001$).

Glucose and lactate measurements in plasma and RBCs revealed that median plasma glucose was 32% higher and lactate was 77% higher in diabetic as compared to non-diabetic subjects ($p=0.0041$ and $p=0.0114$, respectively; Figure 4-1C, D). Similarly, median RBC glucose and lactate levels were 38% and 55% higher in diabetic as compared to non-diabetic subjects ($p=0.0133$ and $p=0.0563$, respectively; Figure 4-1G, H). In contrast to glutamine and glutamate, median RBC glucose and lactate concentrations were ~2 times lower than plasma concentrations (Figure 4-1K, L). Thus, RBC glutamate was lower while RBC glucose was higher in diabetic RBC, and there were significant gradients between plasma and RBC metabolite concentrations.

4.3.3 Diabetic RBC had similar basal ROS but may have higher induced ROS than non-diabetic RBC.

RBCs from diabetic subjects have been reported to have increased ROS [213]. RBCs use glutamine-derived glutamate to synthesize glutathione (GSH) to reduce intracellular ROS[106]. Therefore, I measured ROS in RBCs at baseline and after treatment with tBHP, a cell-permeable oxidant, using both a plate reader and flow cytometry. I hypothesized that diabetic RBCs would have higher ROS due to reduced intracellular glutamate and, consequently, reduced antioxidant defense.

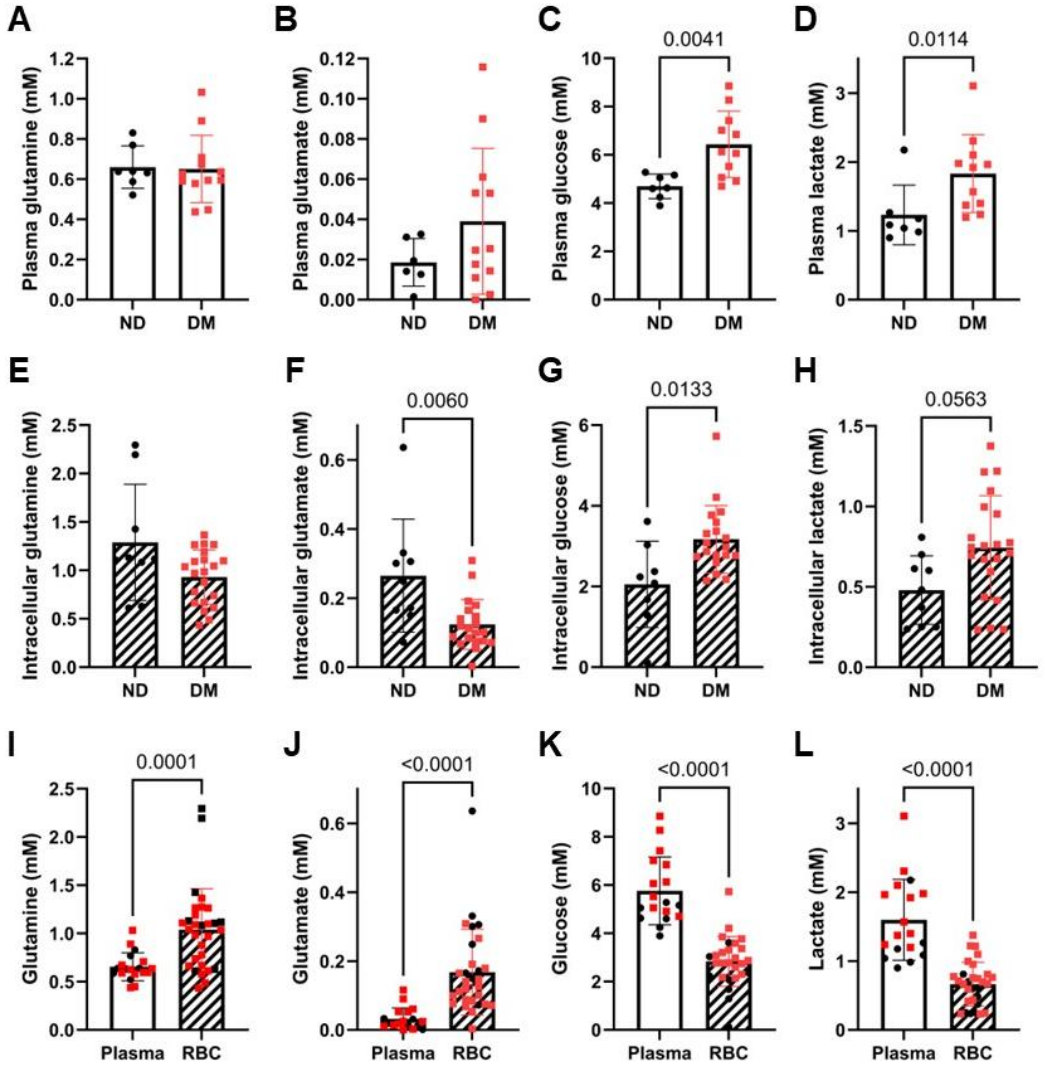

Figure 4-1 Intracellular glutamine and glutamate were significantly lower in RBC from diabetic subjects. Metabolite concentrations in plasma and RBC from diabetic and non-diabetic subjects were measured using a YSI bioanalyzer. Plasma: (A) glutamine, (B) glutamate, (C) glucose, and (D) lactate. n=7 for non-diabetic and 12 for diabetic subjects. RBC: (E) glutamine, (F) glutamate, (G) glucose, and (H) lactate. n=9 for non-diabetic and 22 for diabetic subjects. Plasma to RBC comparison for: (I) glutamine, (J) glutamate, (K) glucose, and (L) lactate. Data were analyzed using a Mann Whitney test after applying a ROUT (Q=1%) outlier test.

No significant differences in basal ROS were observed between diabetic and non-diabetic RBCs (Figure 4-2A, G). Upon tBHP treatment, RBC ROS increased. While diabetic RBC did show more ROS than non-diabetic RBC when treated with tBHP, as measured by both a plate reader and flow cytometry, the data were highly variable and did not reach statistical significance

(Figure 4-2D, J). When I evaluated correlations between basal and tBHP-induced RBC ROS and intracellular glutamine and glutamate concentrations, there was a consistent negative correlation between ROS and intracellular glutamine and glutamate; however, these associations did not always reach statistical significance (Figure 4-2E, F, K, L). Together, these findings suggest that RBCs from diabetic patients may have reduced antioxidant capacity, which may correlate with intracellular glutamine and glutamate levels; however, more data or improved processes are needed to reduce sample variability.

I then analyzed the impact of medications, including insulin (I), metformin (M), or GLP-1 receptor agonists and/or SGLT2 inhibitors (G/S) on RBC ROS levels. With small samples sizes, few robust differences could be detected (Figure 4-3). However, the data suggest that RBC from subjects taking insulin may have higher ROS in basal and tBHP treated conditions. RBC from subjects taking metformin or GLP-1/SGLT2 did not demonstrate consistent differences in basal or tBHP-induced ROS compared to RBC from subjects who were not taking that medication. These exploratory analyses are hypothesis-generating and suggest that insulin therapy may be associated with higher RBC ROS. However, additional investigation is required to establish mechanism and causality.

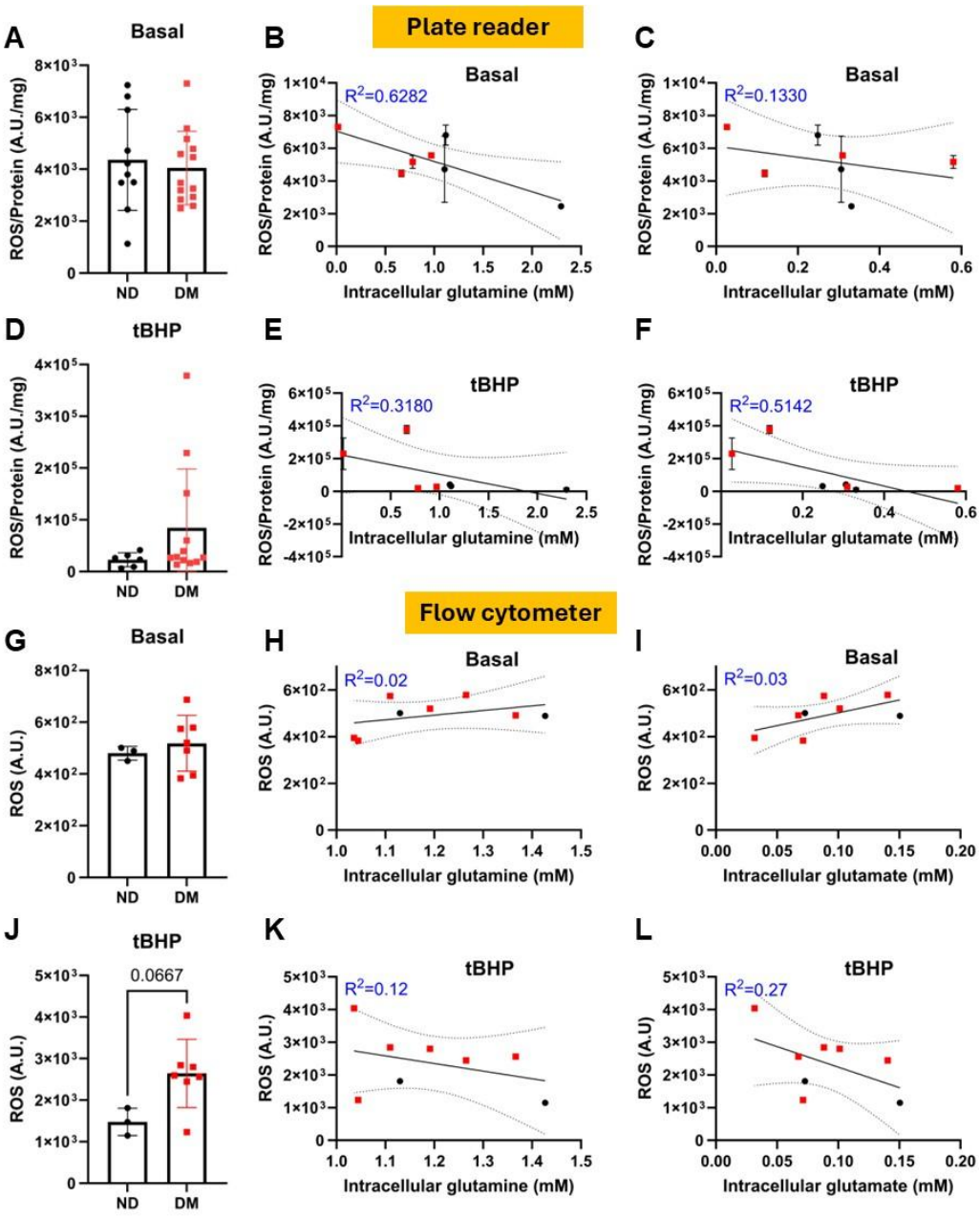

Figure 4-2: Diabetic RBC had similar basal ROS but higher induced ROS than non-diabetic RBC. RBCs from diabetic and non-diabetic subjects were treated with H2DCFDA and ROS were measured with (A) plate reader or (G) flow cytometer. A subset of RBCs were treated with 60 µM tBHP for 30 minutes at 37ºC to increase oxidative stress. RBC were then treated with H2DCFDA and ROS were measured with (D) plate reader or (J) flow cytometer. Each point represents one subject. n = 3-12 subjects. Data were analyzed using a Mann Whitney test after applying a ROUT (Q=1%) outlier test. Correlation between RBC ROS and intracellular glutamine (B, E, H, K) and glutamate (C, F, I, L). Simple regression analysis was used to determine R. $p<0.05$ only in B and F.

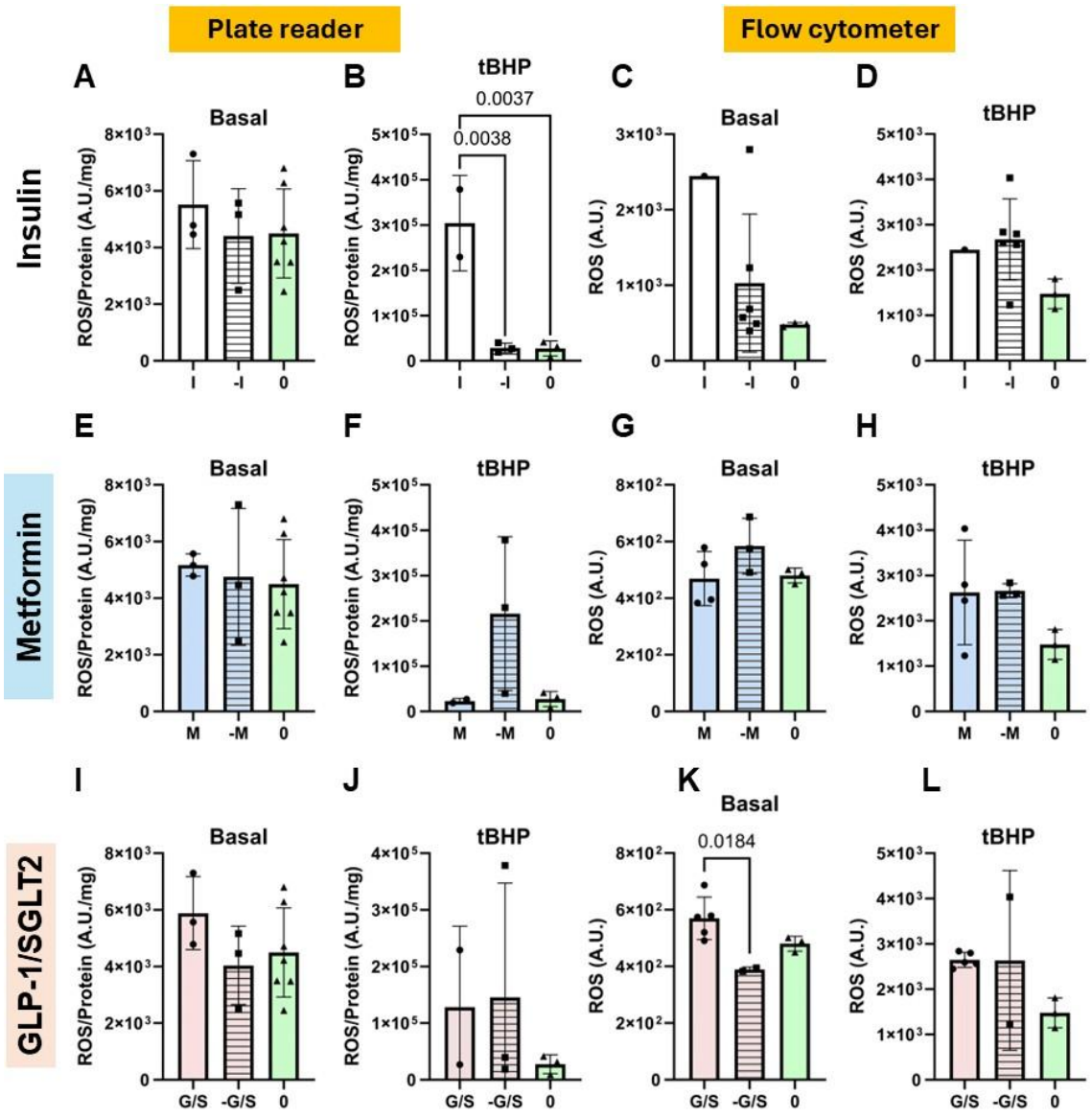

Figure 4-3: Insulin may increase ROS in diabetic RBC. RBC ROS data from Figure 4-2 were separated to analyze the impact of insulin (I), metformin (M), GLP-1 receptor agonists/SGLT2 inhibitors (G/S), or no medications (0). A-D) Insulin; E-H) Metformin; I-L) GLP-1/SGLT2 Each point represents RBC from one subject. Data were analyzed using ordinary one-way ANOVA with a Tukey post-hoc multiple comparisons test.

4.3.4 RBC took up extracellular glutamine, which increased tBHP-induced ROS at 1 day.

Since diabetic RBCs have low glutamate and yet are impermeable to glutamate [227], I investigated how glutamine supplementation impacts RBC ROS in basal conditions and after tBHP

treatment. I hypothesized that glutamine supplementation would decrease RBC ROS, as more glutamine-derived glutamate would increase RBC GSH. When RBCs were incubated with 10 and 20 mM glutamine for 24 hours, intracellular glutamine increased by more than 4 and 8 times, respectively, compared to 0 mM glutamine ($p=0.0058$ and $p=0.006$; Figure 4-4A). Glutamate also was 3 times higher at 2 mM glutamine compared to 0 mM glutamine ($p=0.0152$), while increasing glutamine to 10 and 20 mM did not further impact intracellular glutamate (Figure 4-4B). RBC lactate and glucose did not change with increasing extracellular glutamine concentration (Figure 4-4C, D).

I then incubated RBCs from diabetic and non-diabetic subjects with 0 or 10 mM glutamine for 1 or 3 days and measured ROS. I did not detect any changes in basal ROS (Figure 4-4E, G). When RBC were also treated with tBHP, 1 day of 10 mM glutamine treatment increased RBC oxidative stress (Figure 4-4F). 3 days of 10 mM glutamine decreased ROS in RBCs from diabetic subjects but not in RBCs from non-diabetic subjects (Figure 4-4H). When I measured RBC intracellular GSH, I did not observe any change in GSH for RBC treated with 2 mM glutamine as compared to 0 mM glutamine (Figure 4-5A). Even when RBC were supplemented with the other two building blocks of GSH, cysteine and glycine, which may be required to increase RBC GSH synthesis [111], I still did not detect an increase in RBC intracellular GSH (Figure 4-5B).

These data suggest that although glutamine is transported into RBCs and significantly increases intracellular glutamate levels, GSH did not increase and oxidative stress increased.

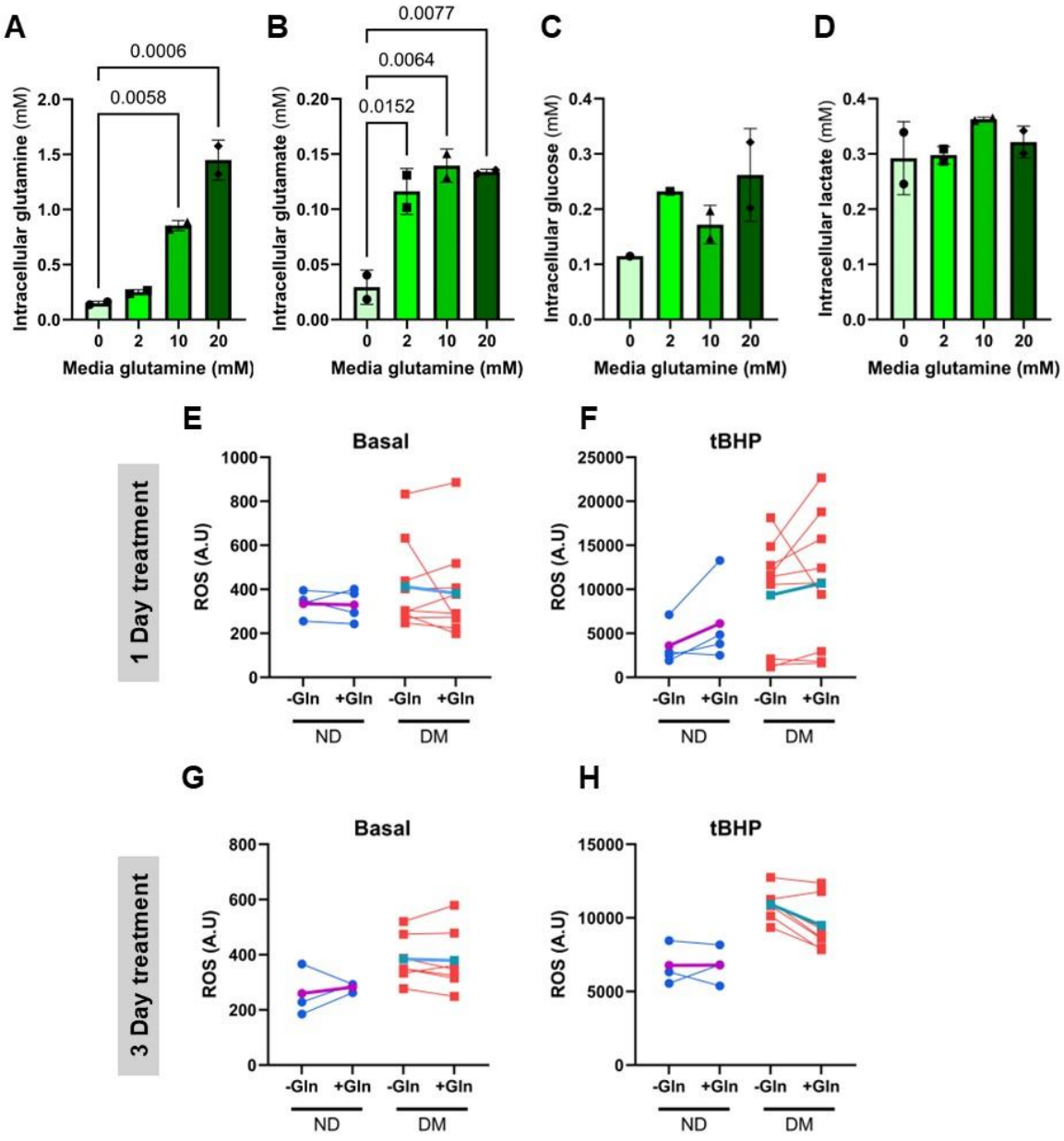

Figure 4-4: RBC glutamine uptake increased as media glutamine increased; glutamine treatment increased tBHP-induced ROS in 1 day and decreased it at 3 days. RBCs were incubated with 0-20 mM glutamine for 24 hours, lysed, and intracellular metabolites were measured using a YSI Bioanalyzer. A) glutamine, B) glutamate, C) glucose, and D) lactate. Data were analyzed using ordinary one-way ANOVA with a Tukey post-hoc multiple comparisons test. RBCs from diabetic and non-diabetic subjects were treated with 10 mM glutamine for 1 day (E, F) or 3 days (G, H). A subset of cells were treated with 60 µM tBHP for 30 minutes, and ROS was measured using a flow cytometer. n=5-7 patients. Each point represents RBC from an individual subject. Purple and blue thick lines represent mean for ND and DM, respectively. Data were analyzed using ordinary two-way ANOVA with a Tukey post-hoc multiple comparisons test.

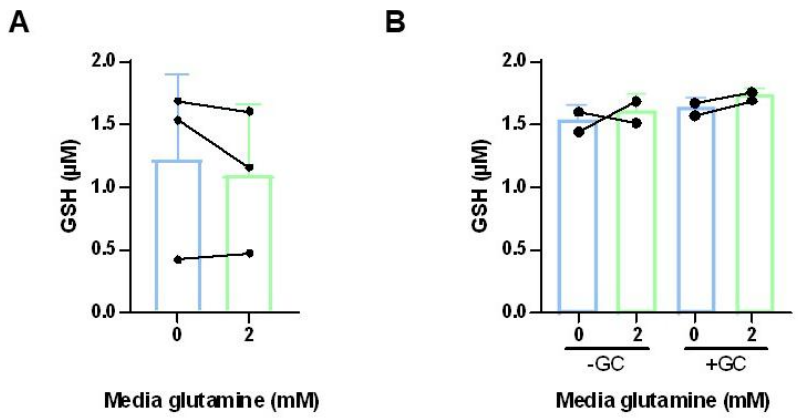

Figure 4-5: Glutamine treatment did not increase RBC GSH even with addition of glycine and cysteine. RBCs were treated with glutamine for 24 hours, lysed, and intracellular GSH was measured using the GSH-Glo assay. In some cases, RBCs were also treated with glycine (250 µM) and cysteine (25 µM). RBC GSH for A) glutamine treatment (n=3 biological replicates) and B) glutamine, glycine, and cysteine treatment (n=2 biological replicates).

4.3.5 NOX inhibition reduced ROS in RBCs.

Since RBC ROS increased with glutamine, I investigated how glutamine increases ROS in RBCs via NOX [216]. I hypothesized that glutamine elevates ROS by enhancing NADPH availability, thereby increasing NOX activity. The NOX inhibitor DPI decreased RBC ROS by 9-23% across all glutamine conditions ($p=0.0045$), with no significant interaction between glutamine and DPI (Figure 4-6). Thus, NOX is unlikely to be the source of the increased RBC ROS with glutamine.

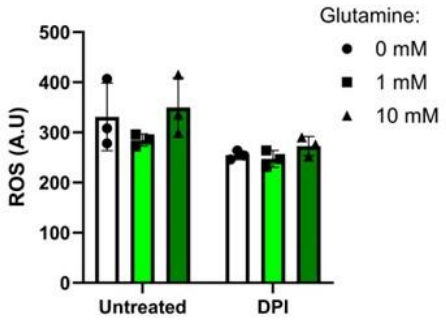

Figure 4-6: NOX inhibition reduced basal ROS in RBCs. RBCs were treated with 0, 1, and 10 mM glutamine with 0 or 10 μM DPI (NOX inhibitor) for 24 hours, labelled with H2DCFDA, and ROS was measured using a flow cytometer. n=3 biological replicate. Data was analyzed using ordinary two-way ANOVA with Tukey post-hoc multiple comparisons test.

4.3.6 Piezo1 stimulation of diabetic and non-diabetic RBCs yielded similar RBC-EVs.

I next determined how diabetic RBCs could impact endothelial cells via extracellular vesicles (RBC-EVs). I generated RBC-EVs using yoda-1, a Piezo-1 channel activist, as has previously been shown in my laboratory [46]. Using Western blot analysis, I detected EV-specific markers including ALIX, TSG101, and CD9 in both non-diabetic and diabetic RBC-EVs. β-actin, which should not be in EVs, was not detected (Figure 4-8A). RBC-EVs from both groups showed a size distribution ranging from 50 to 200 nm (Figure 4-8B). Although the total concentration and mean particle size of non-diabetic and diabetic RBC-EVs were similar at approximately 7×10^{12} particles/mL and 109 nm, respectively (Figure 4-8C, D), diabetic RBC-EVs had a higher particle concentration from 60–120 nm diameter compared to non-diabetic RBC-EVs.

4.3.7 HCAECs took up RBC-EVs, and neither ND-RBC-EV nor D-RBC-EV impacted cell viability.

Next, I determined if RBC-EVs were taken up by HCAECs by analyzing Hb-α and band3 protein within the HCAECs. HCAECs treated with 1×10^{10} RBC-EVs for 24 hours contained band3 and Hb-α (Figure 4-9A), while untreated and EV conditioned media (EV-CM) treated HCAECs

did not (p=0.0079 and p=0.021 for band3 and Hb-α, respectively; Figure 4-9B, C). RBC-EV treatment did not impact HCAEC viability after 24 hours, with cell viability remaining around 97% in both treated and untreated groups (Figure 4-9D, E).

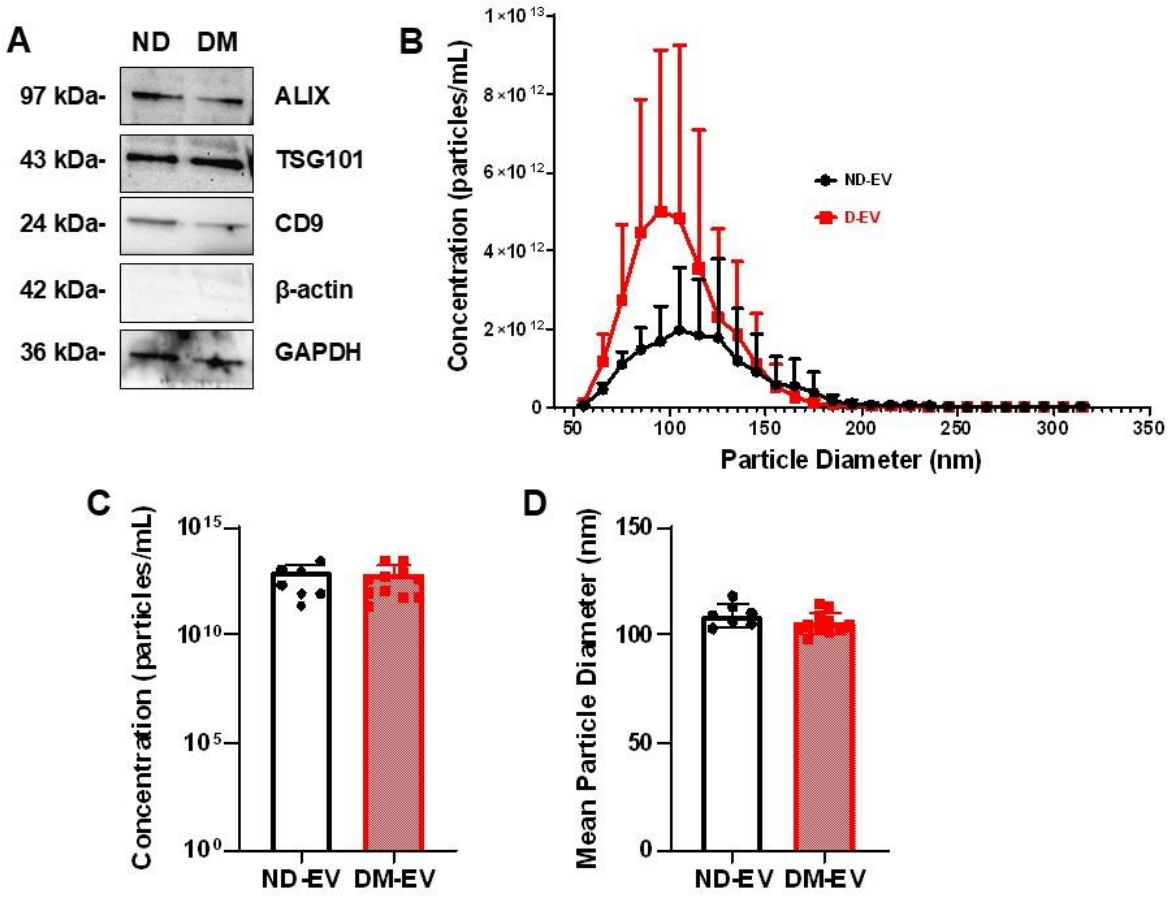

Figure 4-8: Piezo1 stimulation of non-diabetic and diabetic RBCs yielded similar EVs, as confirmed by EV specific markers and size distribution. RBCs from diabetic and non-diabetic patients were resuspended at 18% hematocrit and treated with 10 μM yoda-1 (piezo1 agonist) for 30 minutes. The supernatant was then collected and EVs were isolated using ultracentrifugation. A) EV specific markers, detected via Western blot. B) representative RBC-EV concentration vs diameter measurement, C) RBC-EV concentration, and D) RBC-EV mean particle diameter, all measured by TRPS. n=7-10/ group

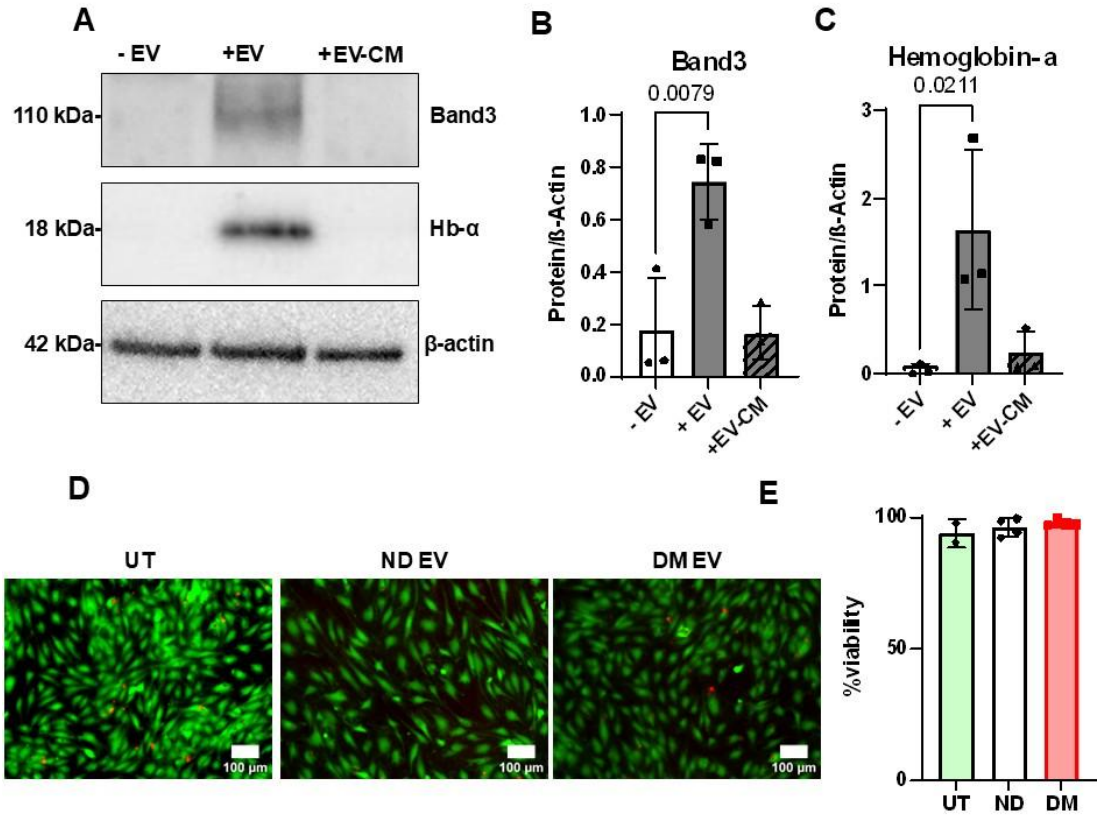

Figure 4-9: HCAECs took up RBC-EVs, and neither non-diabetic nor diabetic RBC-EV impacted cell viability. HCAECs were treated with 10^{10} EVs (+EVs), without EVs (-EVs), and with EV conditioned media (EV-CM) for 24 hours. HCAEC were lysed and intracellular proteins analyzed by Western blot, or cell viability was measured using Calcein-AM and Eth-1 for live and dead cells, respectively. Viability was quantified as percent Calcein-AM positive cells (Live). A) Representative Western blots with B, C) quantification for band3, hemoglobin, and β-actin (loading control). n=3 biological replicates D) Representative fluorescent microscopy images of live dead assay with E) viability quantification. n=4 subjects/group.

4.3.8 Neither non-diabetic nor diabetic RBC-EVs increased WBC adhesion to HCAECs.

Finally, I determined how RBC-EVs affected HCAEC inflammation and ROS as functional readouts. After 24 hours of treatment with 1×10^{10} diabetic or non-diabetic RBC-EVs, there were no significant changes in the number of leukocytes adhered to the endothelium (Figure 4-10A, B). Both diabetic and non-diabetic RBC-EVs decreased HCAEC oxidative stress by approximately 40% compared to untreated HCAECs; however, the difference did not reach statistical significance (Figure 4-11A, B). Together, these data suggest that RBC-EVs, regardless

of whether they originate from diabetic or non-diabetic individuals, may decrease ROS levels in HCAECs.

4.4 Discussion

Prior studies suggested that RBCs from diabetic subjects had higher oxidative stress, and that their RBC-EVs cause more damage to endothelial cells. I therefore measured diabetic and non-diabetic RBC oxidative stress, with and without glutamine supplementation, as well as the impact of RBC-EVs on cultured endothelial cells. My data do not show increased oxidative stress in RBCs from diabetic subjects; however, the data suggest that RBCs from diabetic subjects have reduced antioxidant capacity. Diabetic RBCs had higher intracellular glucose and lactate but lower intracellular glutamate, despite no difference in plasma glutamate. RBCs overall maintained a large gradient between intra- and extra-cellular metabolite concentration. RBCs took up extracellular glutamine and produced glutamate with a plateau at 2 mM glutamine, but extracellular glutamate did not increase RBC GSH. Instead, extracellular glutamine may have increased RBC oxidative stress. Lastly, RBC-EVs produced via piezo-1 stimulation were efficiently taken up by HCAECs, and both non-diabetic and diabetic RBC-EVs reduced endothelial ROS without triggering inflammation or cell death. These data show that glutamine supplementation alone in RBCs does not improve antioxidant defense system and other strategy for increasing GSH inside the RBCs may be required. Additionally, this data show that RBC-EVs generated via piezo1 stimulation may not cause endothelial cell dysfunction, unlike those generated by storage of RBCs.

The diabetic subjects had higher blood glucose and HbA1c than the non-diabetic subjects, which is consistent with established diabetic glycemic criteria. However, the difference in blood

glucose and HbA1c was not as extreme as in other studies, showing that these diabetic subjects had relatively well controlled diabetes [213]. The non-diabetic subjects were younger, which could be confounding as RBCs from older adults differ from RBCs from younger adults [228]. However, since I did not observe worse function in the diabetic RBCs, the increased RBC age did not seem to affect the results, perhaps since RBC are regenerated every 120 days. Other cardiovascular risk factors that could impact RBC function (e.g., blood pressure, lipids, BMI) were statistically similar across the two groups. Thus, the primary difference between the groups related to high glucose, and therefore any differences in diabetic RBC function can be interpreted principally as hyperglycemic effects.

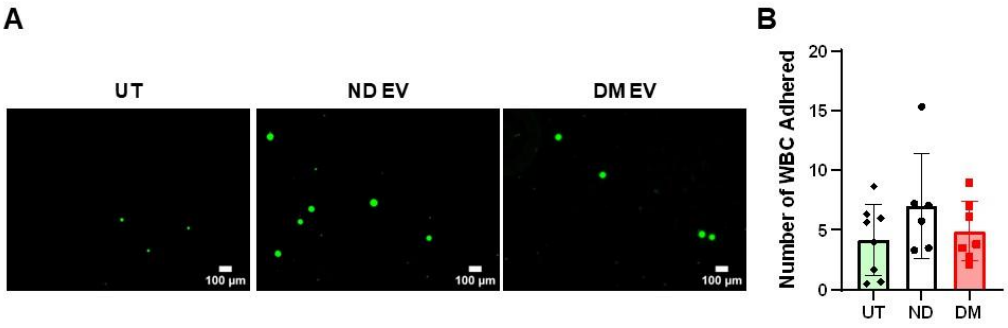

Figure 4-10: Neither D-RBC-EVs nor ND-RBC-EVs increased WBC adhesion to HCAECs. HCAECs were incubated with 10^{10} RBC-EVs from diabetic and non-diabetic patients for 24 hours. Leukocytes were isolated from fresh whole blood and stained with 2 µM Calcein AM (green) for 30 minutes. HCAECs were then incubated with 2 million leukocytes for 10 minutes and imaged by fluorescent microscopy at 10X. The number of leukocytes adhered to the HCAECs was counted using ImageJ. A) Representative fluorescent microscopy images of leukocytes (green) adhered to HCAECs. B) Quantification of adhered leukocytes. n= 6 samples.

RBC glutamate was lower in diabetic than non-diabetic subjects despite statistically similar plasma glutamate. RBCs do not have membrane transporters for negatively charged amino acids such as glutamate, and plasma glutamate enters RBC at <5% the rate of glutamate incorporation

into GSH. Instead, RBCs rely on internal synthesis of glutamate from glutamine [222,223]. In contrast, plasma glucose and lactate followed the same trends as intracellular glucose and lactate, with them all being higher in the diabetic subjects. I also observed that plasma glucose and lactate were higher than intracellular glucose and lactate, while plasma glutamine and glutamate were lower than intracellular glutamine and glutamate. This observation can be explained by their transporters, as glucose is transported by GLUT1 which is a diffusive transporter and maintains gradient, while glutamine is transported by Na^+ coupled transporters that can actively concentrate glutamine inside the cells.

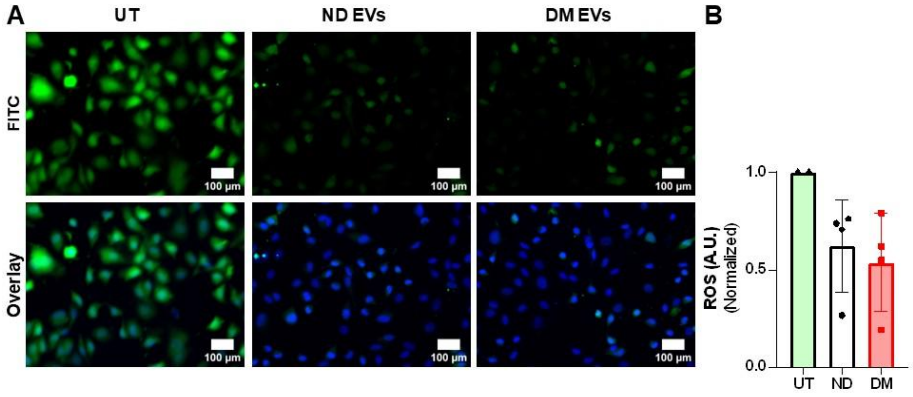

Figure 4-10: Neither D-RBC-EVs nor ND-RBC-EVs increased WBC adhesion to HCAECs. HCAECs were incubated with 10^{10} RBC-EVs from diabetic and non-diabetic patients for 24 hours. Leukocytes were isolated from fresh whole blood and stained with 2 µM Calcein AM (green) for 30 minutes. HCAECs were then incubated with 2 million leukocytes for 10 minutes and imaged by fluorescent microscopy at 10X. The number of leukocytes adhered to the HCAECs was counted using ImageJ. A) Representative fluorescent microscopy images of leukocytes (green) adhered to HCAECs. B) Quantification of adhered leukocytes. n= 6 samples.

Basal ROS was statistically similar in diabetic and non-diabetic RBCs. This contrasts with previous studies that reported higher ROS in RBC from diabetic subjects or due to hyperglycemic culture [69,213,229]. For example, ROS measured *ex vivo* using fluorescent probe was 39% higher in diabetic RBCs (n=12) compared to non-diabetic RBCs (n=9) [213]. The difference between my results and the existing literature may be due to experimental conditions. Specifically, Turpin *et*

al. reported a higher average HbA1c in their diabetic subjects (11± 2.6) than I measured in my experiment (7.63±2.28). They also incubated RBCs at 37°C for 5 days after isolation, which may have increased Hb-α oxidation leading to superoxide production [230]. I measured ROS shortly after the blood draw. Additionally, RBCs in my experiments were isolated from plasma and maintained under controlled conditions that do not reflect the diabetic condition, like glucose fluctuation, increased inflammation or free lipids, which may further change the results.

Diabetic RBCs challenged with oxidative stress (tBHP) showed a greater increase in ROS compared to non-diabetic RBCs. This finding is consistent with prior studies indicating impaired RBC antioxidant capacity in diabetes. Dincer *et al.* observed that RBCs from diabetic subjects that were exposed to H_2O_2 for 2 hours exhibited a greater reduction in GSH compared to RBCs from non-diabetic subjects, which may be due to the reduced ability of diabetic RBCs to regenerate GSH [221]. Our diabetic RBCs may similarly have impaired GSH synthesis and regeneration, which would need to be measured in future work. Exposure to oxidative stress could result in elevated oxidative damage to diabetic RBCs, which in turn could impact vascular cells such as endothelial cells, thereby increasing the risk of cardiovascular complications in diabetic subjects.

Insulin, metformin, and GLP-1 or SGLT2 medication groups did not show differences in baseline ROS. Followed by tBHP treatment, the insulin-treated group showed a greater increase in ROS compared to those not taking insulin in their medication. These observations should be interpreted cautiously and considered hypothesis-generating due to the limited sample size, the fact that most subjects were taking combinations of medications, and potential experimental variability. Notably, a higher increase in tBHP treated ROS in insulin-treated subjects was not observed in the experiment in which flow cytometry was used. The potential finding of reduced antioxidant capacity in the insulin-treated group compared to the non-insulin group aligns with

previous research indicating that insulin-dependent diabetic subjects have significant defects in their antioxidant defense systems. Maxwell *et al.* reported that subjects with insulin-dependent diabetes mellitus exhibited significantly reduced total serum antioxidant activity compared to non-diabetic controls [231]. Thus, we hypothesize that insulin treatment may be associated with reduced antioxidant capacity in RBCs of diabetic subjects; however, further research is required to confirm this finding and investigate the underlying mechanisms.

RBC incubated with glutamine increased intracellular glutamine and glutamate but did not increase GSH or reduce oxidative stress. Glutamate increased only up to 2 mM glutamine, which is consistent with previous reports indicating that RBCs use glutamine as a precursor to glutamate [222]. The glutamate plateau at higher glutamine concentrations may be due to GLS-1 saturation or inhibition by glutamate. Glutamine alone may not have conferred antioxidant protection after tBHP treatment, as others have shown that co-treatment with glutamine, cysteine, and glycine was required to reduce RBC ROS after treatment with 50 μM H_2O_2 [111]. However, glutamine supplementation has been shown to reduce oxidative stress in sickle cell disease. In a study by Sadaf *et al.*, increasing oral glutamine from 0.1 g/kg to 0.6 g/kg over 3 weeks decreased ROS in reticulocytes (immature RBCs) but not in mature RBCs [224]. The differences between our results and others may relate to mature RBCs vs reticulocytes, presence of other amino acids, or incubation times.

RBC-EV generation via the piezo1 agonist yoda-1 yielding particles positive for canonical EV markers (ALIX, TSG101, CD9), consistent with a previous study from our laboratory [46]. Diabetic and non-diabetic RBC-EVs were of similar size distribution and concentration. Other studies report varied impact of hyperglycemia and diabetes on RBC-EV concentration. A study comparing EVs isolated from diabetic and non-diabetic RBCs after 18 hours incubation at 37°C

reported significantly lower RBC-EV concentrations from diabetic subjects [67]. Another study analyzing serum from diabetic and non-diabetic subjects reported increased plasma EVs, specifically RBC-EVs, in diabetic subjects [68]. Similarly, *in vitro* incubation of RBCs in 45 and 100 mM glucose led to increased RBC-EV release compared to RBCs in 5 mM glucose [69]. These differences may be due to the RBC-EV production mechanisms, which vary from piezo1 stimulation in my study to RBC storage, plasma isolation, and *in vitro* hyperglycemic conditions. My method of EV isolation is closer to physiological conditions, in which RBCs shed EVs in response to shear stress. To our knowledge, this is the first study isolating EVs from diabetic RBCs in a physiologically relevant manner.

RBC-EVs were taken up by HCAECs and did not affect cell viability or leukocyte adhesion and actually decreased oxidative stress. Some studies have similarly shown that endothelial cells internalize RBC-EVs, even under flow conditions, [232] and that EV treatment did not reduce cell viability [67,232]. However, other studies have shown that RBC-EVs can have pro-inflammatory effects. RBC-EVs carry cell-free Hb or heme, which acts as a ligand for toll like receptor 4 (TLR4). When heme binds to TLR4, endothelial cells express pro-inflammatory genes like IL-6, ICAM-1 and VCAM-1 [225]. Collado *et al.* also reported that T2D RBC-EVs induced oxidative stress and impaired endothelial function through the transfer of arginase-1 [67]. RBC-EVs have been extensively investigated across other conditions, including pulmonary hypertension, obstructive sleep apnea, and acute coronary syndrome and were associated with vascular disorders [60,61]. Several factors might explain the discrepancy between prior studies and our work. In some studies, RBC-EVs were generated after RBC storage, which may alter RBC-EV content. Others also included smokers and subjects with cardiovascular complications, whereas we excluded these groups. Another possibility is an assay artifact. Hemoglobin in RBC-EVs may quench the

H_2DCFDA signal in endothelial cell. Additional research is required to clarify the underlying mechanisms for reduced ROS in our studies.

4.5 Limitations:

This study has some limitations related to our study population. The diabetic subjects who donated blood in our study had well-controlled glucose, which could have contributed to the low ROS in the diabetic RBCs. In the future, we may need to set a threshold for HbA1c values to better understand the impact of chronic hyperglycemia on RBC oxidative stress. In addition, the diabetic subjects were older on average than non-diabetic subjects. Since RBC ROS increases with age, this could confound our results.

4.6 Conclusion:

Diabetic RBCs had less intracellular glutamate and higher ROS following tBHP treatment. Although RBCs took up glutamine to make glutamate, this did not reduce RBC oxidative stress. Neither diabetic nor non-diabetic piezo1-induced RBC-EVs negatively impacted endothelial cell function. Together, these results suggest that diabetic RBCs exhibit impaired redox adaptability rather than elevated basal oxidative stress, and that RBC-EVs generated through piezo-1 stimulation may influence endothelial redox balance differently than RBC-EVs generated via storage.

Chapter 5: Conclusion and Future work

5.1 Thesis summary

Cardiovascular complications are the leading cause of morbidity and mortality in subjects with diabetes. Endothelial cells and red blood cells (RBCs) become dysfunctional when exposed to hyperglycemia associated with diabetes, partially driven by disruption of redox balance leading to increased oxidative stress. The adverse effects of hyperglycemia may be further amplified through interactions between dysfunctional RBCs and the endothelium via extracellular vesicles (EVs), which can carry pro-oxidant and pro-inflammatory cargo. Glutamine, the most abundant amino acid in the body, is reduced in the serum of diabetic subjects, and glutamine supplementation has been shown to have anti-inflammatory and antioxidant effects. In this thesis, I investigated how glutamine affects the metabolism and function of endothelial cells under hyperglycemic conditions and RBCs from diabetic subjects. I further examined how diabetic RBC-EVs influence endothelial cell function. I demonstrated that glutamine enhanced NADPH and glutathione synthesis in endothelial cells, thereby reducing oxidative stress. In contrast, glutamine supplementation did not decrease RBC oxidative stress. Glutamine supplementation altered endothelial cell systemic metabolism by enhancing oxidative respiration, succinate dehydrogenase activity, UDP-GlcNAc formation, and ornithine cycle flux while decreasing membrane fatty acids and 1C metabolites. These findings suggest the potential of glutamine supplementation to reduce oxidative stress in diabetes while emphasizing the need for cell-type specific considerations to optimize its therapeutic impact.

5.2 Specific discoveries

The overall goal of this thesis is to understand how glutamine impacts vascular cells, including endothelial cells and RBCs, under diabetic conditions. I modeled hyperglycemia *in vitro* and obtained RBCs from diabetic subjects and measured the impact of glutamine on oxidative stress. Maintaining oxidative balance in the vasculature is critical because oxidative stress impairs vasodilation and promotes inflammation. *I hypothesized that glutamine supplementation above physiological concentrations would protect endothelial cells and RBCs from oxidative stress induced in diabetic conditions.*

In Chapter 2, I treated endothelial cells with varied glutamine concentrations in both normo- and hyper-glycemia. I showed that glutamine deficiency increased oxidative stress regardless of glucose concentration, whereas glutamine supplementation significantly decreased oxidative stress through increased NADPH and GSH synthesis. I also demonstrated that in normal glucose conditions, 2 mM glutamine improved vasodilation *ex vivo,* with no changes to NO synthesis *in vitro*. These findings suggest that glutamine promotes vascular relaxation primarily through reduced ROS and decreased NO scavenging, rather than by increasing NO synthesis. This clarifies inconsistencies in the literature regarding the relationship between glutamine and NO. Overall, these results support a beneficial role for glutamine in maintaining endothelial antioxidant defense under both physiological and hyperglycemic conditions and suggest that glutamine depletion or defect metabolism may impair endothelial function.

In Chapter 3, I further investigated endothelial cell glutamine metabolism in physiological and supraphysiological glutamine concentrations. I incubated endothelial cells with 0-10 mM glutamine in both normo- and hyperglycemia conditions. While endothelial cells continued to take up glutamine, they stopped secreting glutamate above 2 mM glutamine. Using optimized isotope

labeling, I traced glutamine carbons through the forward and reverse TCA cycle and demonstrated that increasing glutamine concentration enhanced forward TCA cycle activity but did not significantly impact reverse TCA cycle flux. The presence of glutamine increased most TCA metabolites, glutathione, proline, aspartate, and UDP-GlcNAc; however, glutamine decreased succinate, citrulline, arginine, the fatty acids EPA and icosatrienoic acid, and 1C metabolites folate and histidine. Decreased total metabolite abundance in the 1C pathway and EPA suggest increased pathway activity and fatty acid oxidation, potentially supporting nucleotide and macromolecule synthesis. Principal component analysis of glutamine-carbon labeled metabolites showed clear separation between endothelial cells cultured with and without glutamine but no separation at higher glutamine concentrations. These data suggest that excess glutamine is largely stored by endothelial cells, perhaps due to limited GLS-1 enzymatic capacity, and that glutamine provides carbon for central metabolic pathways while also impacting interconnected metabolic networks.

In Chapter 4, I incorporated a clinical model of diabetes by analyzing RBCs collected from diabetic and non-diabetic subjects. Diabetic RBCs showed significantly higher intracellular glucose and lactate and significantly lower intracellular glutamate compared to non-diabetic RBCs. At baseline, oxidative stress was similar between diabetic and non-diabetic RBCs. However, upon exposure to the oxidant tBHP, diabetic RBCs exhibited a greater increase in ROS, suggesting reduced antioxidant capacity. Unlike endothelial cells, RBCs did not increase GSH or reduce oxidative stress in response to glutamine supplementation after 24 hours. This may reflect enzymatic constraints within the RBC glutamate and glutathione synthesis pathway.

I also investigated the interaction between RBCs and endothelial cells through RBC-EVs. RBC-EVs were generated through piezo1 stimulation, which mimics physiological shear stress. In contrast to storage derived RBC-EVs reported in previous studies, piezo1 stimulated EVs from

both diabetic and non-diabetic RBCs did not increase endothelial inflammation and may even have reduced oxidative stress. These findings suggest that EV generation methodology significantly influences functional outcomes and that physiologically generated RBC-EVs from diabetic subjects may not impair endothelial function.

5.3 Contributions to the field

Although current diabetes treatments are effective in controlling blood glucose levels, diabetic subjects continue to experience a higher risk of cardiovascular complications[39,67]. Glycemic control alone is not sufficient to protect diabetic subjects from cardiovascular disease, and additional strategies are needed to reduce cardiovascular risk in diabetes. Several *in vivo*, *ex vivo*, and *in vitro* studies suggest that glutamine supplementation can reduce oxidative stress and vascular damage [128,129,233] However, the impact of glutamine availability on the metabolism and function of circulating RBCs and endothelial cells and their interaction under diabetic conditions is not fully understood.

In this thesis, I demonstrated the impact of glutamine availability in an *in vitro* hyperglycemic model and, for the first time, showed that glutamine prevents oxidative stress in hyperglycemia through enhanced NADPH and GSH synthesis. Because glutamine and glucose metabolism are interconnected, it was important to determine how changes in glutamine availability influence endothelial metabolism and function under elevated glucose. While previous studies showed that glutamine decreases ROS under normal glucose conditions [85], its role in hyperglycemia had not been investigated. In addition, this study used primary HCAECs and 15 mM glucose, which more closely reflect pathophysiological conditions compared to supraphysiological glucose concentrations commonly used in other studies.

This work is also the first to systematically investigate glutamine's metabolic fate across a range of concentrations, including supraphysiological levels typically present in cell culture media. I demonstrated that increasing glutamine above physiological concentrations does not significantly alter major metabolic pathways, likely due to enzymatic limitations. Instead, endothelial cells store intracellular glutamine, potentially as a carbon reservoir to account for future nutrient variability. These findings suggest that if the goal of glutamine supplementation is to enhance glutamine metabolic flux, key glutaminolysis enzymes would also need to be modified to fully benefit from glutamine metabolism's antioxidant and anti-inflammatory effects.

Furthermore, my data revealed that increasing glutamine availability significantly reduced succinate, 1C metabolites, and intracellular membrane fatty acids in endothelial cells. These findings suggest novel mechanisms through which glutamine may regulate endothelial function by limiting succinate-induced HIF-1α signaling and inflammation [199–201], supporting redox balance and biosynthetic capacity through enhanced 1C metabolism [181], and modulating PUFA eicosanoids and vascular signaling molecules[168,209].

The findings of this work suggest that glutamine can metabolically support endothelial cells by enhancing antioxidant capacity, particularly through promoting glutathione synthesis, thereby reducing oxidative stress. In this context, while therapies such as semaglutide address upstream metabolic dysfunction, glutamine may act downstream by mitigating oxidative stress–induced endothelial dysfunction. This distinction highlights a potential role for glutamine in targeting vascular-specific mechanisms that are not directly addressed by current systemic therapies.

This study is also the first to demonstrate that intracellular glutamate is significantly decreased in RBCs from diabetic subjects, suggesting glutamate restoration as a potential

therapeutic target to improve antioxidant capacity. In addition, this is the first study to investigate the impact of glutamine supplementation on RBCs isolated from diabetic subjects. Unlike endothelial cells, RBCs did not increase GSH synthesis in response to glutamine supplementation, suggesting enzymatic constraints in RBCs glutathione metabolism.

Finally, this work is the first to generate RBC-EVs from diabetic subjects using a physiologically relevant piezo1 mediated stimulation method previously established in our laboratory [46]. In contrast to EVs generated through RBC storage, which may induce cellular stress, piezo1 stimulated RBC-EVs did not increase inflammation or oxidative stress in endothelial cells. These findings provide new insight into RBC-EV biology in diabetes and highlight the importance of EV generation methodology when interpreting functional outcomes.

5.4 Future studies

5.4.1 Incorporation of multifactorial metabolic changes and sex-specific variability.

Diabetes is associated with metabolic alterations beyond hyperglycemia, including changes in lipid profiles and increased inflammatory cytokines [166,167,234]. Therefore, future studies should incorporate these multifactorial metabolic changes to better reflect the diabetic environment.

Additionally, the endothelial cells used in this study were derived from a single male donor. Given that cardiovascular disease differs in males and female subjects [235], it is important to repeat these experiments using cells from multiple donors of different sexes to confirm the robustness and generalizability of these findings.

5.4.2 Investigating the interplay between glutamine and glucose and transient metabolic responses

In this work, I used 1-^{13}C-glutamine and 5-^{13}C-glutamine to trace glutamine metabolism. However, glutamine and glucose metabolism are interconnected, and changes in one pathway can impact the other. Future experiments using U-^{13}C-glucose with increasing glutamine concentration would provide deeper insight into how glutamine availability influences glucose carbon flux. This will be especially important under hyperglycemic conditions, in which both metabolites may be altered.

In addition, the current study assessed glutamine metabolism at steady state. We do not yet have information on the transient effects of glutamine on endothelial metabolic activity. This is particularly relevant for rapid processes such as glycolysis, where steady-state metabolite levels may not accurately reflect real time flux changes. Real time isotope tracing would help clarify these dynamic effects.

5.4.3 Overcoming potential enzymatic constraints in RBCs and glutathione loading.

While RBC intracellular glutamate was lower in RBCs from diabetic subjects, glutamine supplementation did not increase RBC GSH or reduce RBC oxidative stress. This may be due to limited enzymatic activity within the RBCs. To overcome this potential constraint, direct GSH loading into RBCs using hypotonic methods could be explored [236]. Hypotonic GSH loading could protect RBCs during clinical interventions such as dialysis or heart-lung bypass or in RBC storage. Since RBCs shed EVs during circulation, increasing intracellular GSH may also increase GSH content within RBC- EVs. This could potentially improve the redox status of recipient cells through EV uptake.

5.4.4 Integrating metabolic disruption in diabetes with RBC-EV effects.

In this study, RBC-EVs from both diabetic and non-diabetic subjects did not increase endothelial inflammation or oxidative stress under our experimental conditions. This suggests that RBC-EVs alone may not be sufficient to induce dysfunction. However, *in vivo*, RBC-EVs are released in the context of hyperglycemia, hyperlipidemia, and systemic inflammation. It is therefore possible that RBC-EVs contribute to endothelial dysfunction only in the presence of these additional stressors. Future studies should investigate the combined effects of RBC-EVs with hyperglycemia, altered lipid profiles, inflammatory cytokines, and inflammatory cells to better model the diabetic environment.

References:

1. Luo Y, Liu J, Zeng J, Pan H. Global burden of cardiovascular diseases attributed to low physical activity: An analysis of 204 countries and territories between 1990 and 2019. *Am J Prev Cardiol*. 2024;17. doi:10.1016/j.ajpc.2024.100633
2. Haupt M, Gerner ST, Bähr M, Doeppner TR. Neuroprotective Strategies for Ischemic Stroke—Future Perspectives. *Int J Mol Sci*. *Multidisciplinary Digital Publishing Institute (MDPI)*. 2023;24(5). doi:10.3390/ijms24054334
3. Nordanstig J, Behrendt CA, Bradbury AW, et al. Peripheral arterial disease (PAD) – A challenging manifestation of atherosclerosis. *Prev Med (Baltim)*. *Academic Press Inc.* 2023;171. doi:10.1016/j.ypmed.2023.107489
4. Schwinger RHG. Pathophysiology of heart failure. *Cardiovasc Diagn Ther*. *AME Publishing Company*. 2021;11(1). doi:10.21037/CDT-20-302
5. Widmer RJ, Lerman A. Endothelial dysfunction and cardiovascular disease. *Glob Cardiol Sci Pract*. *HBKU Press*. 2014;2014(3). doi:10.5339/gcsp.2014.43
6. Lorenty K, Harding E, Fenton O. A Call to Action to Address the Burden of Cardiovascular Disease in People with Diabetes. *Glob Heart*. 2022;17(1). doi:10.5334/GH.1176
7. Krause M, De Vito G. Type 1 and Type 2 Diabetes Mellitus: Commonalities, Differences and the Importance of Exercise and Nutrition. *Nutrients*. *Multidisciplinary Digital Publishing Institute (MDPI)*. 2023;15(19). doi:10.3390/nu15194279
8. Okorigba EM, Akinade O, Emore E, et al. Prevalence and Hospitalization Trends of Cardiovascular Disease in Diabetic Populations: An Analysis of the United States Diabetes Surveillance System (USDSS) Data From 2000 to 2022. *Cureus*. Published online July 14, 2025. doi:10.7759/cureus.87886
9. Cade WT. Diabetes-Related Microvascular and Macrovascular Diseases in the Physical Therapy Setting. *Phys Ther*. 2008;88(11):1322-1335. doi:10.2522/ptj.20080008
10. Einarson TR, Acs A, Ludwig C, Panton UH. Prevalence of cardiovascular disease in type 2 diabetes: A systematic literature review of scientific evidence from across the world in 2007-2017. *Cardiovasc Diabetol*. *BioMed Central Ltd.* 2018;17(1). doi:10.1186/s12933-018-0728-6
11. Caldarera. *Prioritizing Health | Residual Cardiovascular Risk: Beyond Traditional Risk Factors*. 2022. https://www.acc.org/Latest-in-Cardiology/Articles/2022/02/12/01/42/Prioritizing-Health-Residual-Cardiovascular-Risk-Beyond-Traditional-Risk-Factors-acc-2022#:~:text=Advances
12. Aristizábal-Colorado D, Corredor-Rengifo D, Sierra-Castillo S, et al. A decade of progress in type 2 diabetes and cardiovascular disease: advances in SGLT2 inhibitors and GLP-1 receptor agonists – a comprehensive review. *Front Endocrinol (Lausanne)*. *Frontiers Media SA*. 2025;16. doi:10.3389/fendo.2025.1605746
13. Liu Z, Lu J, Sha W, Lei T. Comprehensive treatment of diabetic endothelial dysfunction based on pathophysiological mechanism. *Front Med (Lausanne)*. *Frontiers Media SA*. 2025;12. doi:10.3389/fmed.2025.1509884
14. Medina-Leyte DJ, Zepeda-García O, Domínguez-Pérez M, González-Garrido A, Villarreal-Molina T, Jacobo-Albavera L. Endothelial dysfunction, inflammation and coronary artery disease: Potential biomarkers and promising therapeutical approaches. *Int J Mol Sci*. *MDPI AG*. 2021;22(8). doi:10.3390/ijms22083850

15. Förstermann U, Sessa WC. Nitric oxide synthases: Regulation and function. *Eur Heart J*. 2012;33(7). doi:10.1093/eurheartj/ehr304
16. Yan XL, Liu XC, Zhang YN, et al. Succinate aggravates intestinal injury in mice with necrotizing enterocolitis. *Front Cell Infect Microbiol*. 2022;12. doi:10.3389/fcimb.2022.1064462
17. Panieri E, Santoro MM. ROS signaling and redox biology in endothelial cells. *Cellular and Molecular Life Sciences*. 2015;72(17):3281-3303. doi:10.1007/s00018-015-1928-9
18. Yan R, Zhang X, Xu W, et al. ROS-Induced Endothelial Dysfunction in the Pathogenesis of Atherosclerosis. *Aging Dis*. *International Society on Aging and Disease*. 2025;16(1):250-268. doi:10.14336/AD.2024.0309
19. Fiorelli S, Porro B, Cosentino N, et al. Activation of Nrf2/HO-1 pathway and human atherosclerotic plaque vulnerability: An in vitro and in vivo study. *Cells*. 2019;8(4). doi:10.3390/cells8040356
20. Yang DR, Wang MY, Zhang CL, Wang Y. Endothelial dysfunction in vascular complications of diabetes: a comprehensive review of mechanisms and implications. *Front Endocrinol (Lausanne)*. *Frontiers Media SA*. 2024;15. doi:10.3389/fendo.2024.1359255
21. Medina-Leyte DJ, Zepeda-García O, Domínguez-Pérez M, González-Garrido A, Villarreal-Molina T, Jacobo-Albavera L. Endothelial dysfunction, inflammation and coronary artery disease: Potential biomarkers and promising therapeutical approaches. *Int J Mol Sci*. *MDPI AG*. 2021;22(8). doi:10.3390/ijms22083850
22. Sun HJ, Wu ZY, Nie XW, Bian JS. Role of endothelial dysfunction in cardiovascular diseases: The link between inflammation and hydrogen sulfide. *Front Pharmacol*. *Frontiers Media S.A.* 2020;10. doi:10.3389/fphar.2019.01568
23. Kopych V, Da Costa ADS, Park K. Endothelial Dysfunction in Atherosclerosis: Experimental Models and Therapeutics. *Biomater Res*. *American Association for the Advancement of Science*. 2025;29. doi:10.34133/bmr.0252
24. Meza CA, La Favor JD, Kim DH, Hickner RC. Endothelial dysfunction: Is there a hyperglycemia-induced imbalance of NOX and NOS? *Int J Mol Sci*. *MDPI AG*. 2019;20(15). doi:10.3390/ijms20153775
25. Yang DR, Wang MY, Zhang CL, Wang Y. Endothelial dysfunction in vascular complications of diabetes: a comprehensive review of mechanisms and implications. *Front Endocrinol (Lausanne)*. *Frontiers Media SA*. 2024;15. doi:10.3389/fendo.2024.1359255
26. Kemeny SF, Figueroa DS, Clyne AM. Hypo- and Hyperglycemia Impair Endothelial Cell Actin Alignment and Nitric Oxide Synthase Activation in Response to Shear Stress. *PLoS One*. 2013;8(6). doi:10.1371/journal.pone.0066176
27. Gray SP, Di Marco E, Okabe J, et al. NADPH Oxidase 1 plays a key role in diabetes mellitus-accelerated atherosclerosis. *Circulation*. 2013;127(18):1888-1902. doi:10.1161/CIRCULATIONAHA.112.132159
28. Wu N, Shen H, Liu H, Wang Y, Bai Y, Han P. Acute blood glucose fluctuation enhances rat aorta endothelial cell apoptosis, oxidative stress and pro-inflammatory cytokine expression in vivo. *Cardiovasc Diabetol*. 2016;15(1). doi:10.1186/s12933-016-0427-0
29. Meyerovich K, Ortis F, Cardozo AK. The non-canonical NF-κB pathway and its contribution to β-cell failure in diabetes. *J Mol Endocrinol*. *BioScientifica Ltd.* 2018;61(2):F1-F6. doi:10.1530/JME-16-0183

30. Fei Y, Sun L, Yuan C, Jiang M, Lou Q, Xu Y. CFTR ameliorates high glucose-induced oxidative stress and inflammation by mediating the NF-κB and MAPK signaling pathways in endothelial cells. *Int J Mol Med*. 2018;41(6):3501-3508. doi:10.3892/ijmm.2018.3547
31. Liu Z, Lu J, Sha W, Lei T. Comprehensive treatment of diabetic endothelial dysfunction based on pathophysiological mechanism. *Front Med (Lausanne)*. *Frontiers Media SA*. 2025;12. doi:10.3389/fmed.2025.1509884
32. Wang L, Guo L, Zhang L, et al. Effects of glucose load and nateglinide intervention on endothelial function and oxidative stress. *J Diabetes Res*. 2013;2013. doi:10.1155/2013/849295
33. Aljofan M, Ding H. High glucose increases expression of cyclooxygenase-2, increases oxidative stress and decreases the generation of nitric oxide in mouse microvessel endothelial cells. *J Cell Physiol*. 2010;222(3):669-675. doi:10.1002/jcp.21986
34. Yu W, Liu X, Feng L, et al. Glycation of paraoxonase 1 by high glucose instigates endoplasmic reticulum stress to induce endothelial dysfunction in vivo. *Sci Rep*. 2017;7. doi:10.1038/srep45827
35. Magenta A, Greco S, Capogrossi MC, Gaetano C, Martelli F. Nitric oxide, oxidative stress, and p66Shc interplay in diabetic endothelial dysfunction. *Biomed Res Int*. 2014;2014. doi:10.1155/2014/193095
36. Wang Y, Yang P, Yan Z, et al. The Relationship between Erythrocytes and Diabetes Mellitus. *J Diabetes Res*. *Hindawi Limited*. 2021;2021. doi:10.1155/2021/6656062
37. McMahon TJ. Red Blood Cell Deformability, Vasoactive Mediators, and Adhesion. *Front Physiol*. *Frontiers Media S.A.* 2019;10. doi:10.3389/fphys.2019.01417
38. Zhang Z, Teo H, Preißing T, Neu B. The role of sialic acid and macromolecular depletion interactions in red blood cell adhesion: Insights from interference reflection microscopy. *Colloids Surf B Biointerfaces*. 2025;254. doi:10.1016/j.colsurfb.2025.114861
39. Pernow J, Mahdi A, Yang J, Zhou Z. Red blood cell dysfunction: A new player in cardiovascular disease. *Cardiovasc Res*. 2019;115(11):1596-1605. doi:10.1093/cvr/cvz156
40. Kuhn V, Diederich L, Keller TCS, et al. Red Blood Cell Function and Dysfunction: Redox Regulation, Nitric Oxide Metabolism, Anemia. *Antioxid Redox Signal*. *Mary Ann Liebert Inc.* 2017;26(13):718-742. doi:10.1089/ars.2016.6954
41. Cortese-Krott MM, Kelm M. Endothelial nitric oxide synthase in red blood cells: Key to a new erythrocrine function? *Redox Biol*. *Elsevier B.V.* 2014;2(1):251-258. doi:10.1016/j.redox.2013.12.027
42. Racine ML, Terwoord JD, Ketelhut NB, et al. Rho-kinase inhibition improves haemodynamic responses and circulating ATP during hypoxia and moderate intensity handgrip exercise in healthy older adults. *J Physiol*. 2022;600(14):3265-3285. doi:10.1113/JP282730
43. Kirby BS, Crecelius AR, Voyles WF, Dinenno FA. Clinical/Translational Research Impaired Skeletal Muscle Blood Flow Control With Advancing Age in Humans Attenuated ATP Release and Local Vasodilation During Erythrocyte Deoxygenation. Published online 2012. doi:10.1161/CIRCRESAHA.112
44. Ulker P, Gunduz F, Meiselman HJ, Baskurt OK. Nitric oxide generated by red blood cells following exposure to shear stress dilates isolated small mesenteric arteries under hypoxic conditions. *Clin Hemorheol Microcirc*. 2013;54(4):357-369. doi:10.3233/CH-2012-1618

45. Leo F, Suvorava T, Heuser SK, et al. Red Blood Cell and Endothelial eNOS Independently Regulate Circulating Nitric Oxide Metabolites and Blood Pressure. *Circulation*. 2021;144(11):870-889. doi:10.1161/CIRCULATIONAHA.120.049606
46. Sangha GS, Weber CM, Sapp RM, et al. Mechanical stimuli such as shear stress and piezo1 stimulation generate red blood cell extracellular vesicles. *Front Physiol*. 2023;14. doi:10.3389/fphys.2023.1246910
47. Sangha GS, Smith L V., Kheradmand M, et al. Piezo1 activates nitric oxide synthase in red blood cells via protein kinase C with increased activity in diabetes. *Mechanobiology in Medicine*. 2025;3(3). doi:10.1016/j.mbm.2025.100145
48. Diesen DL, Hess DT, Stamler JS. Hypoxic vasodilation by red blood cells: Evidence for an s-nitrosothiol-based signal. *Circ Res*. 2008;103(5):545-553. doi:10.1161/CIRCRESAHA.108.176867
49. Helms CC, Gladwin MT, Kim-Shapiro DB. Erythrocytes and vascular function: Oxygen and nitric oxide. *Front Physiol*. *Frontiers Media S.A.* 2018;9(FEB). doi:10.3389/fphys.2018.00125
50. Rifkind JM, Mohanty JG, Nagababu E, Salgado MT, Cao Z. Potential modulation of vascular function by nitric oxide and reactive oxygen species released from erythrocytes. *Front Physiol*. 2018;9(JUN). doi:10.3389/fphys.2018.00690
51. Wautier JL, Paton RC, Wautier MP, et al. increased adhesion of RBCs. *N Engl J Med*. Published online 1981:237-242.
52. Wautier JL, Wautier MP. Cellular and molecular aspects of blood cell–endothelium interactions in vascular disorders. *Int J Mol Sci*. 2020;21(15):1-16. doi:10.3390/ijms21155315
53. Mahdi A, Tratsiakovich Y, Tengbom J, et al. Erythrocytes Induce Endothelial Injury in Type 2 Diabetes Through Alteration of Vascular Purinergic Signaling. *Front Pharmacol*. 2020;11. doi:10.3389/fphar.2020.603226
54. Zhang H, Wang C, Sun H, et al. Glutamine supplementation alleviated aortic atherosclerosis in mice model and in vitro. *Proteomics*. Published online 2023. doi:10.1002/pmic.202300179
55. Yang J, Gonon AT, Sjöquist PO, Lundberg JO, Pernow J. Arginase regulates red blood cell nitric oxide synthase and export of cardioprotective nitric oxide bioactivity. *Proc Natl Acad Sci U S A*. 2013;110(37):15049-15054. doi:10.1073/pnas.1307058110
56. Zhou Z, Mahdi A, Tratsiakovich Y, et al. Erythrocytes From Patients With Type 2 Diabetes Induce Endothelial Dysfunction Via Arginase I. *J Am Coll Cardiol*. 2018;72(7):769-780. doi:10.1016/j.jacc.2018.05.052
57. Jiang M, Ding Y, Su Y, Hu X, Li J, Zhang Z. Arginase-flotillin interaction brings arginase to red blood cell membrane. *FEBS Lett*. 2006;580(28-29):6561-6564. doi:10.1016/j.febslet.2006.11.003
58. Thangaraju K, Neerukonda SN, Katneni U, Buehler PW. Extracellular vesicles from red blood cells and their evolving roles in health, coagulopathy and therapy. *Int J Mol Sci*. *MDPI AG*. 2021;22(1):1-25. doi:10.3390/ijms22010153
59. Khalyfa A, Sanz-Rubio D. The mystery of red blood cells extracellular vesicles in sleep apnea with metabolic dysfunction. *Int J Mol Sci*. *MDPI*. 2021;22(9). doi:10.3390/ijms22094301
60. He Y, Wu Q. The Effect of Extracellular Vesicles on Thrombosis. *J Cardiovasc Transl Res*. *Springer*. 2023;16(3):682-697. doi:10.1007/s12265-022-10342-w

61. Peng L, Li Y, Li X, et al. Extracellular Vesicles Derived from Intermittent Hypoxia-Treated Red Blood Cells Impair Endothelial Function Through Regulating eNOS Phosphorylation and ET-1 Expression. doi:10.1007/s10557-020-07117-3/Published
62. Rubin O, Delobel J, Prudent M, et al. Red blood cell–derived microparticles isolated from blood units initiate and propagate thrombin generation. *Transfusion (Paris)*. 2013;53(8):1744-1754. doi:10.1111/trf.12008
63. Sweeney J, Kouttab N, Kurtis J. Stored red blood cell supernatant facilitates thrombin generation. *Transfusion (Paris)*. 2009;49(8):1569-1579. doi:10.1111/j.1537-2995.2009.02196.x
64. An R, Man Y, Cheng K, et al. Sickle red blood cell-derived extracellular vesicles activate endothelial cells and enhance sickle red cell adhesion mediated by von Willebrand factor. *Br J Haematol*. 2023;201(3):552-563. doi:10.1111/bjh.18616
65. Liu C, Zhao W, Christ GJ, Gladwin MT, Kim-Shapiro DB. Nitric oxide scavenging by red cell microparticles. *Free Radic Biol Med*. 2013;65:1164-1173. doi:10.1016/j.freeradbiomed.2013.09.002
66. Chiangjong W, Netsirisawan P, Hongeng S, Chutipongtanate S. Red Blood Cell Extracellular Vesicle-Based Drug Delivery: Challenges and Opportunities. *Front Med (Lausanne)*. *Frontiers Media S.A.* 2021;8. doi:10.3389/fmed.2021.761362
67. Collado A, Humoud R, Kontidou E, et al. Erythrocyte-derived extracellular vesicles induce endothelial dysfunction through arginase-1 and oxidative stress in type 2 diabetes. *Journal of Clinical Investigation*. 2025;135(10). doi:10.1172/JCI180900
68. Freeman DW, Noren Hooten N, Eitan E, et al. Altered extracellular vesicle concentration, cargo, and function in diabetes. *Diabetes*. 2018;67(11):2377-2388. doi:10.2337/db17-1308
69. Sukati S, Chunglok W, Naulkaew T, et al. Elevated red blood cell-derived extracellular vesicles under hyperglycemic conditions are associated with CD47 expression and production of intracellular reactive oxygen species. *Biomed Rep*. 2025;23(2). doi:10.3892/br.2025.2007
70. Xu S, Liao J, Liu B, Zhang C, Xu X. Aerobic glycolysis of vascular endothelial cells: a novel perspective in cancer therapy. *Mol Biol Rep*. *Springer Science and Business Media B.V.* 2024;51(1). doi:10.1007/s11033-024-09588-1
71. Wong BW, Marsch E, Treps L, Baes M, Carmeliet P. Endothelial cell metabolism in health and disease: impact of hypoxia. *EMBO J*. 2017;36(15):2187-2203. doi:10.15252/embj.201696150
72. Du W, Ren L, Hamblin MH, Fan Y. Endothelial cell glucose metabolism and angiogenesis. *Biomedicines*. 2021;9(2):1-17. doi:10.3390/biomedicines9020147
73. Moiz B, Garcia J, Basehore S, et al. metabolites 13 C Metabolic Flux Analysis Indicates Endothelial Cells Attenuate Metabolic Perturbations by Modulating TCA Activity. Published online 2021. doi:10.3390/metabo
74. Liu B, Dai Z. Fatty Acid Metabolism in Endothelial Cell. *Genes (Basel)*. *MDPI*. 2022;13(12). doi:10.3390/genes13122301
75. Mirveis Z, Howe O, Cahill P, Patil N, Byrne HJ. Monitoring and modelling the glutamine metabolic pathway: a review and future perspectives. *Metabolomics*. *Springer*. 2023;19(8). doi:10.1007/s11306-023-02031-9
76. Liu Y, Zhao T, Li Z, Wang L, Yuan S, Sun L. The role of ASCT2 in cancer: A review. *Eur J Pharmacol*. *Elsevier B.V.* 2018;837:81-87. doi:10.1016/j.ejphar.2018.07.007

77. Kim B, Li J, Jang C, Arany Z. Glutamine fuels proliferation but not migration of endothelial cells. *EMBO J*. 2017;36(16):2321-2333. doi:10.15252/embj.201796436
78. Huang H, Vandekeere S, Kalucka J, et al. Role of glutamine and interlinked asparagine metabolism in vessel formation. *EMBO J*. 2017;36(16):2334-2352. doi:10.15252/embj.201695518
79. Yoo HC, Yu YC, Sung Y, Han JM. Glutamine reliance in cell metabolism. *Exp Mol Med*. *Springer Nature*. 2020;52(9):1496-1516. doi:10.1038/s12276-020-00504-8
80. Lu SC. Glutathione synthesis. *Biochim Biophys Acta Gen Subj*. 2013;1830(5):3143-3153. doi:10.1016/j.bbagen.2012.09.008
81. Lu SC. Regulation of glutathione synthesis. *Mol Aspects Med*. 2009;30(1-2):42-59. doi:10.1016/j.mam.2008.05.005
82. Lyssiotis CA, Son J, Cantley LC, Kimmelman AC. Pancreatic cancers rely on a novel glutamine metabolism pathway to maintain redox balance. *Cell Cycle*. *Taylor and Francis Inc.* 2013;12(13):1987-1988. doi:10.4161/cc.25307
83. Katayama N, Iwazumi K, Suzuki H, Osanai T, Ito S. Malic Enzyme, not Malate Dehydrogenase, Mainly Oxidizes Malate That Originates from the Tricarboxylic Acid Cycle in Cyanobacteria. *mBio*. 2022;13(6). doi:10.1128/mbio.02187-22
84. Durante W. The emerging role of l-glutamine in cardiovascular health and disease. *Nutrients*. 2019;11(9). doi:10.3390/nu11092092
85. Peyton KJ, Liu X ming, Yu Y, Yates B, Behnammanesh G, Durante W. Glutaminase-1 stimulates the proliferation, migration, and survival of human endothelial cells. *Biochem Pharmacol*. 2018;156:204-214. doi:10.1016/j.bcp.2018.08.032
86. Peng H, Wang X, Du J, Cui Q, Huang Y, Jin H. Metabolic Reprogramming of Vascular Endothelial Cells: Basic Research and Clinical Applications. *Front Cell Dev Biol*. *Frontiers Media S.A.* 2021;9. doi:10.3389/fcell.2021.626047
87. Wu G, Haynes TE, Li H, Meininger CJ. *Glutamine Metabolism in Endothelial Cells: Ornithine Synthesis from Glutamine via Pyrroline-5-Carboxylate Synthase*. Vol 126. 2000. www.elsevier.com/locate/cbpa
88. de Ingeniis J, Ratnikov B, Richardson AD, et al. Functional Specialization in Proline Biosynthesis of Melanoma. *PLoS One*. 2012;7(9). doi:10.1371/journal.pone.0045190
89. Teo CF, Wollaston-Hayden EE, Wells L. Hexosamine flux, the O-GlcNAc modification, and the development of insulin resistance in adipocytes. *Mol Cell Endocrinol*. 2010;318(1-2):44-53. doi:10.1016/j.mce.2009.09.022
90. Wu G, Haynes TE, Li H, Yan W, Meininger CJ. *Glutamine Metabolism to Glucosamine Is Necessary for Glutamine Inhibition of Endothelial Nitric Oxide Synthesis*. Vol 353. 2001.
91. Beleznai T, Bagi Z. Activation of hexosamine pathway impairs nitric oxide (NO)-dependent arteriolar dilations by increased protein O-GlcNAcylation. *Vascul Pharmacol*. 2012;56(3-4):115-121. doi:10.1016/j.vph.2011.11.003
92. Addabbo F, Chen Q, Patel DP, et al. Glutamine Supplementation Alleviates Vasculopathy and Corrects Metabolic Profile in an In Vivo Model of Endothelial Cell Dysfunction. *PLoS One*. 2013;8(6). doi:10.1371/journal.pone.0065458
93. Kawakami A, Sato H, Nakadate Y, et al. Cardioprotective effects of L-glutamine in an ischemic rat heart model. *Microvasc Res*. 2025;158. doi:10.1016/j.mvr.2024.104764
94. Brownlee M. Biochemistry and molecular cell biology of diabetic complications. *Nature*. 2001;414(6865):813-820. doi:10.1038/414813a

95. Du X, Matsumura T, Edelstein D, et al. Inhibition of GAPDH activity by poly(ADP-ribose) polymerase activates three major pathways of hyperglycemic damage in endothelial cells. *Journal of Clinical Investigation*. 2003;112(7):1049-1057. doi:10.1172/JCI18127
96. Pabitra B Pal, Himangshu Sonowal, Kirtikar Shukla, Satish K Srivastava, Kota V Ramana. Aldose reductase regulates hyperglycemia-induced HUVEC death via SIRT1/AMPK-α1/mTOR pathway. *Journal of Molecular Endocrinology*. 2019;63(1):11-25.
97. Wu G, Haynes TE, Li H, Yan W, Meininger CJ. *Glutamine Metabolism to Glucosamine Is Necessary for Glutamine Inhibition of Endothelial Nitric Oxide Synthesis*. Vol 353. 2001.
98. Ge T, Yang J, Zhou S, Wang Y, Li Y, Tong X. The Role of the Pentose Phosphate Pathway in Diabetes and Cancer. *Front Endocrinol (Lausanne)*. *Frontiers Media S.A.* 2020;11. doi:10.3389/fendo.2020.00365
99. Mansour A, Mohajeri- Tehrani MR, Qorbani M, Heshmat R, Larijani B, Hosseini S. Effect of glutamine supplementation on cardiovascular risk factors in patients with type 2 diabetes. *Nutrition*. 2015;31(1):119-126. doi:10.1016/j.nut.2014.05.014
100. Singh VP, Bali A, Singh N, Jaggi AS. Advanced glycation end products and diabetic complications. *Korean Journal of Physiology and Pharmacology*. *Korean Physiological Soc. and Korean Soc. of Pharmacology*. 2014;18(1):1-14. doi:10.4196/kjpp.2014.18.1.1
101. Lorenzi M. The polyol pathway as a mechanism for diabetic retinopathy: Attractive, elusive, and resilient. *Exp Diabesity Res*. 2007;2007. doi:10.1155/2007/61038
102. Kukreja RC, Xi L. eNOS phosphorylation: A pivotal molecular switch in vasodilation and cardioprotection? *J Mol Cell Cardiol*. 2007;42(2):280-282. doi:10.1016/j.yjmcc.2006.10.011
103. Du XL, Edelstein D, Dimmeler S, Ju Q, Sui C, Brownlee M. Hyperglycemia inhibits endothelial nitric oxide synthase activity by posttranslational modification at the Akt site. *Journal of Clinical Investigation*. 2001;108(9):1341-1348. doi:10.1172/jci200111235
104. Zang Z, Apse K, Pang J, Stanton RC. High glucose inhibits glucose-6-phosphate dehydrogenase via cAMP in aortic endothelial cells. *Journal of Biological Chemistry*. 2000;275(51):40042-40047. doi:10.1074/jbc.M007505200
105. Van Wijk R, Van Solinge WW. The energy-less red blood cell is lost: Erythrocyte enzyme abnormalities of glycolysis. *Blood*. *American Society of Hematology*. 2005;106(13):4034-4042. doi:10.1182/blood-2005-04-1622
106. Whillier S, Garcia B, Chapman BE, Kuchel PW, Raftos JE. Glutamine and α-ketoglutarate as glutamate sources for glutathione synthesis in human erythrocytes. *FEBS Journal*. 2011;278(17):3152-3163. doi:10.1111/j.1742-4658.2011.08241.x
107. Morris CR. *Role of Arginase in Sickle Cell Lung Disease and Hemolytic Anemias*. Vol 2. 2010. doi:10.2174/1875042701002010041
108. Jafri F, Seong G, Jang T, et al. L-glutamine for sickle cell disease: more than reducing redox. *Ann Hematol*. *Springer Science and Business Media Deutschland GmbH*. 2022;101(8):1645-1654. doi:10.1007/s00277-022-04867-y
109. Niihara Y, Miller ST, Kanter J, et al. A Phase 3 Trial of l -Glutamine in Sickle Cell Disease . *New England Journal of Medicine*. 2018;379(3):226-235. doi:10.1056/nejmoa1715971
110. Elenga N, Loko G, Etienne-Julan M, Al-Okka R, Adel AM, Yassin MA. Real-World data on efficacy of L-glutamine in preventing sickle cell disease-related complications in

pediatric and adult patients. *Front Med (Lausanne)*. 2022;9. doi:10.3389/fmed.2022.931925
111. Binns HC, Alipour E, Sherlock CE, et al. Amino acid supplementation confers protection to red blood cells before Plasmodium falciparum bystander stress. *Blood Adv*. 2024;8(10):2552-2564. doi:10.1182/bloodadvances.2023010820
112. Travis SF, Morrison AD, Clements RS, Winegrad AI, Oski FA. Metabolic alterations in the human erythrocyte produced by increases in glucose concentration. The role of the polyol pathway. *J Clin Invest*. 1971;50(10):2104-2112. doi:10.1172/JCI106704
113. Ciuchi E, Odetti P, Prando R. Relationship Between Glutathione and Sorbitol Concentrations in Erythrocytes From Diabetic Patients. *Metabolism*. 1996;45(5):611-613.
114. Wang Y, Yang P, Yan Z, et al. The Relationship between Erythrocytes and Diabetes Mellitus. *J Diabetes Res*. *Hindawi Limited*. 2021;2021. doi:10.1155/2021/6656062
115. Cortese-Krott MM, Rodriguez-Mateos A, Sansone R, et al. Human red blood cells at work: identification and visualization of erythrocytic eNOS activity in health and disease. Published online 2012. doi:10.1182/blood-2012
116. Daraghmeh DN, Karaman R. The Redox Process in Red Blood Cells: Balancing Oxidants and Antioxidants. *Antioxidants*. *Multidisciplinary Digital Publishing Institute (MDPI)*. 2025;14(1). doi:10.3390/antiox14010036
117. Ting Li, Anne Le. Glutamine Metabolism in Cancer. *Advances in Experimental Medicine and Biology*. 1063.
118. Sadaf A, Quinn CT. L-glutamine for sickle cell disease: Knight or pawn? *Exp Biol Med*. *SAGE Publications Inc.* 2020;245(2):146-154. doi:10.1177/1535370219900637
119. Chen J, Zhang S, Wu J, Wu S, Xu G, Wei D. Essential Role of Nonessential Amino Acid Glutamine in Atherosclerotic Cardiovascular Disease. *DNA Cell Biol*. *Mary Ann Liebert Inc.* 2020;39(1):8-15. doi:10.1089/dna.2019.5034
120. Jin J, Byun JK, Choi YK, Park KG. Targeting glutamine metabolism as a therapeutic strategy for cancer. *Exp Mol Med*. *Springer Nature*. 2023;55(4):706-715. doi:10.1038/s12276-023-00971-9
121. Yu M, Chen H, Chen C, et al. Hyperglycemia-depleted glutamine contributes to the pathogenesis of diabetic corneal endothelial dysfunction. *Exp Eye Res*. 2024;249. doi:10.1016/j.exer.2024.110124
122. Mahdi A, Jiao T, Yang J, et al. The effect of glycemic control on endothelial and cardiac dysfunction induced by red blood cells in type 2 diabetes. *Front Pharmacol*. 2019;10(JULY). doi:10.3389/fphar.2019.00861
123. Tsai PH, Liu JJ, Yeh CL, Chiu WC, Yeh SL. Effects of glutamine supplementation on oxidative stress-related gene expression and antioxidant properties in rats with streptozotocin-induced type 2 diabetes. *Br J Nutr*. 2012;107(8):1112-1118. doi:10.1017/S0007114511004168
124. Zhao M, Zhou J, Hu Y, et al. Defective Endothelial Glutaminolysis Contributes to Impaired Angiogenesis and Poor Ischemic Tissue Repair in Diabetes. *Research*. 2025;8. doi:10.34133/research.0706
125. Safi SZ, Batumalaie K, Mansor M, et al. Glutamine treatment attenuates hyperglycemia-induced mitochondrial stress and apoptosis in umbilical vein endothelial cells. *Clinics*. 2015;70(8):569-576. doi:10.6061/clinics/2015(08)07

126. Li K, Cui YC, Zhang H, et al. Glutamine reduces the apoptosis of H9C2 cells treated with high-glucose and reperfusion through an oxidation-related mechanism. *PLoS One*. 2015;10(7). doi:10.1371/journal.pone.0132402
127. Kim B, Li J, Jang C, Arany Z. Glutamine fuels proliferation but not migration of endothelial cells. *EMBO J*. 2017;36(16):2321-2333. doi:10.15252/embj.201796436
128. Ko CH, Yeh SL, Yeh CL. Dietary Supplemental Glutamine Enhances the Percentage of Circulating Endothelial Progenitor Cells in Mice with High-Fat Diet-Induced Obesity Subjected to Hind Limb Ischemia. *Mediators Inflamm*. 2020;2020. doi:10.1155/2020/3153186
129. Mansour A, Mohajeri- Tehrani MR, Qorbani M, Heshmat R, Larijani B, Hosseini S. Effect of glutamine supplementation on cardiovascular risk factors in patients with type 2 diabetes. *Nutrition*. 2015;31(1):119-126. doi:10.1016/j.nut.2014.05.014
130. Galera SC, Fechine FV, Teixeira MJ, Coelho ZCB, de Vasconcelos RC, Leitão de Vasconcelos PR. The safety of oral use of l-glutamine in middle-aged and elderly individuals. *Nutrition*. 2010;26(4):375-381. doi:10.1016/j.nut.2009.05.013
131. Kassab A, Piwowar A. Cell oxidant stress delivery and cell dysfunction onset in type 2 diabetes. *Biochimie*. 2012;94(9):1837-1848. doi:10.1016/j.biochi.2012.01.020
132. Kim B, Li J, Jang C, Arany Z. Glutamine fuels proliferation but not migration of endothelial cells. *EMBO J*. 2017;36(16):2321-2333. doi:10.15252/embj.201796436
133. Peyton KJ, Liu X ming, Yu Y, Yates B, Behnammanesh G, Durante W. Glutaminase-1 stimulates the proliferation, migration, and survival of human endothelial cells. *Biochem Pharmacol*. 2018;156:204-214. doi:10.1016/j.bcp.2018.08.032
134. Zhao M, Zhou J, Hu Y, et al. Defective Endothelial Glutaminolysis Contributes to Impaired Angiogenesis and Poor Ischemic Tissue Repair in Diabetes. *Research*. 2025;8. doi:10.34133/research.0706
135. Arnal JF, Münzel T, Venema RC, et al. Interactions between L-arginine and L-glutamine change endothelial NO production: An effect independent of NO synthase substrate availability. *Journal of Clinical Investigation*. 1995;95(6):2565-2572. doi:10.1172/JCI117957
136. Kawaguchi T, Brusilow SW, Traystman RJ, Koehler RC. Glutamine-dependent inhibition of pial arteriolar dilation to acetylcholine with and without hyperammonemia in the rat. *First Am J Physiol Regul Integr Comp Physiol*. 2005;288:1612-1619. doi:10.1152/ajpregu.00783.2004.-Glu
137. Wu G, Haynes TE, Li H, Yan W, Meininger CJ. *Glutamine Metabolism to Glucosamine Is Necessary for Glutamine Inhibition of Endothelial Nitric Oxide Synthesis*. Vol 353. 2001.
138. Basehore SE, Bohlman S, Weber C, et al. Laminar Flow on Endothelial Cells Suppresses eNOS O-GlcNAcylation to Promote eNOS Activity. *Circ Res*. 2021;129(11):1054-1066. doi:10.1161/CIRCRESAHA.121.318982
139. Ellis AC, Patterson M, Dudenbostel T, Calhoun D, Gower B. Effects of 6-month supplementation with β-hydroxy-β-methylbutyrate, glutamine and arginine on vascular endothelial function of older adults. *Eur J Clin Nutr*. 2016;70(2):269-273. doi:10.1038/ejcn.2015.137
140. Mansour A, Mohajeri- Tehrani MR, Qorbani M, Heshmat R, Larijani B, Hosseini S. Effect of glutamine supplementation on cardiovascular risk factors in patients with type 2 diabetes. *Nutrition*. 2015;31(1):119-126. doi:10.1016/j.nut.2014.05.014

141. Safi SZ, Batumalaie K, Mansor M, et al. Glutamine treatment attenuates hyperglycemia-induced mitochondrial stress and apoptosis in umbilical vein endothelial cells. *Clinics*. 2015;70(8):569-576. doi:10.6061/clinics/2015(08)07
142. Lee SM, Koh D, Fun SN, Sum CF. Diabetes management and hyperglycemia in safety sensitive jobs. *Saf Health Work*. *Elsevier Science B.V.* 2011;2(4):380-384. doi:10.5491/SHAW.2011.2.4.380
143. Low SY, Salter M, Knowles RG, Pogsont C 1, Rennie MJ. *A Quantitative Analysis of the Control of Glutamine Catabolism in Rat Liver Cells Use Ot Selective Inhibitors*. Vol 295. 1993.
144. Wals PA, Katz J. A concentration gradient of glucose from liver to plasma. *Metabolism*. 1993;42(11):1492-1496. doi:10.1016/0026-0495(93)90204-2
145. Shukla K, Ferraris D V., Thomas AG, et al. Design, synthesis, and pharmacological evaluation of bis-2-(5- phenylacetamido-1,2,4-thiadiazol-2-yl)ethyl sulfide 3 (BPTES) analogs as glutaminase inhibitors. *J Med Chem*. 2012;55(23):10551-10563. doi:10.1021/jm301191p
146. Uggeri J, Gatti R, Belletti S, et al. Calcein-AM is a detector of intracellular oxidative activity. *Histochem Cell Biol*. 2000;122(5):499-505. doi:10.1007/s00418-004-0712-y
147. Wedel S, Martic I, Hrapovic N, et al. tBHP treatment as a model for cellular senescence and pollution-induced skin aging. *Mech Ageing Dev*. 2020;190. doi:10.1016/j.mad.2020.111318
148. Bongard RD, Lindemer BJ, Krenz GS, Merker MP. Preferential utilization of NADPH as the endogenous electron donor for NAD(P)H:quinone oxidoreductase 1 (NQO1) in intact pulmonary arterial endothelial cells. *Free Radic Biol Med*. 2009;46(1):25-32. doi:10.1016/j.freeradbiomed.2008.09.007
149. Schoonjans CA, Mathieu B, Joudiou N, et al. Targeting endothelial cell metabolism by inhibition of pyruvate dehydrogenase kinase and glutaminase-1. *J Clin Med*. 2020;9(10):1-14. doi:10.3390/jcm9103308
150. Das S, Kar Mahapatra S, Gautam N, Das A, Roy S. Oxidative stress in lymphocytes, neutrophils, and serum of oral cavity cancer patients: Modulatory array of L-glutamine. *Supportive Care in Cancer*. 2007;15(12):1399-1405. doi:10.1007/s00520-007-0266-3
151. Nakhostin-Roohi B, Javanamani R. The Effect of Glutamine Supplementation on Exercise-Induced Oxidative Stress. *Journal of Advanced Agricultural Technologies*. 2015;2(1). doi:10.12720/joaat.2.1.8-12
152. Liu XM, Peyton KJ, Durante W. Ammonia promotes endothelial cell survival via the heme oxygenase-1-mediated release of carbon monoxide. *Free Radic Biol Med*. 2017;102:37-46. doi:10.1016/j.freeradbiomed.2016.11.029
153. Zhang H, Forman HJ. Glutathione synthesis and its role in redox signaling. *Semin Cell Dev Biol*. *Elsevier Ltd*. 2012;23(7):722-728. doi:10.1016/j.semcdb.2012.03.017
154. Li M, Chiu JF, Kelsen A, Lu SC, Fukagawa NK. Identification and characterization of an Nrf2-mediated ARE upstream of the rat glutamate cysteine ligase catalytic subunit gene (GCLC). *J Cell Biochem*. 2009;107(5):944-954. doi:10.1002/jcb.22197
155. Huang CS, Lii CK, Lin AH, et al. Protection by chrysin, apigenin, and luteolin against oxidative stress is mediated by the Nrf2-dependent up-regulation of heme oxygenase 1 and glutamate cysteine ligase in rat primary hepatocytes. *Arch Toxicol*. 2013;87(1):167-178. doi:10.1007/s00204-012-0913-4

156. Ying M, You D, Zhu X, Cai L, Zeng S, Hu X. Lactate and glutamine support NADPH generation in cancer cells under glucose deprived conditions. *Redox Biol*. 2021;46. doi:10.1016/j.redox.2021.102065
157. Lin TY, Cantley LC, DeNicola GM. NRF2 Rewires Cellular Metabolism to Support the Antioxidant Response. In: *A Master Regulator of Oxidative Stress - The Transcription Factor Nrf2*. InTech; 2016. doi:10.5772/65141
158. Chen Z, Hu Y, Hu FB, et al. Dietary Glutamine and Glutamate in Relation to Cardiovascular Disease Incidence and Mortality in the United States Men and Women with Diabetes Mellitus. *Journal of Nutrition*. 2023;153(11):3247-3258. doi:10.1016/j.tjnut.2023.08.031
159. Durante W. The emerging role of l-glutamine in cardiovascular health and disease. *Nutrients*. 2019;11(9). doi:10.3390/nu11092092
160. Aulak KS, Barnes JW, Tian L, et al. Specific O-GlcNAc modification at Ser-615 modulates eNOS function. *Redox Biol*. 2020;36. doi:10.1016/j.redox.2020.101625
161. Meininger CJ, Guoyao WU. L-glutamine inhibits nitric oxide synthesis in bovine venular endothelial cells. *Journal of Pharmacology and Experimental Therapeutics*. 1997;281(1):448-453. doi:10.1016/s0022-3565(24)36584-x
162. Hecker M, Mitchell JA, Swierkosz TA, Sessa WC, Vane JR. *Jy Inhibition by L-Glutamine of the Release of Endothelium-Derived Relaxing Factor from Cultured Endothelial Cells*.
163. Sessa WC, Hecker M, Mitchell JA, Vane JR. *The Metabolism of L-Arginine and Its Significance for the Biosynthesis of Endothelium-Derived Relaxing Factor: L-Glutamine Inhibits the Generation of L-Arginine by Cultured Endothelial Cells*. Vol 87. 1990.
164. Kemeny SF, Figueroa DS, Clyne AM. Hypo- and Hyperglycemia Impair Endothelial Cell Actin Alignment and Nitric Oxide Synthase Activation in Response to Shear Stress. *PLoS One*. 2013;8(6). doi:10.1371/journal.pone.0066176
165. Serizawa K ichi, Yogo K, Aizawa K, Tashiro Y, Ishizuka N. Nicorandil prevents endothelial dysfunction due to antioxidative effects via normalisation of NADPH oxidase and nitric oxide synthase in streptozotocin diabetic rats. *Cardiovasc Diabetol*. 2011;10. doi:10.1186/1475-2840-10-105
166. BERGMAN R, ADER M. Free Fatty Acids and Pathogenesis of Type 2 Diabetes Mellitus. *Trends in Endocrinology and Metabolism*. 2000;11(9):351-356. doi:10.1016/S1043-2760(00)00323-4
167. Muniandy S, Qvist R, Ong Siok Yan G, Jack Bee C, Koon Chu Y, Vinsent Rayappan A. The oxidative stress of hyperglycemia and the inflammatory process in endothelial cells. *The Journal of Medical Investigation*. 2009;56(1,2):6-10. doi:10.2152/jmi.56.6
168. Balakumar P, Taneja G. Fish oil and vascular endothelial protection: Bench to bedside. *Free Radic Biol Med*. 2012;53(2):271-279. doi:10.1016/j.freeradbiomed.2012.05.005
169. Huang H, Li G, He Y, et al. Cellular succinate metabolism and signaling in inflammation: implications for therapeutic intervention. *Front Immunol*. *Frontiers Media SA*. 2024;15. doi:10.3389/fimmu.2024.1404441
170. Schoors S, Bruning U, Missiaen R, et al. Fatty acid carbon is essential for dNTP synthesis in endothelial cells. *Nature*. 2015;520(7546):192-197. doi:10.1038/nature14362
171. Kaczara P, Czyzynska-Cichon I, Kus E, et al. Liver sinusoidal endothelial cells rely on oxidative phosphorylation but avoid processing long-chain fatty acids in their mitochondria. *Cell Mol Biol Lett*. 2024;29(1). doi:10.1186/s11658-024-00584-8

172. Wellen KE, Lu C, Mancuso A, et al. The hexosamine biosynthetic pathway couples growth factor-induced glutamine uptake to glucose metabolism. *Genes Dev*. 2010;24(24):2784-2799. doi:10.1101/gad.1985910
173. Mann GE, Yudilevich DL, Sobrevia L. Regulation of Amino Acid and Glucose Transporters in Endothelial and Smooth Muscle Cells. Published online 2003. doi:10.1152/physrev.00022.2002.-While
174. Taslimifar M, Faltys M, Kurtcuoglu V, Verrey F, Makrides V. Analysis of L-leucine amino acid transporter species activity and gene expression by human blood brain barrier hCMEC/D3 model reveal potential LAT1, LAT4, B0AT2 and y+LAT1 functional cooperation. *Journal of Cerebral Blood Flow and Metabolism*. 2022;42(1):90-103. doi:10.1177/0271678X211039593
175. Blot A, Billups D, Bjørkmo M, et al. Functional expression of two system A glutamine transporter isoforms in rat auditory brainstem neurons. *Neuroscience*. 2009;164(3):998-1008. doi:10.1016/j.neuroscience.2009.09.015
176. Hinca SB, Salcedo C, Wagner A, et al. Brain endothelial cells metabolize glutamate via glutamate dehydrogenase to replenish TCA-intermediates and produce ATP under hypoglycemic conditions. *J Neurochem*. 2021;157(6):1861-1875. doi:10.1111/jnc.15207
177. Darley-Usmar VM, Ball LE, Chatham JC. Protein O-linked β-N-acetylglucosamine: A novel effector of cardiomyocyte metabolism and function. *J Mol Cell Cardiol*. 2012;52(3):538-549. doi:10.1016/j.yjmcc.2011.08.009
178. Paneque A, Fortus H, Zheng J, Werlen G, Jacinto E. The Hexosamine Biosynthesis Pathway: Regulation and Function. *Genes (Basel)*. *Multidisciplinary Digital Publishing Institute (MDPI)*. 2023;14(4). doi:10.3390/genes14040933
179. Sivashanmugam M, J. J, V. U, K.N. S. Ornithine and its role in metabolic diseases: An appraisal. *Biomedicine and Pharmacotherapy*. *Elsevier Masson SAS*. 2017;86:185-194. doi:10.1016/j.biopha.2016.12.024
180. Chalecka M, Kazberuk A, Palka J, Surazynski A. P5c as an interface of proline interconvertible amino acids and its role in regulation of cell survival and apoptosis. *Int J Mol Sci*. *MDPI*. 2021;22(21). doi:10.3390/ijms222111763
181. Ducker GS, Rabinowitz JD. One-Carbon Metabolism in Health and Disease. *Cell Metab*. *Cell Press*. 2017;25(1):27-42. doi:10.1016/j.cmet.2016.08.009
182. Hwang Y, Yun HJ, Jeong JW, et al. Co-inhibition of glutaminolysis and one-carbon metabolism promotes ROS accumulation leading to enhancement of chemotherapeutic efficacy in anaplastic thyroid cancer. *Cell Death Dis*. 2023;14(8). doi:10.1038/s41419-023-06041-2
183. Hinshaw DB, Burger JM. *Protective Effect of Glutamine on Endothelial Cell ATP in Oxidant Injury'*. Vol 49. 1990.
184. Wischmeyer PE, Kahana M, Wolfson R, Ren H, Musch MM, Chang EB. GLUTAMINE REDUCES CYTOKINE RELEASE, ORGAN DAMAGE, AND MORTALITY IN A RAT MODEL OF ENDOTOXEMIA. *Shock*. 2001;16(5):398-402. doi:10.1097/00024382-200116050-00014
185. Desler C, Hansen TL, Frederiksen JB, Marcker ML, Singh KK, Juel Rasmussen L. Is there a link between mitochondrial reserve respiratory capacity and aging? *J Aging Res*. 2012;2012. doi:10.1155/2012/192503

186. Bisbach CM, Hass DT, Thomas ED, Cherry TJ, Hurley JB. Monocarboxylate Transporter 1 (MCT1) Mediates Succinate Export in the Retina. *Invest Ophthalmol Vis Sci*. 2022;63(4). doi:10.1167/iovs.63.4.1
187. Xia L, Zhang H, Wang X, Zhang X, Nie K. The Role of Succinic Acid Metabolism in Ovarian Cancer. *Front Oncol*. *Frontiers Media S.A.* 2021;11. doi:10.3389/fonc.2021.769196
188. Liu Y, Liu K, Thorne RF, et al. Mitochondrial SENP2 regulates the assembly of SDH complex under metabolic stress. *Cell Rep*. 2023;42(2). doi:10.1016/j.celrep.2023.112041
189. Bannai S, Ishii T. A novel function of glutamine in cell culture: Utilization of glutamine for the uptake of cystine in human fibroblasts. *J Cell Physiol*. 1988;137(2):360-366. doi:10.1002/jcp.1041370221
190. Crane CS, McIssac TK, Milano SK, Cerione RA, Ulrich SM. Structure and enzymology of glutaminase mutants that disrupt glutamine-glutamate homeostasis and cause neurological disease. Preprint posted online September 17, 2025. doi:10.1101/2025.09.14.674662
191. Kheradmand M, Sangha G, Sissons CM, et al. Glutamine enhances endothelial cell survival and vasodilation by increasing glutathione to reduce oxidative stress. *Physiol Rep*. 2026;14(2):e70737. doi:10.14814/phy2.70737
192. Jiang J, Yin L, Li JY, et al. Glutamate attenuates lipopolysaccharide-induced oxidative damage and mRNA expression changes of tight junction and defensin proteins, inflammatory and apoptosis response signaling molecules in the intestine of fish. *Fish Shellfish Immunol*. 2017;70:473-484. doi:10.1016/j.fsi.2017.09.035
193. Fernando Rubio-Atonal L, Chang J, Jacquemyn J, Ralhan I, Ilarraza I, Ioannou MS. *Glutamate Decreases Oxidative Stress and Lipid Droplet Formation in Astrocytes*. 2025.
194. Metallo CM, Gameiro PA, Bell EL, et al. Reductive glutamine metabolism by IDH1 mediates lipogenesis under hypoxia. *Nature*. 2012;481(7381):380-384. doi:10.1038/nature10602
195. Piccoli C, Ria R, Scrima R, et al. Characterization of mitochondrial and extra-mitochondrial oxygen consuming reactions in human hematopoietic stem cells: Novel evidence of the occurrence of NAD(P)H oxidase activity. *Journal of Biological Chemistry*. 2005;280(28):26467-26476. doi:10.1074/jbc.M500047200
196. PITHON-CURI TC, LEVADA AC, LOPES LR, DOI SQ, CURI R. Glutamine plays a role in superoxide production and the expression of p47phox, p22phox and gp91phox in rat neutrophils. *Clin Sci*. 2002;103(4):403-408. doi:10.1042/cs1030403
197. Weber CM, Moiz B, Kheradmand M, et al. Glutamine metabolism is systemically different between primary and induced pluripotent stem cell-derived brain microvascular endothelial cells. *Journal of Cerebral Blood Flow and Metabolism*. 2025;45(6):1082-1099. doi:10.1177/0271678X241310729
198. Atallah R, Gindlhuber J, Platzer W, Rajesh R, Heinemann A. Succinate Regulates Endothelial Mitochondrial Function and Barrier Integrity. *Antioxidants*. 2024;13(12). doi:10.3390/antiox13121579
199. Huang H, Cui J, Tang D, et al. Succinate accumulation induces pyroptosis and mitochondrial damage via the inhibition of ATP5F1D in HUVECs. *Acta Biochim Biophys Sin (Shanghai)*. 2025;57(12):2011-2021. doi:10.3724/abbs.2025116

200. Mills EL, Kelly B, Logan A, et al. Succinate Dehydrogenase Supports Metabolic Repurposing of Mitochondria to Drive Inflammatory Macrophages. *Cell*. 2016;167(2):457-470.e13. doi:10.1016/j.cell.2016.08.064
201. Tannahill GM, Curtis AM, Adamik J, et al. Succinate is an inflammatory signal that induces IL-1β through HIF-1α. *Nature*. 2013;496(7444):238-242. doi:10.1038/nature11986
202. Richman PG, Meister A. Regulation of γ glutamyl cysteine synthetase by nonallosteric feedback inhibition by glutathione. *Journal of Biological Chemistry*. 1975;250(4):1422-1426. doi:10.1016/s0021-9258(19)41830-9
203. Gialeli C, Shami A, Gonçalves I. Extracellular matrix: Paving the way to the newest trends in atherosclerosis. *Curr Opin Lipidol*. *Lippincott Williams and Wilkins*. 2021;32(5):277-285. doi:10.1097/MOL.0000000000000775
204. Howard B V., Macarak EJ, Gunson D, Kefalides NA. Characterization of the collagen synthesized by endothelial cells in culture. *Proc Natl Acad Sci U S A*. 1976;73(7):2361-2364. doi:10.1073/pnas.73.7.2361
205. Wu G, Meininger CJ. *Regulation of L-Arginine Synthesis from L-Citrulline by L-Glutamine in Endothelial Cells*. 1993. www.physiology.org/journal/ajpheart
206. Campbell S, Mesaros C, Izzo L, et al. Glutamine deprivation triggers nagk-dependent hexosamine salvage. *Elife*. 2021;10. doi:10.7554/eLife.62644
207. Oberkersch RE, Lidonnici J, Andreuzza S, et al. Transsulfuration metabolism is essential for ferroptosis resistance in quiescent endothelial cells. *Cell Death Dis*. Published online December 20, 2025. doi:10.1038/s41419-025-08333-1
208. Héliès-Toussaint C, Gambert S, Roller P, Tricot S, Lacour B, Grynberg A. Lipid metabolism in human endothelial cells. *Biochimica et Biophysica Acta (BBA) - Molecular and Cell Biology of Lipids*. 2006;1761(7):765-774. doi:10.1016/j.bbalip.2006.05.013
209. Long B, Muhamad R, Yan G, et al. Quantitative proteomics analysis reveals glutamine deprivation activates fatty acid β-oxidation pathway in HepG2 cells. *Amino Acids*. 2016;48(5):1297-1307. doi:10.1007/s00726-016-2182-7
210. Oberkersch RE, Pontarin G, Astone M, et al. Aspartate metabolism in endothelial cells activates the mTORC1 pathway to initiate translation during angiogenesis. *Dev Cell*. 2022;57(10):1241-1256.e8. doi:10.1016/j.devcel.2022.04.018
211. Wol~ SP, Jiang ZY, Huwr J V. *PROTEIN GLYCATION AND OXIDATIVE STRESS IN DIABETES MELLITUS AND AGEING*. Vol 10. 1991.
212. Nishigaki I, Hagihara M, Tsunekawa H, Maseki M, Yagi K. *Lipid Peroxide Levels of Serum Lipoprotein Fractions of Diabetic Patients*.
213. Turpin C, Catan A, Guerin-Dubourg A, et al. Enhanced oxidative stress and damage in glycated erythrocytes. *PLoS One*. 2020;15(7 July). doi:10.1371/journal.pone.0235335
214. Williams A, Bissinger R, Shamaa H, et al. Pathophysiology of Red Blood Cell Dysfunction in Diabetes and Its Complications. *Pathophysiology*. *Multidisciplinary Digital Publishing Institute (MDPI)*. 2023;30(3):327-345. doi:10.3390/pathophysiology30030026
215. Obeagu EI. Red blood cells as biomarkers and mediators in complications of diabetes mellitus: A review. *Medicine (United States)*. *Lippincott Williams and Wilkins*. 2024;103(8):E37265. doi:10.1097/MD.0000000000037265

216. George A, Pushkaran S, Konstantinidis DG, et al. Erythrocyte NADPH oxidase activity modulated by Rac GTPases, PKC, and plasma cytokines contributes to oxidative stress in sickle cell disease Key Points. Published online 2013. doi:10.1182/blood-2012-07
217. Orrico F, Laurance S, Lopez AC, et al. Oxidative Stress in Healthy and Pathological Red Blood Cells. *Biomolecules*. *Multidisciplinary Digital Publishing Institute (MDPI)*. 2023;13(8). doi:10.3390/biom13081262
218. Gradinaru D, Borsa C, Ionescu C, Margina D. Advanced oxidative and glycoxidative protein damage markers in the elderly with type 2 diabetes. *J Proteomics*. 2013;92:313-322. doi:10.1016/j.jprot.2013.03.034
219. Nowotny K, Jung T, Höhn A, Weber D, Grune T. Advanced glycation end products and oxidative stress in type 2 diabetes mellitus. *Biomolecules*. *MDPI AG*. 2015;5(1):194-222. doi:10.3390/biom5010194
220. Bila I, Dzydzan O, Brodyak I, Sybirna N. Agmatine prevents oxidative-nitrative stress in blood leukocytes under streptozotocin-induced diabetes mellitus. *Open Life Sci*. 2019;14(1):299-310. doi:10.1515/biol-2019-0033
221. Dincer Y, Akcay T, Alademir Z, Ilkova H. Effect of oxidative stress on glutathione pathway in red blood cells from patients with insulin-dependent diabetes mellitus. *Metabolism*. 2002;51(10):1360-1362. doi:10.1053/meta.2002.35192
222. Raftos JE, Whillier S, Kuchel PW. Glutathione synthesis and turnover in the human erythrocyte: Alignment of a model based on detailed enzyme kinetics with experimental data. *Journal of Biological Chemistry*. 2010;285(31):23557-23567. doi:10.1074/jbc.M109.067017
223. Ellory JC, Preston RL, Osotimehin B, Young JD. Transport of amino acids for glutathione biosynthesis in human and dog red cells. *Biomed Biochim Acta*. 1983;42(11-12):S48-52.
224. Sadaf A, Dong M, Pfeiffer A, et al. A pharmacokinetic–pharmacodynamic analysis of l-glutamine for the treatment of sickle cell disease: Implications for understanding the mechanism of action and evaluating response to therapy. *Br J Haematol*. 2024;205(3):1147-1158. doi:10.1111/bjh.19632
225. Joshi U, George LB, Highland H. Red blood cell extracellular vesicles: new frontiers in hematological biomarker discovery. *Front Med (Lausanne)*. *Frontiers Media SA*. 2025;12. doi:10.3389/fmed.2025.1644077
226. Reis J, Massari M, Marchese S, et al. A closer look into NADPH oxidase inhibitors: Validation and insight into their mechanism of action. *Redox Biol*. 2020;32. doi:10.1016/j.redox.2020.101466
227. Niihara Y, Zerez CR, Akiyama DS, Tanaka Torrance KR. *Increased Red Ceil Glutamine Availability in Sickle Cell Anemia: Demonstration of Increased Active Transport, Affinity, and Increased Glutamate Level in Intact Red Cells*. 1997.
228. Rifkind JM, Nagababu E. Hemoglobin redox reactions and red blood cell aging. *Antioxid Redox Signal*. 2013;18(17):2274-2283. doi:10.1089/ars.2012.4867
229. Pandey KB, Mishra N, Rizvi SI. Myricetin May Provide Protection against Oxidative Stress in Type 2 Diabetic Erythrocytes. *Zeitschrift für Naturforschung C*. 2009;64(9-10):626-630. doi:10.1515/znc-2009-9-1004
230. Gwozdzinski K, Pieniazek A, Gwozdzinski L. Reactive Oxygen Species and Their Involvement in Red Blood Cell Damage in Chronic Kidney Disease. *Oxid Med Cell Longev*. *Hindawi Limited*. 2021;2021. doi:10.1155/2021/6639199

231. Maxwell SRJ, Thomason H, Sandler D, et al. Antioxidant status in patients with uncomplicated insulin-dependent and non-insulin-dependent diabetes mellitus. *Eur J Clin Invest*. 1997;27(6):484-490. doi:10.1046/j.1365-2362.1997.1390687.x
232. Qin X, Zhang K, Qiu J, et al. Uptake of oxidative stress-mediated extracellular vesicles by vascular endothelial cells under low magnitude shear stress. *Bioact Mater*. 2022;9:397-410. doi:10.1016/j.bioactmat.2021.10.038
233. Tsai PH, Liu JJ, Yeh CL, Chiu WC, Yeh SL. Effects of glutamine supplementation on oxidative stress-related gene expression and antioxidant properties in rats with streptozotocin-induced type 2 diabetes. *Br J Nutr*. 2012;107(8):1112-1118. doi:10.1017/S0007114511004168
234. Li L, Sun J, Xia S, Tian X, Cheserek MJ, Le G. Mechanism of antifungal activity of antimicrobial peptide APP, a cell-penetrating peptide derivative, against Candida albicans: intracellular DNA binding and cell cycle arrest. *Appl Microbiol Biotechnol*. 2016;100(7):3245-3253. doi:10.1007/s00253-015-7265-y
235. Madonna R, Balistreri CR, De Rosa S, et al. Impact of sex differences and diabetes on coronary atherosclerosis and ischemic heart disease. *J Clin Med*. *MDPI*. 2019;8(1). doi:10.3390/jcm8010098
236. Gutierrez-Millan C, Barez Diaz C, Alvarez Vizan L, Colino CI. Evaluation of Two Osmosis-Based Methods for the Preparation of Drug Delivery Systems Based on Red Blood Cells. *Pharmaceutics*. 2023;15(9). doi:10.3390/pharmaceutics15092281